BRANZ

STUDY REPORT

SR No. 204 (2009)

Seismic performance of brick veneer houses

Phase 4. Cyclic racking of a two-storey clay-brick veneer building

S.J. Thurston and G.J. Beattie

The work reported here was funded by the Building Research Levy.

ISSN: 1178-4938

Preface

This is the fourth BRANZ investigation of a series looking into the seismic performance of brick veneer.

In Phase 1 slow cyclic tests were performed on two full-scale veneer specimens where the veneer clad a rectangular room which had both window and door openings. In Phase 2 and 3 a shake table test was performed on a clay brick veneer clad room and concrete brick veneer clad room respectively. These used an inertial mass to simulate roof loads. In this latest study a two-storey brick veneer building was cyclically racked to investigate its seismic performance.

The quality of brick veneer construction has improved markedly in recent years, with requirements for the ties to be screw-fixed to the timber framing and with the advent of lighter bricks with vertical penetrations. It is considered that the veneer may no longer be just a driver, but rather that it may have some lateral load-resisting capability.

The complete study is intended to improve the understanding of brick veneer construction in earthquakes, in particular:

- To determine if brick veneer can be relied upon to carry some of the building seismic load or whether the building light timber framing (LTF) construction should be designed to carry the entire load.
- To identify the level of seismic damage that can be expected in modern brick veneer construction.

Acknowledgments

This work was funded by the Building Research Levy. Elephant Plasterboard New Zealand donated the wall linings used in the testing in this report. MonierBricks donated the bricks and Eagle Wire Products Ltd the brick ties used in the testing.

Note

This report is intended for the Department of Building Housing (DBH), standards committees, structural engineers, architects, designers, plasterboard and brick manufacturers and others researching this topic.

Seismic performance of brick veneer houses
Phase 4. Cyclic racking of a two-storey clay-brick veneer building

BRANZ Study Report SR 204
S.J. Thurston and G. J. Beattie

Reference
Thurston SJ and Beattie GJ. 2009. 'Seismic Performance of Brick Veneer Houses. Phase 4. Cyclic racking of a two-storey clay-brick veneer building'. BRANZ *Study Report 204*. BRANZ Ltd, Judgeford, New Zealand.

Abstract

Historically brick veneer houses have not performed well in earthquakes. However, in Phases 1 and 2 of this project, modern construction using better brick ties which are screwed to studs, and the use of bricks with internal holes which allow mortar to penetrate and act as dowels, were shown to result in good performance.

In this study, BRANZ performed a slow cyclic racking test on a timber-framed two-storey brick veneer building with plan dimension 6.7 m x 3.9 m. The construction included flooring at the first floor level and ceilings at ground and first floor level. The walls were lined with plasterboard and incorporated window and door openings. At racking displacements expected in design level earthquakes the veneer exhibited few cracks. These followed mortar courses and almost fully closed when the building was unloaded. Raking out the mortar at crack lines and re-pointing is expected to provide an effective repair strategy. The building appearance, weathertightness and seismic resistance is not expected to be unduly compromised. At top and middle floor racking displacements of ±143 mm and ±69 mm respectively, few bricks had fallen. Cracks could readily be seen at unload and some of these crossed bricks. The veneer would have likely suffered partial collapse if seismic out-of-plane loading had been imposed at this stage. The veneer on a building in such a state is likely to require demolition. However, these extreme displacements are unlikely to occur in practice.

The seismic shear force carried by the veneer was measured directly. This was a high proportion of the total load at design level seismic displacements.

It was concluded that two-storey construction without seismic separations using these bricks and ties is likely to perform very well in a design level earthquake and a conservative estimate of the lateral load carrying capacity of the brick veneer may be used during building design.

Contents Page

Figures Page

Tables Page

1. INTRODUCTION

1.1 Background

The existing NZS 3604 design philosophy assumes the veneer ties accommodate expected differential in-plane displacements between the framing and the veneer and the ties are expected to transfer all the inertial forces from the face-loaded veneer panels to the timber framing.

The veneer tie testing standard, AS/NZS 2699.1:2000 (SA/SNZ 2000), requires the ties to withstand 10 mm vertical differential movement between the veneer and the framing, ±20 mm in-plane differential racking displacement and then be adequately strong under face load tests to withstand expected inertial loads derived using the parts provisions of NZS 4203:1992 (SNZ 1992).

However, in modern veneer construction, the pick-up of in-plane load by the veneer may indeed assist the overall performance of the building in an earthquake by reducing the displacement of the frame. On the other hand, it may also result in damage to the brick veneer.

Slow cyclic and shake table tests on single-storey clay brick veneer specimens have been conducted in Phases 1 and 2 of this research programme (Thurston and Beattie 2008a and 2008b). These reports also discuss the use of this style of construction in New Zealand and include a literature review on the topic. The results of this research indicated that the seismic performance of brick veneers is now much better than it was prior to the introduction of screw fixing of ties and light-weight penetrated bricks. The testing referred to above (Thurston and Beattie 2008a and 2008b) showed that single-storey brick veneer panels tend to rock as single elements under in-plane actions, returning to their at-rest position after the earthquake with little damage. These elements generally cantilever vertically between window and door openings and there is no continuity of the veneer over the tops of the openings, allowing the rocking to occur. Because it was uncertain whether a similar behaviour would be possible in two-storey construction, where there was a continuity of the veneer over the lower-storey window and door openings, the current research programme was devised.

1.2 Current design method for two-storey brick veneer construction

The expectation for brick veneer houses under earthquake loading is that the light timber-framing in each storey will be subjected to ±20 mm racking displacement in a design level earthquake. Because the brick veneer may have zero in-plane displacement under this loading (i.e. does not rock or slide), then in-plane differential movements of ±40 mm could occur across the ties at the top of two-storey veneer construction which does not incorporate horizontal separations. This is expected to rupture the ties which could result in out-of-plane collapse of the veneer.

Further considerations before the acceptance of two-storey veneer are:

- The lower storey of two-storey construction usually carries higher shear loads per unit area than corresponding single-storey construction

- The veneer axial load is higher due to the weight of the veneer above and resistance to veneer uplift provided by the ties
- Openings in the upper and lower storey may be offset.

NZS 3604 does not cover two-storey brick veneer construction largely for the reason discussed above. Thus, specific design is required, where the usual method of dealing with the problem is to separate the lower and upper-storey veneer near the top of the first storey to reduce the maximum design differential movement across the ties back to ±20 mm. The two construction techniques commonly employed are to:

- Support the top storey veneer on a steel angle section which is screwed to the LTF construction. Thus the full weight of the top-storey brick veneer is transferred to the timber framing, or
- Provide a horizontal slip layer within the veneer construction near veneer mid-height (MonierBrick 2006).

The first of these methods ensures that if large in-plane displacements of the LTF structure occurs, the veneer will be able to move with it without the development of large differential displacements. The second method expects the upper section of the veneer to move separately from the lower section (as in the first method) but with the added advantage that the weight of the upper section of the veneer is transferred directly to the foundation rather than via the timber framing.

In the racking test described herein neither of the veneer separation techniques listed above was used because the results of the single-storey veneer tests indicated that the strength and stiffness of the veneer was such that the building would not likely be subjected to large displacements in a design earthquake. Further, the strength of the ties in the plane of the wall was shown to be sufficient to transfer forces from the framing to the veneer. Tie ruptures are unlikely if the design earthquake induces sufficient movement of the brick veneer to reduce tie differential movements to safe values. Whether this occurs under design level earthquake displacements, and whether the veneer rocks back into the uncracked position when the excitation is removed, is the major interest of this study.

1.3 Literature survey

The review of previous investigations on the seismic in-plane performance of brick veneer, both in New Zealand and overseas, is presented in BRANZ *Study Report 190* (Thurston and Beattie 2008b).

In parallel with this current research study, uni-directional shake table testing has been conducted at the University of California in San Diego. Testing of individual panels was reported by Okail et al (2008). Further testing has recently been undertaken at the same facility on a single-storey timber-framed building clad with brick veneer but this work is yet to be reported. It is worth noting that the details of the test specimens are representative of American construction techniques and therefore differ significantly from New Zealand construction. The American ties are either nail fixed to the framing or screwed through the bend in the tie where it butts against the wall stud. Furthermore, the exterior of the American framing is completely clad with either oriented strand board (OSB) or plywood, which results in a significantly stiffer timber-framed structure than typical construction in New Zealand.

1.4 Outline of this report

Section 2 of this report summarises the results of slow cyclic testing of the test building. This testing is described in greater detail in Appendix A.

Section 3 uses the observations from the testing described in Section 2 to describe the racking behaviour and cracking mechanisms qualitatively.

Section 4 calls on the behaviour described in Section 3 to develop computer models to predict brick veneer behaviour under lateral load from which the relationship between LTF wall displacement and load carried by the veneer can be determined. To achieve this, it uses the measured brick tie stiffness characteristics given in Phase 1 (Thurston and Beattie 2008a). A conservative method for calculating the bracing rating of both single-storey and two-storey brick veneer construction is proposed for adoption into NZS 3604. Predictions from the theory are compared with test results.

Section 4 also compares the measured test results with the predictions to help validate the theory.

Conclusions and recommendations are given in Section 5.

Appendix A describes in detail the slow cyclic testing of the test building.

Appendix B describes the measurement of the brickwork mortar bond strength in both shear and tension and in both brick-to-brick and brick-to-foundation concrete.

Appendix C gives details of a Ruaumoko computer analysis of the two-storey building.

1.5 Bricks, brick ties and mortar used in the testing

Details of the brick construction used in the tests that are described in the Appendices are given below. The choice of these products is expected to have a significant influence on the test results. Further tests are required before general applicability can be determined.

The MonierBricks brand clay bricks used had dimensions 230 mm long x 76 mm high x 70 mm wide. When assembled using the standard 10 mm of mortar between bricks, the veneer weighs approximately 130 kg/m^2.

The bricks used had five vertical holes, of cross-section 32 x 23 mm, for the full brick depth which partially filled with mortar, as shown in Figure 1.

The bricks were laid by tradesmen using Dricon Trade Mortar with approximately 10 mm thick mortar being used between the bricks on both horizontal and vertical surfaces. This mortar was stated to comply with NZS 4210 (SNZ 2001) for masonry construction.

The average strength of the standard cured 28-day-old mortar was determined in Phase 1 (Thurston and Beattie 2008a) to be 20.2 MPa which is 62% more than the 12.5 MPa minimum strength specified by NZS 4210. Hot-dipped galvanised steel, 85 mm long, Eagle brand brick ties were dry-bedded onto the bricks rather than being fully encapsulated within the mortar. The ties were stated to be rated “heavy earthquake to NZS 3604:1999 and the draft AS/NZS 2699 Standards”.

Ties were secured to the face of the timber studs using galvanised, self-drilling, 35 mm long, Tek screws which were supplied with the ties.

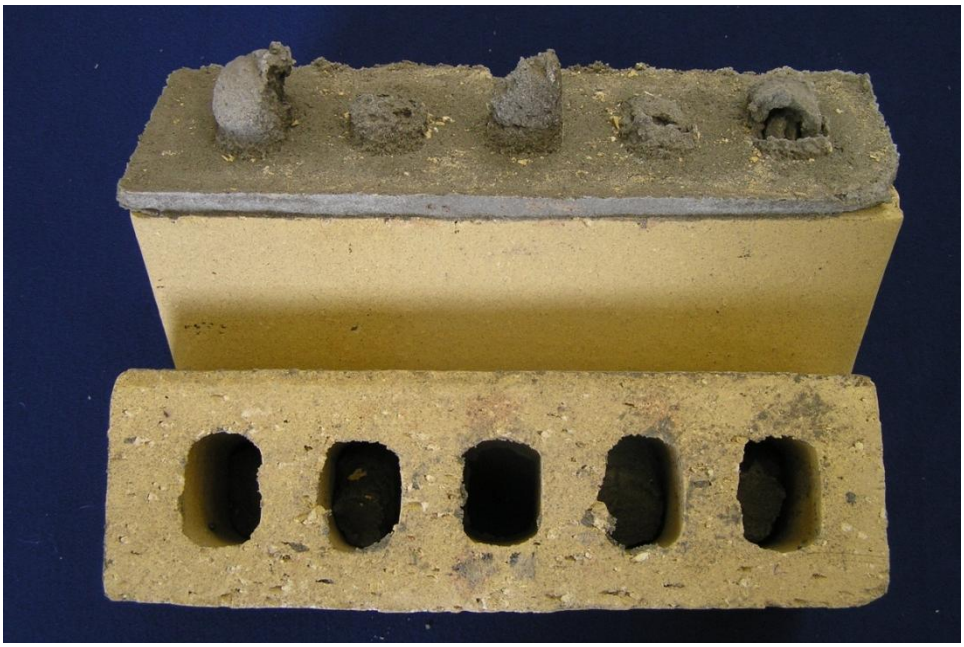

Figure 1. Holes in bricks – mortar formed dowels linking bricks

2. SUMMARY OF TEST SPECIMEN CONSTRUCTION AND TEST METHOD

Appendix A provides the details of the construction and racking tests on the test building. This was a two-storey timber-framed single room on each floor building, with ceilings at the ground and first floor levels and a floor at first floor level. The brick veneer cladding incorporated window and door openings. The specimen had plasterboard-lined LTF walls, timber-framed plasterboard-lined ceilings and brick veneer on all four sides. The outside plan dimensions of the room were 6.73 x 3.93 m. Generally the brickwork was constructed in a running bond pattern but soldier bricks were used above two windows. The brickwork cracking pattern, the load carried by the veneer and various displacements were monitored.

The brick veneer was constructed on a steel ring beam with concrete infill which was supported on rollers. An arrow in Figure 3 points to this ring beam. Appendix A explains how this enabled the force in the brick veneer to be measured using the ring beam restraints.

Figure 2. Laying brickwork against the LTF during construction

Figure 3. Photograph of building Side 1 before testing

Figure 4. Photograph of building Side 2 before testing

Aluminium windows were installed in three of the four bottom-storey side wall openings. The windows were fitted into the timber-framed walls so that they extended out into the plane of the veneer with a touch fit to the veneer, typical of normal construction. Any relative movement between the brickwork and the LTF walls required the window framing to deform. This was observed to occur as distortion of the window frames into a trapezoidal shape and rotation of the gasketed glazing within the window frames. No window damage or glass breakage was observed. The remaining window opening was framed in timber, to simulate a window. The lintel of this window was formed with a soldier course of bricks.

Initially the first floor and roof were horizontally displaced using two actuators such that the force in the top actuator was twice that at the first floor. This was done to match the design lateral load distribution stipulated by NZS 4203. However, as the bottom-storey veneer was far stronger and stiffer than the upper storey, when the strength of the upper storey had been reached the shear force in the bottom storey was well short of its ultimate strength and hence the displacement and cracking of the lower-storey veneer was low. Therefore, to investigate the strength of the lower storey the test regime was changed to deflection control so that the inter-storey deflection was similar in each storey.

3. BRICK VENEER MOVEMENT AND CRACK PATTERNS IN EARTHQUAKES

3.1 Introduction

In the discussion below veneer panels are referred to using the labelling system of Figure 21 to Figure 23. Full details of the labelling system used are given in Section A.1. The brickwork above the top windows is referred to as the top spandrel, between the two window levels as the middle spandrel and below the bottom windows as the bottom spandrel.

In Section 3.2 the predicted building crack pattern (predicted before the racking test was performed) is given. This was based on simple veneer rocking mechanisms and assumed no cracking in the spandrels.

The measured crack pattern is discussed in Section 3.3. The spandrels did crack, but as the theory of Section 3.2 is the basis of the two-storey veneer model given in Section 4.4.6, the simple rocking models in Section 3.2 need to be discussed.

3.2 Predicted veneer crack pattern

To the writers' knowledge, racking tests have not previously been performed on two-storey brick veneer houses and the veneer cracking pattern was difficult to predict in advance.

In Phases 1 and 2 of this project (Thurston and Beattie 2008a and 2008b) the single-storey brickwork piers rocked as a single unit or in some cases slid on the base. In all cases 'L-shaped corner veneer elements' rocked. No diagonal cracks occurred within rocking or sliding units. They basically retained their original rectangular shapes and no vertical cracks occurred (e.g. at corners). However, a more complex crack pattern was expected for two-storey construction because of the continuity of the veneer above lower-storey openings and the extra axial load from the upper-storey veneer. Possible deformation mechanisms are discussed below:

1. The whole building rocks as a single unit. This was discounted as other mechanisms were shown to occur at lower loads.
2. The whole veneer slides along the base as a single unit. This was considered to be unlikely as the ties connecting the end face-loaded veneer to the LTF would resist this movement.
3. The full two-storey height veneer piers between windows rock. A possible mechanism to achieve this is drawn in Figure 5. Here, the spandrels beneath windows are considered to rock separately thereby inducing vertical cracks. However, this mechanism was considered unlikely (even when the windows are aligned in upper and lower storeys) as there would be a clash of two portions of brickwork trying to occupy the same space as illustrated in Figure 5.
4. The piers rock between window openings with the entire brickwork between window levels remaining uncracked, as shown in Figure 6. This drawing includes the axial and shear transfer forces which would exist between veneer panels. The resistance to rocking of the lower-

storey panels was expected to be high due to high axial forces on the rocking corner panels which would resist this motion. These axial forces arise from both the weight of brick above and the resistance to veneer uplift from the brick ties in the brickwork above. It was recognised that spandrel diagonal cracks emanating from window corners (due to the forces shown in Figure 6) may occur before a full rocking mechanism had developed and may limit the maximum shear that the veneer could carry.

It was considered that the mechanism detailed in point 4 above would be the most likely.

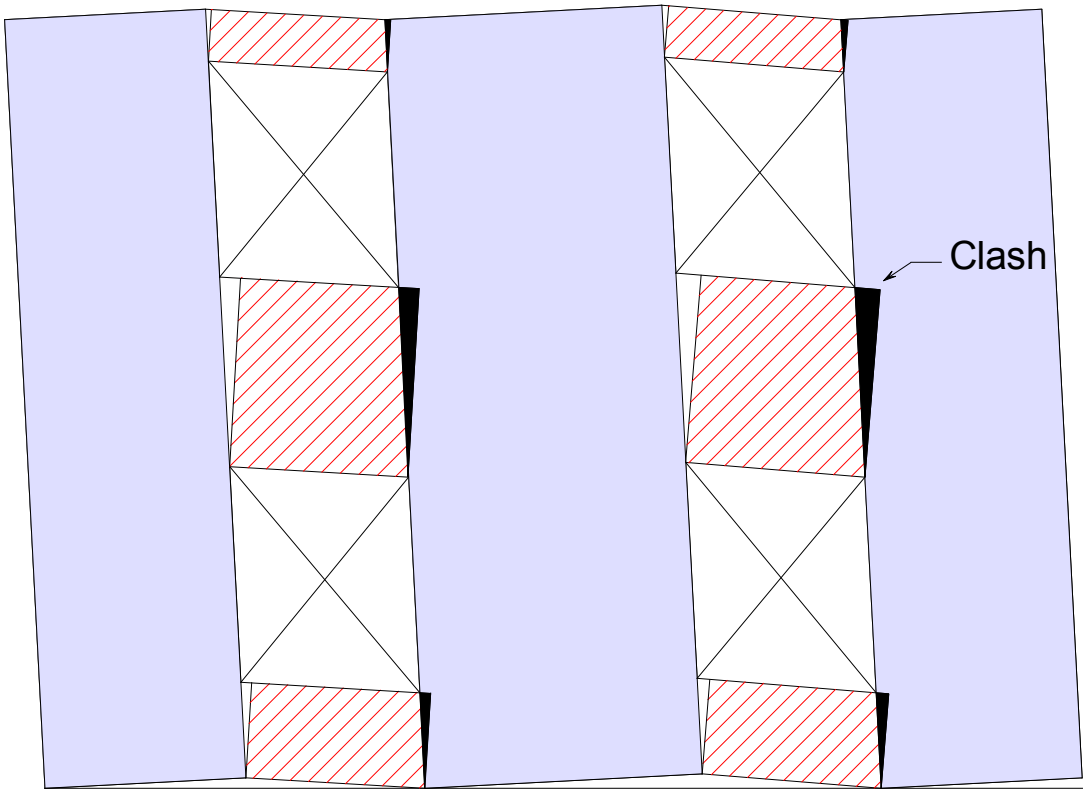

Figure 5. Possible deformation mechanism No 1 of two-storey veneer under in-plane racking – considered unlikely

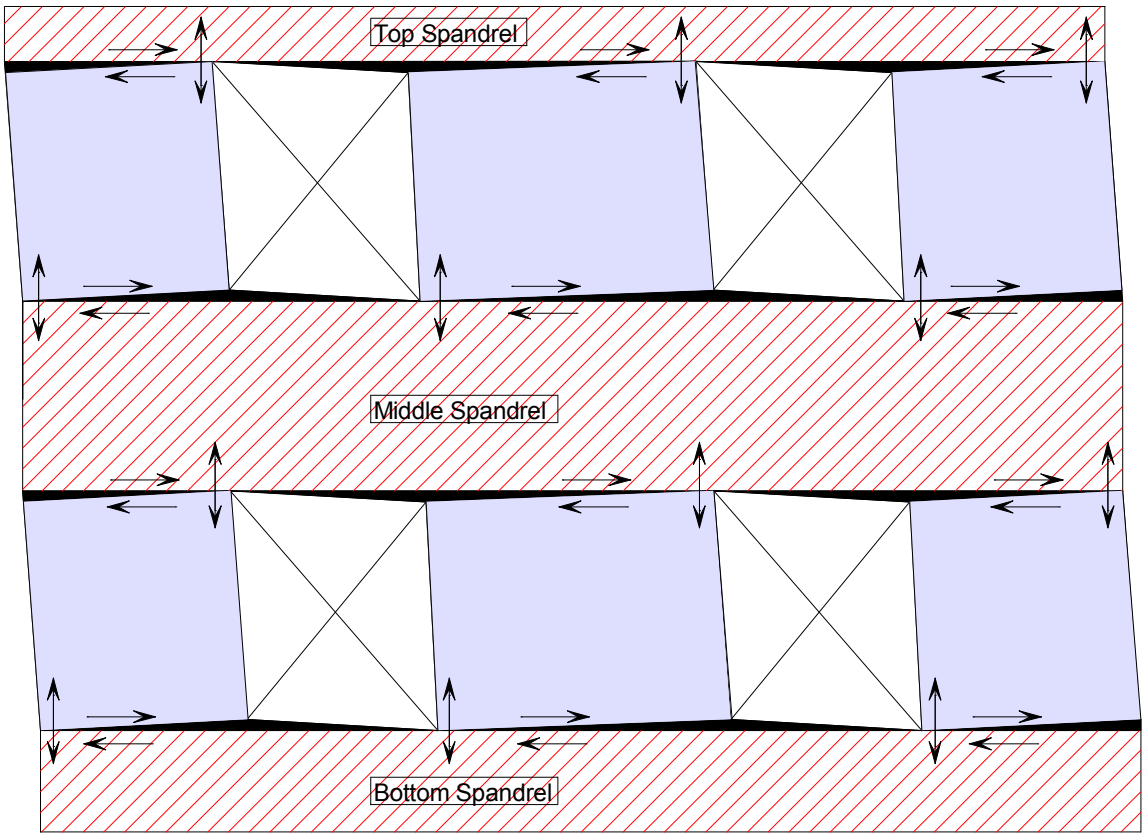

Figure 6. Possible deformation mechanism No 4 for two-storey veneer under in-plane racking

Note gaps are shown shaded in black. Transfer forces between veneer panels only are shown and not forces from brick ties

3.3 Measured veneer cracking and deformation

Observed cracking in the brick veneer during testing is sketched in Figure 34 to Figure 41. Photographs of cracking in the top spandrel are given in Figure 48 to Figure 54. Photographs of veneer cracking at progressive stages of the testing are given in Figure 55 to Figure 103.

The test was conducted in nine stages (called Stage A to Stage I). The corresponding applied building displacements are summarised in Table 6. In Stage D the inter-storey drifts were approximately ±27 mm for the upper storey and ±8 mm for the lower storey and the peak shear forces carried by the veneer were ±68 kN (as directly measured by the base load cells and summarised in Table 6). This was 75% of the total applied load. Cracks were very narrow and difficult to detect immediately after the applied floor displacements were returned to zero.

In Stage E the inter-storey drifts were approximately 36 mm for the upper storey and 10 mm for the lower storey and the shear carried by the veneer was 69 kN. The major veneer deformation mechanism for Stages A to E was rocking of the veneer panels over the top window heights about cracks emanating from the bottom corners of the upper-storey windows. These cracks were mainly horizontal

in the Side 1 veneer and diagonal through the middle spandrel in the Side 2 veneer except the cracks in Panel G middle spandrel were horizontal not diagonal. Cracks emanated from the top window corners, extending through the full depth of the top spandrels. The cracks emanating from lower-storey window corners were narrow and only just visible at peak loads.

In the latter stages of testing (after Stage F) the major veneer deformation mechanism was still rocking of the veneer panels between windows. This rocking was about cracks emanating from the window bottom corners. These cracks were now mainly diagonal cracks cutting through the spandrel below for panels located between a window and a veneer corner and horizontal cracks for panels between adjacent windows.

Rather than the predicted horizontal cracks shown in Figure 6 the cracks were now:

(a) Top spandrel: diagonal or near vertical

(b) Middle spandrel: diagonal or near vertical linking upper and lower-storey window corners

(c) Bottom spandrel: diagonal cracks cutting through the spandrel below for panels located between a window and a veneer corner and horizontal cracks for panels between adjacent windows.

4. MODELS OF BRICK VENEER SEISMIC BEHAVIOUR

4.1 Introduction

This section develops models for predicting the shear load carried by homogeneous single and two-storey brick veneer construction based on the observed veneer crack pattern. This is construction in which the veneer is continuous for the full height and does not have either a horizontal slip joint or the top veneer separately supported on steel angles fastened to the LTF.

In Section 4.2 a complex (Ruaumoko) computer model which assumes no spandrel cracks is discussed. This model predicts far greater lower-storey veneer shear loads than were actually measured for the two-storey building reported on here although the agreement for the upper storey is reasonable.

A simple computer model is developed in Section 4.3. This gives better agreement with the measured strength of the two-storey veneer.

Section 4.4 presents a conservative method of estimating the shear load that can be carried by brick veneer, which is proposed to be incorporated in NZS 3604.

4.2 Analysis 1 – Ruaumoko computer model of two-storey test building

4.2.1 Introduction

A proposed model of the deformation of the brick veneer is shown in Figure 6. If a vertical section is drawn through the walls then the brick veneer and LTF on this section will displace as shown in Figure 7. The LTF deflection is linear over each storey but the inter-storey deflection is different for each storey. The veneer

rotation only occurs between top and bottom cracks over the height of the windows and the spandrels do not rotate. The difference between LTF and brick veneer deflection profiles represents the brick tie in-plane displacement plus any in-plane weak axis bending of the timber studs. If the spandrels do not crack then the brick veneer in-plane displacement at any particular spandrel will be constant along the building sides that are parallel with the driving motion but it will vary by the accumulated crack widths should cracking occur.

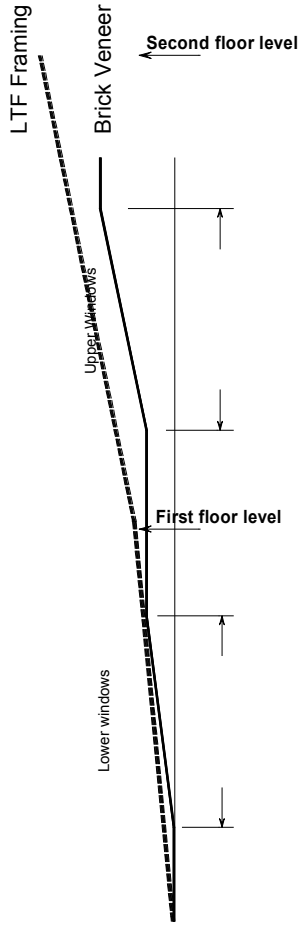

Figure 7. Theoretical deflection profiles of two-storey brick veneer sides

4.2.2 Model used

A Ruaumoko computer model was developed, as discussed further in Appendix C. The single-storey displacement pattern was simple and led to a relatively easy solution (Thurston and Beattie 2008a). However, the two-storey situation is more complex and requires the following assumptions before the analysis can be run:

1. Horizontal cracks occur in the side (in-plane loaded) walls and end (out-of-plane loaded) walls at the levels of the top and bottom of the windows as shown in Figure 6
2. There is no cracking in the spandrels and thus the end walls and spandrels displace the same amount at the level of the spandrels

3. The difference between LTF and veneer displacement is partially resisted by end wall ties and side wall ties
4. The shear load versus deflection of the brick piers can be modelled with the forces shown in Figure 9 using the theory given in Section 4.3.

4.2.3 Comparison of theory and test results

Figure 8 plots the recorded total shear load applied to each storey plotted against the LTF inter-storey displacement. Note that the lower-storey shear load is the shear force directly measured at the base of the veneer. The upper-storey shear load is taken as the load applied at the roof. This would have been partially resisted by the lined LTF. As the upper-storey lining was only screwed at 600 mm centres and vertical joints were not stopped, the upper-storey LTF bracing strength was expected to be low, particularly at large displacements when the lining fixings had effectively failed.

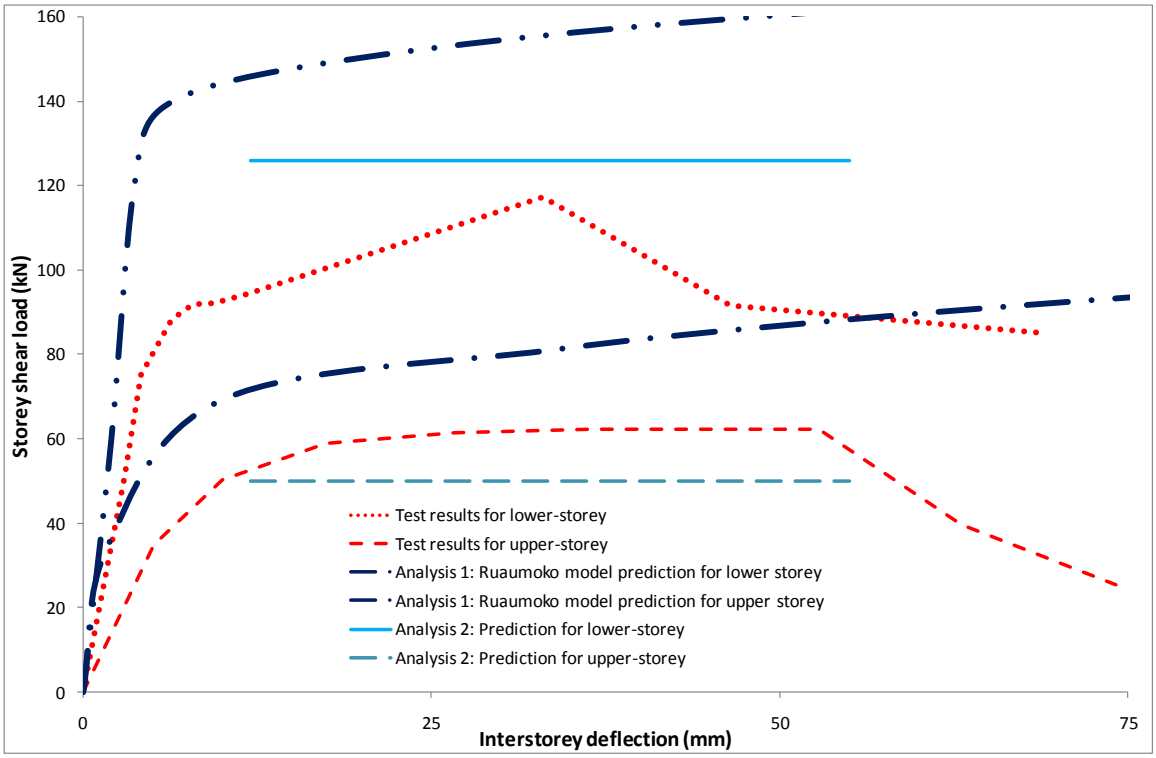

Figure 8. Comparison of backbone curve of inter-storey shear force versus inter-storey displacement for theory and test results for the two-storey building

Figure 8 also gives the Analysis 1 (Ruaumoko model) prediction. Analysis 2 results are also shown but these are discussed in Section 4.3.

The Ruaumoko model grossly overestimates the load carried by the veneer, particularly for the lower storey. This is largely attributed to the cracking mechanism assumed by the theory (Figure 6) varying from that found in the test. The main difference was that the horizontal cracking assumed at the top of windows did not occur in the test. Instead cracks (often diagonal cracks)

occurred in the spandrels, particularly the middle spandrel. Thus, the test had found a weaker mechanism than assumed. The agreement between theory and test is better for the upper storey which will be less affected by the diagonal cracks in the middle-storey spandrels.

4.3 Analysis 2 – simplified analysis of two-storey test building

4.3.1 Introduction

The test building can be analysed as two single-storey buildings, one on top of the other using the method discussed below. If there is no top spandrel (lintel) the method derived by Thurston and Beattie (2008a) may be used for the top storey. Section 4.3.2 develops a model for the upper-storey or single-storey case where there is a top spandrel (lintel).

4.3.2 Analysis of a rocking pier with spandrel above

Assumptions (1) to (3) in Section 4.2.2 are used. In addition, it is assumed that the compression of end (face-loaded) wall ties is zero. Thus, the end wall veneer displaces the same as the LTF. Test results (see Table 6) show that the differential movement between the two was small except at the very top of the veneer near corners. As the spandrels are assumed to remain uncracked the side wall veneer also displaces the same as the LTF and therefore the horizontal forces in the side wall ties are zero. Thus, the shear load on side wall rocking elements between windows is applied via the spandrels (i.e. at the top of the window openings). These assumptions lead to the model in Figure 9.

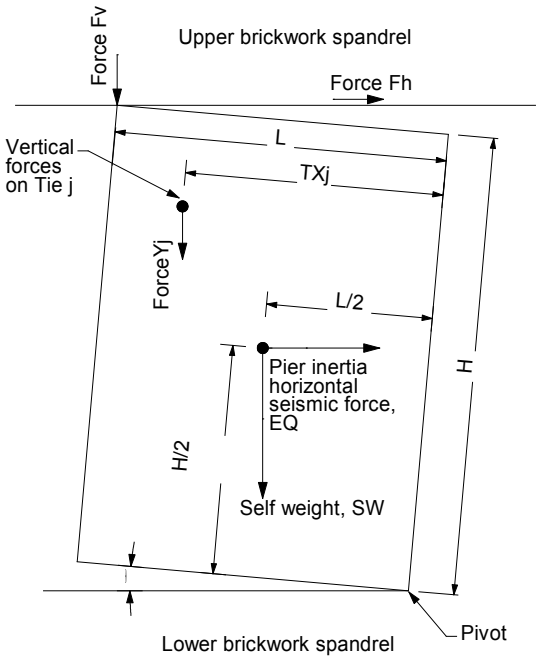

Figure 9. Forces on a rocking brick pier

A theory is developed below for predicting the relationship between shear force in the brick pier and LTF displacement. The pier is assumed to be located between adjacent windows with a spandrel below and a spandrel (i.e. lintel) above.

Figure 9 shows the forces on a rocking pier of brick, of height H and length L, which has rotated by θ radians by pivoting at one end. The rotation occurs about a crack at the height of the sill of the adjacent windows. The upper spandrel is lifted by the rocking action of the pier below by θ x L. This will attract a resisting force, Fv, at the highest corner of the pier (shown in Figure 9) due to the attributed weight of brickwork above plus the resistance provided by the attributed ties in the veneer above the pier being lifted by θ x L.

It is assumed that uplift of the LTF is zero and there is negligible slip of both the brick ties in the mortar and the ties at the screw interface with the timber stud. Thus, the vertical deformation of Tie j relative to the stud is given by:

$$TieDefYj = TXj \times \theta \quad \ldots (1)$$

The relationship of tie force versus vertical displacement has been measured (Thurston and Beattie 2008a) and thus the vertical force in Tie j (ForceYj) can be derived from the measured TieDefYj.

By taking moments about the pivot point of the pier:

$$Fh \times H + EQ \times H/2 = SW \times L/2 + \Sigma ForceYj \times TXj + Fv \times L \ldots (2)$$

where:

EQ = $C_{EQ} \times \rho \times H \times L$

C_{EQ} = the seismic lateral load coefficient = 0.241 for Zone A (Shelton 2007). Note that in the tests C_{EQ} = 0 because there were no inertial forces

ρ = the brick veneer weight per unit area in kN/m^2

SW = pier self-weight = ρ x H x L

Fv = vertical force at lifting corner due to the weight of veneer above and sum of forces from uplift of ties which are attributed to this lifting corner

Fh = horizontal shear force in brick pier.

The parameters can be found as described below:

- For any pier horizontal displacement, Δh, the rotation, θ, can be found from $\theta = \Delta h/H$
- The uplift of the veneer spandrel above the pier, Δv, can be found from $\Delta v = L \times \theta$
- The uplift forces in each tie above the pier, Force Yj, can be found from the tie force versus upward deflection relationship given in Appendix D of Thurston and Beattie (2008a)
- The vertical force at the pier corners, Fv, can be found from the attributed weight plus force for each tie lifted by Δv in the brickwork in the spandrel above.

Thus, the shear force, Fh, can be found from any specified horizontal displacement of the pier, Δh, by substituting into Eqn (2).

4.3.3 Rocking 'L-shaped corner veneer element'

This is identical to a rocking pier except Fv now includes the weight of half the end (face-loaded) wall above the rocking element and the force from the ties in the end wall above at lifting corners.

4.3.4 Total building

The method described above was used to predict the shear load carried by the test building. The results are summarised in Table 1. This is compared with the measured strength in Figure 8. The theoretical values are lower than the Ruaumoko values. Compared to the test results, the prediction is slightly conservative for the upper storey. However, as the test results include some shear carried by the lined LTF and the model does not, all that can be said is the prediction is reasonable. The prediction is slightly unconservative for the lower storey. It is concluded that cracking of the middle height spandrels was a weaker failure mechanism which limited the shear that could be taken by the lower storey.

Table 1. Predicted shear strength of test building brick veneer (note that panel positions are shown in Figure 21 and Figure 22)

Panel	Upper Storey (kN)	Lower Storey (kN)
A	7.5	20.3
B	6.5	23.1
C	7.5	20.3
F	16.4	34.7
G	5.0	8.8
H	7.1	19.0
Sum	50.0	126.1

4.4 Proposed design level of seismic shear to be carried by brick veneer

4.4.1 Introduction

A conservative method to calculate the bracing resistance provided by brick veneer is derived below for both single and two-storey buildings. It is proposed that this be incorporated into the next revision of NZS 3604.

The main assumption is that the veneer may **only** carry the in-plane seismic inertia load attributed to it by NZS 3604 i.e. that assumed to be transferred to the top of the adjacent LTF. In the tests reported here, a large shear load in the LTF was transferred to, and carried by, the veneer but this is conservatively ignored. The resistance to the veneer upward rocking provided by the ties and also the weight of

brick veneer return walls is also conservatively ignored. The predictions are shown to be very conservative relative to test results but still provide a useful bracing function. However, at this stage the method is limited to similar construction to that tested, namely bricks of certain aspect ratios, which have full depth voids as defined in Section 1.5. It is also limited to brickwork with a minimum mortar strength of 12.5 MPa. The tie type and distribution must still meet the current criteria from the various standards.

The self-weight seismic shear force is assumed to be distributed up the height of the veneer as shown in Figure 10(a). This can be integrated over the height of the veneer to give the total force, V1. This is the shear force carried at the bottom of the veneer and is the value to use when comparing with test results as these too are measured at the bottom of the veneer. However, the inter-storey shear force assumed by NZS 3604 is 0.5V1 as sketched in Figure 10(b).

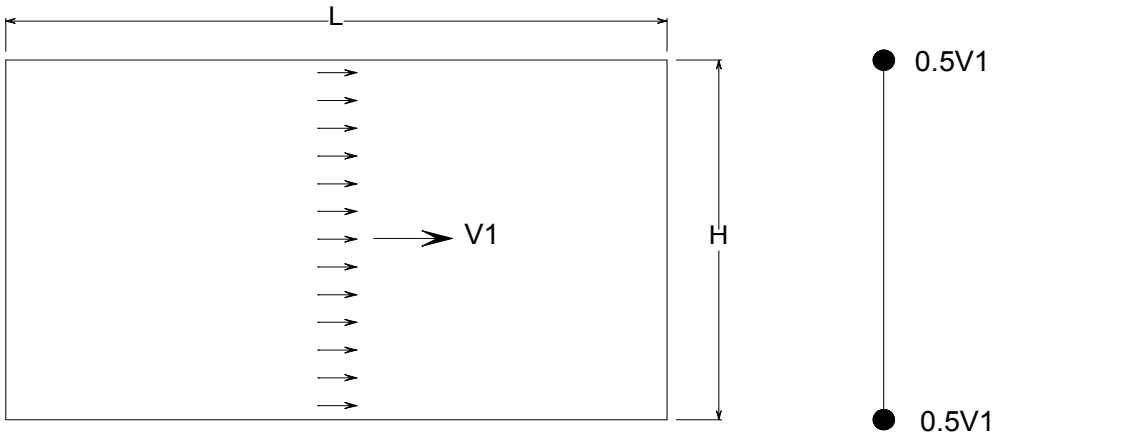

(a) Seismic loading on veneer wall (b) NZS 3604 assumed distribution

Figure 10. Self-weight induced seismic shear forces on a single-storey veneer wall

4.4.2 Single-storey pier

It is proposed that the design seismic shear that can be carried by a brick pier be the minimum of the shear forces determined using the following three criteria:

1. The veneer to carry the in-plane self-weight seismic inertia force assumed by NZS 3604, V1, given by:

   $$V1 = C\rho LH \quad ... (3)$$

   Where:

   C = lateral force coefficient. Shelton (2007) stated that C = 0.241 for Zone A, C = 0.181 for Zone B and C = 0.121 for Zone C

   ρ = veneer weight per unit area. Shelton (2007) also stated that ρ = 2.2 kN/m^2 for heavy-weight veneer and ρ = 0.8 kN/m^2 for medium-weight veneer. As all brick veneer is expected to weigh over ρ = 0.8 kN/m^2 it will be assumed all brick veneer is heavy-weight veneer.

   However, the veneer contains window and door openings. Shelton (2007) stated that NZS 3604 assumes that 30% of the area of a cladding is

openings. If this area is called Openingfraction then the design bracing resistance (DBR), assumed by NZS 3604, is given by:

$$DBR = 0.5V1 = 0.5C\rho LH \times (1\text{-Openingfraction}) \ (kN) \ \ldots (4)$$

Factoring by 20 to convert to Bracing Units (BUs) and substituting Shelton's values for the other parameters gives:

$$DBR = KLH \ldots (5)$$

where K is a constant given in Table 2.

Table 2. Value of K to calculate design bracing resistance (DBR)

Zone A	Zone B	Zone C
3.71	2.78	1.86

2. The shear force to slide the pier on the foundation, V2. For bricks with holes where mortar dowel action helps resist shear slip between bricks this displacement mechanism is expected to be limited to isolated piers. These are moderately rare and occur only where there are full height windows or a pier is adjacent to doorway openings, and is longer than it is high. Thurston and Beattie (2008a) showed that the sliding strength was:

   $$V2 = 0.63\rho LH \ldots (6)$$

   where 0.63 was the measured sliding friction coefficient for a mortar course on a flat surface.

   Note that from the two equations above that V2/V1 = 0.63/C = 2.6 for Zone A and 5.2 for Zone C. Thus, V2 is always significantly greater than V1 and will not govern and so this criteria can be ignored.

3. The force to make the pier rock. It is assumed that there is no load horizontal transfer between veneer and LTF. Thus, there are no forces in the ties connecting the two and the forces on the pier are shown in Figure 9. From Figure 9 the pier will rock when:

   $$V1 \times H/2 = SW \times L/2 \ldots (7)$$
   $$\text{Or} \quad V1 = \rho L^2 \ldots (8)$$

   By examining Eqn 3 and Eqn 8, the latter only governs when L is less than CH (= 0.241 x 2.2 m = 0.53 m). In practice this means that this criteria can be ignored too.

The predictions from Eqn 3 and Eqn 8 are plotted in Figure 12 for the case of a 2.2 m high heavy-weight veneer pier for Zones A and C. The predictions from the theory of Section 5.2 of Thurston and Beattie (2008a) with no top spandrel (lintel), and also from the theory of Section 4.3.2 for a 0.344 m high spandrel, have also been plotted in this figure for the ties used in the tests. It can be seen that the

design method is very conservative relative to the more detailed theory for piers more than 1 m long.

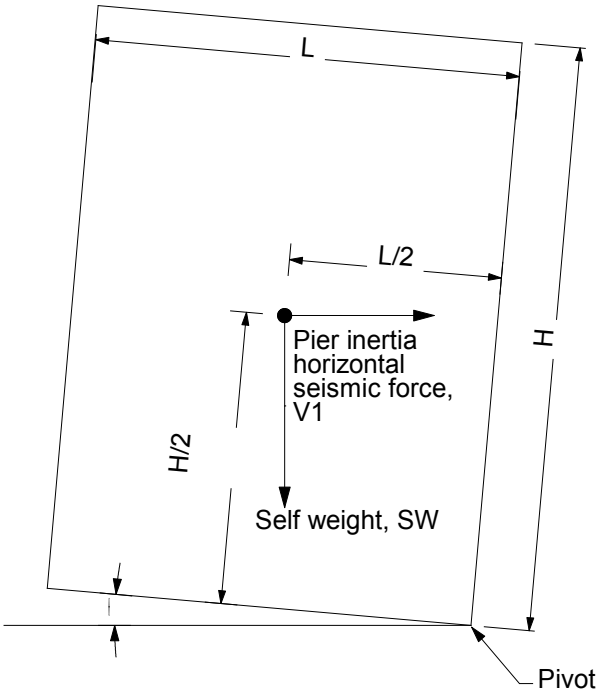

Figure 11. Rocking pier for design method calculation

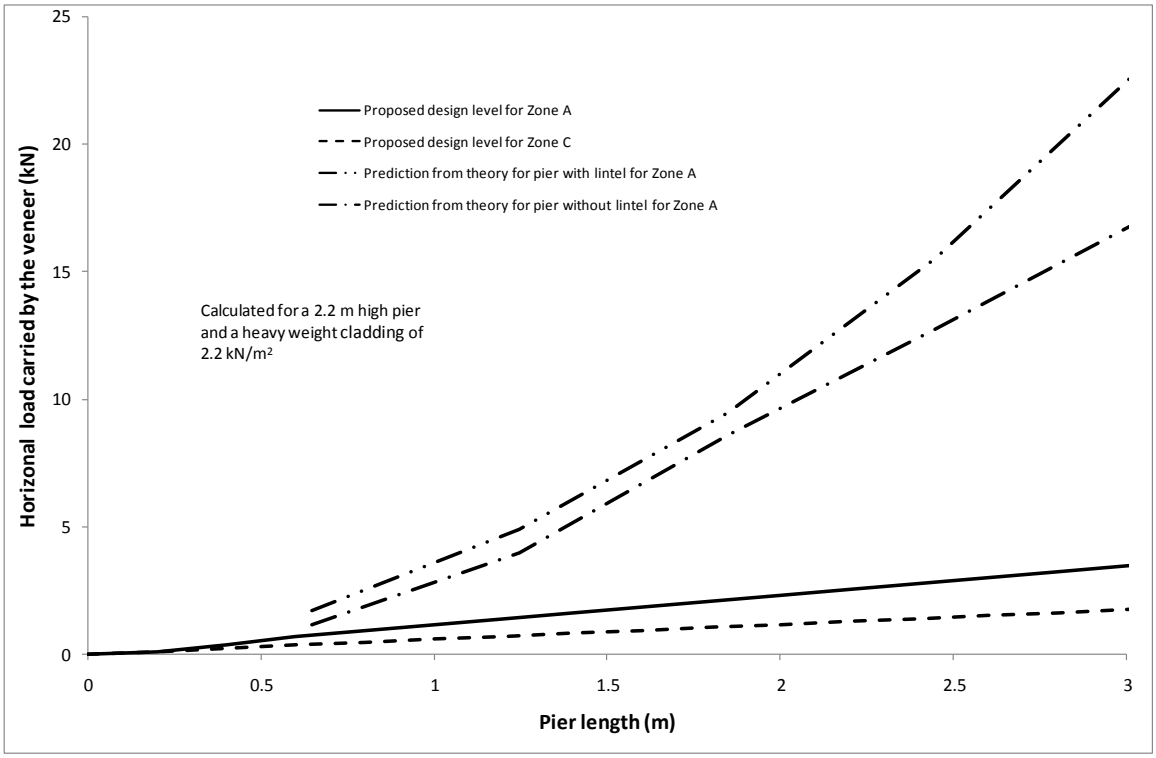

Figure 12. Design pier bracing resistance (DBR)

4.4.3 Single-storey corner veneer rocking element

These will provide significantly more resistance to rocking than side wall veneer piers of the same length when the earthquake is in a direction that lifts the return walls, due to the moment resistance provided by the weight of the return end walls. However, this strength enhancement is conservatively ignored in this design method.

4.4.4 Comparison between proposed design level of seismic shear and single-storey test result

The percentage of openings in the Thurston and Beattie (2008a) Room 1 side wall veneer was 19.9%. The self-weight seismic inertia force from the veneer for a heavy-weight cladding in Zone A is therefore given by:

V1 = Cρ x (inter-storey height) x (total length of veneer) x (1-0.199)

= 0.241 x 2.2 x 2.42 x 13.46 x 0.801 = 13.83 kN.

This is plotted in Figure 13 for comparison with the test results. Clearly this design method is very conservative. The shear carried by the veneer in the test came from load transfer from the LTF via the brick ties, which is ignored in the proposed method. Note that the proposed design level of shear to be used is 0.5V1, as discussed in Section 4.4.1.

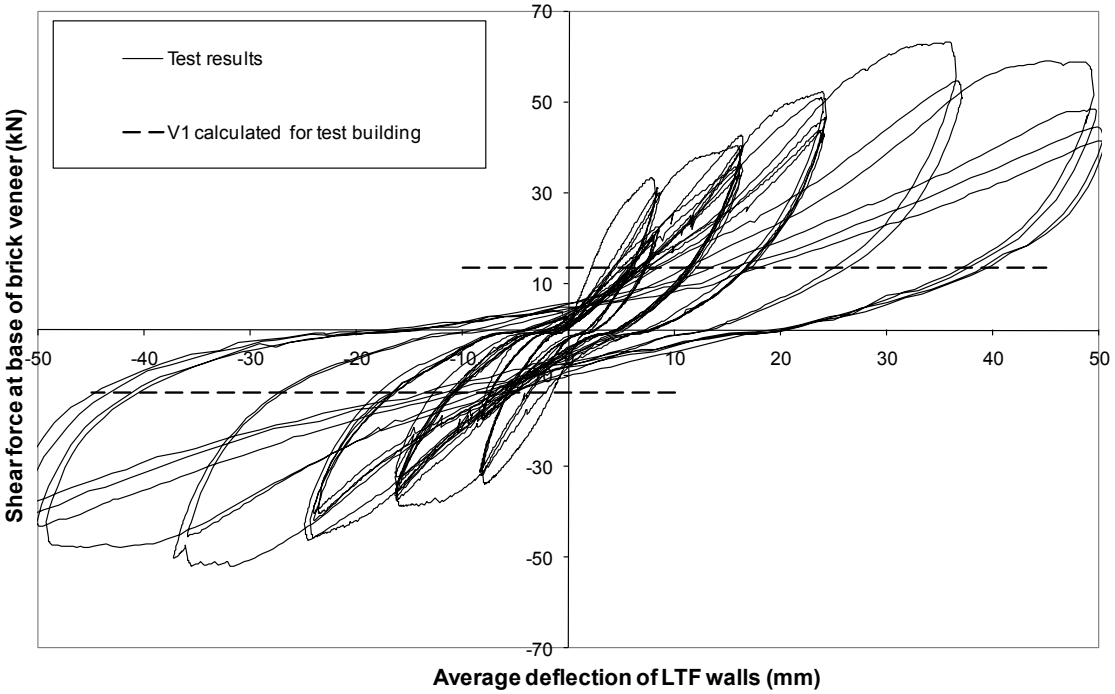

Figure 13. Comparison of design load for Room 1 and measured shear strength

4.4.5 Proposed brick veneer bracing rating for NZS 3604 single-storey veneer construction

The proposed clause for the standard is: “Provided the brick veneer construction complies with the following required features then each veneer wall may be assumed to have a DBR in the direction of the wall plane of:

$$DBR = KxHxL \quad \ldots (9)$$

Where:

H is the inter-storey height in metres
L is the wall length in metres
K is given in Table 2.

Walls within two metres of a bracing line may be assumed to be on the bracing line. The bracing rating for the veneer is additive to that due to the timber-framed wall bracing elements in the structure that are parallel to the veneer.

Required veneer features

- The mortar has a compressive strength of at least 12.5 MPa
- The bricks have a height to length ratio no greater than 0.5
- The bricks have full depth holes comprising not less than 12% of the horizontal cross-section of the brick and having a minimum dimension of 20 mm”.

The bracing resistances derived from the above method are compared with the bracing demand ratings for Zone A in Table 3 for both earthquake directions on three buildings shapes and for both heavy and light 25˚ slope roofs. The assumed stud height was 2.4 m. The first building shape is the small standard building assumed in the calculation of the bracing demand tables in NZS 3604.

The percentages shown in Table 3 are independent of the seismic zone. It can be seen that the percentage of load carried by the brick veneer is always less than 50% and decreases rapidly for squarer buildings and larger buildings. The load to be carried by the LTF is almost independent of the cladding weight used, which is as expected as the design method simply assumes the veneer carries its own seismic weight in the in-plane direction. This observation does provide a useful check though.

Table 3. Comparison of proposed brick veneer bracing ratings with demand loads from NZS 3604 for three single-storey building shapes

Building plan dimensions		Roof Weight	Percentage of load carried by brick veneer	Load to be carried by LTF bracing walls (BU's) *
Parallel to earthquake (m)	Perpendicular to earthquake (m)			
Building Number 1. Small building with rectagular plan shape (ratio of sides 2:1)				
14.14	7.07	Light	48.5%	268
7.07	14.14	Light	24.2%	394
14.14	7.07	Heavy	31.9%	538
7.07	14.14	Heavy	15.9%	664
Building Number 2. Square plan shaped building.				
12	12	Light	28.5%	535
12	12	Light	28.5%	535
12	12	Heavy	18.8%	924
12	12	Heavy	18.8%	924
Building Number 3. Large building with rectagular plan shape (ratio of sides 2:1)				
24	12	Light	28.5%	1070
12	24	Light	14.3%	1284
24	12	Heavy	18.8%	1848
12	24	Heavy	9.4%	2061

Legend: * Value shown is demand load minus the proposed design veneer resistance

4.4.6 Proposed brick veneer bracing rating for NZS 3604 two-storey buildings

It is proposed that a two-storey brick veneer building be considered as a single-storey brick veneer above the lower-storey veneer. Thus, the bracing rating for the upper storey is calculated as in Section 4.4.5. The lower storey can be treated similarly except H in Eqn 5 is now the height from the concrete floor to the eaves. These assumptions are shown to be conservative in the paragraph below, but this is desirable as it is considered that greater conservatism in two-storey design is justified (particularly for the lower storey).

The demand seismic shear forces on a two-storey veneer wall are shown in Figure 14., Table 4 used the values in this figure to give a comparison of the veneer resistance for the proposed design method and also the demand veneer seismic inertia shear force assumed in NZS 3604. If V1(Upper) is set = V1(Lower) then both the upper and lower-storey design shear resistances in the proposed method are only approximately two-thirds of the shear demand due to veneer self-weight imposed by NZS 3604 for in-plane veneer.

The NZS 3604 revision may need to prohibit two-storey veneer construction where the openings in the lower storey are too large or the piers too narrow or the openings in upper and lower storeys are located inappropriately with respect to each other. Suitable clauses to capture this have yet to be developed.

Table 4. Comparison of veneer shear resistance from the proposed design method and the demand veneer seismic inertia shear force assumed in NZS 3604

Location	Shear force assumed in proposed design method	Veneer seismic inertia force assumed by NZS 3604
Upper storey	0.5V1(Upper)	Approximately 0.8V1*
Lower storey	0.5(V1(Upper)+ V1(Lower))	V1(Upper)+ 0.5V1(Lower)

Legend. * Estimated using the redistribution of NZS 4203, Clause 4.8 (SNZ 1992)

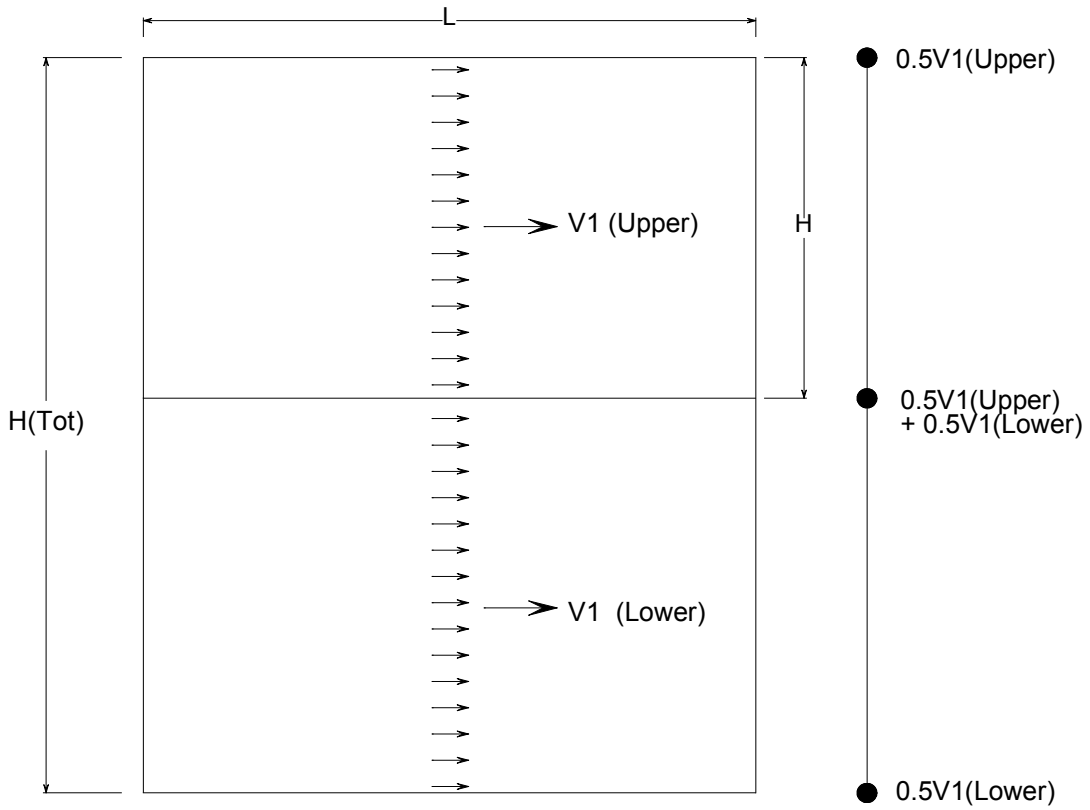

(a) Seismic loading on veneer wall

(b) Initial assumed shear forces before redistribution

Figure 14. Self-weight induced seismic shear forces on a two-storey veneer wall

4.4.7 Comparison between proposed design level of seismic shear and two-storey test result

The percent of openings in the two-storey side wall veneer was 21.5%.

The upper-storey design resistance for the veneer in Zone A is thus given by:

V1 = Cρ x (inter-storey height) x (total length of veneer) x (1-0.215)

= 0.241 x 2.2 x 2.42 x 13.46 x 0.785 = 13.56 kN.

The lower-storey design resistances for the veneer in Zone A are given by:

V1 = Cρ x (height of veneer to eaves) x (total length of veneer) x (1-0.215)

= 0.241 x 2.2 x 4.985 x 13.46 x 0.785 = 27.93 kN.

These are plotted in Figure 15 and Figure 16 for comparison with the measured shear carried by the upper and lower storey respectively of the two-storey brick veneer building. Clearly this design method is very conservative for the top storey and conservative for the bottom storey. The shear carried by the veneer in the test came from load transfer from the LTF via the brick tie, which is ignored in the proposed method.

4.4.8 Proposed changes in NZS 3604

It is proposed that NZS 3604 now allow two-storey brick veneer construction without requiring specific design.

Veneer bracing resistances may be derived with Eqn (9) where H is the upper-storey height for the upper-storey bracing rating and the height from concrete floor slab to the eaves for the lower-storey bracing rating.

The bracing resistances derived for two-storey veneer using the above method are compared with the bracing demand for Zone A in Table 5 for both earthquake directions on three buildings shapes and for both heavy and light roofs of 25˚ slope. The assumed upper-storey stud height was 2.4 m and the height from the slab to the eaves was assumed to be 5.1 m. The first building shape was the small standard building assumed by NZS 3604.

It can be seen that the percentage of load carried by the brick veneer is always less than 30% and decreases rapidly for more square buildings and larger buildings.

Table 5. Comparison of proposed brick veneer bracing ratings with demand loads for two-storey buildings from NZS 3604

(a) Upper storey

Building plan dimensions		Roof Weight	Percentage of load carried by brick veneer	Load to be carried by LTF bracing walls (BU's) *
Parallel to earthquake (m)	Perpendicular to earthquake (m)			
Building Number 1. Small building with rectagular plan shape (ratio of sides 2:1)				
14.14	7.07	Light	29.0%	618
7.07	14.14	Light	14.5%	744
14.14	7.07	Heavy	21.0%	948
7.07	14.14	Heavy	10.5%	1074
Building Number 2. Square plan shaped building.				
12	12	Light	17.1%	1039
12	12	Light	17.1%	1039
12	12	Heavy	12.4%	1514
12	12	Heavy	12.4%	1514
Building Number 3. Large building with rectagular plan shape (ratio of sides 2:1)				
24	12	Light	17.1%	2078
12	24	Light	8.5%	2292
24	12	Heavy	12.4%	3028
12	24	Heavy	6.2%	3242

(b) Lower storey

Building Number 1. Small building with rectagular plan shape (ratio of sides 2:1)				
14.14	7.07	Light	29.8%	1284
7.07	14.14	Light	14.9%	1557
14.14	7.07	Heavy	26.0%	1554
7.07	14.14	Heavy	13.0%	1826
Building Number 2. Square plan shaped building.				
12	12	Light	17.6%	2172
12	12	Light	17.6%	2172
12	12	Heavy	15.3%	2561
12	12	Heavy	15.3%	2561
Building Number 3. Large building with rectagular plan shape (ratio of sides 2:1)				
24	12	Light	17.6%	4344
12	24	Light	8.8%	4807
24	12	Heavy	15.3%	5122
12	24	Heavy	7.7%	5585

Legend: * Value shown is demand load minus the proposed design veneer resistance

Figure 15. Comparison of design shear resistance for the upper-storey veneer of the two-storey building and the applied load at the roof level

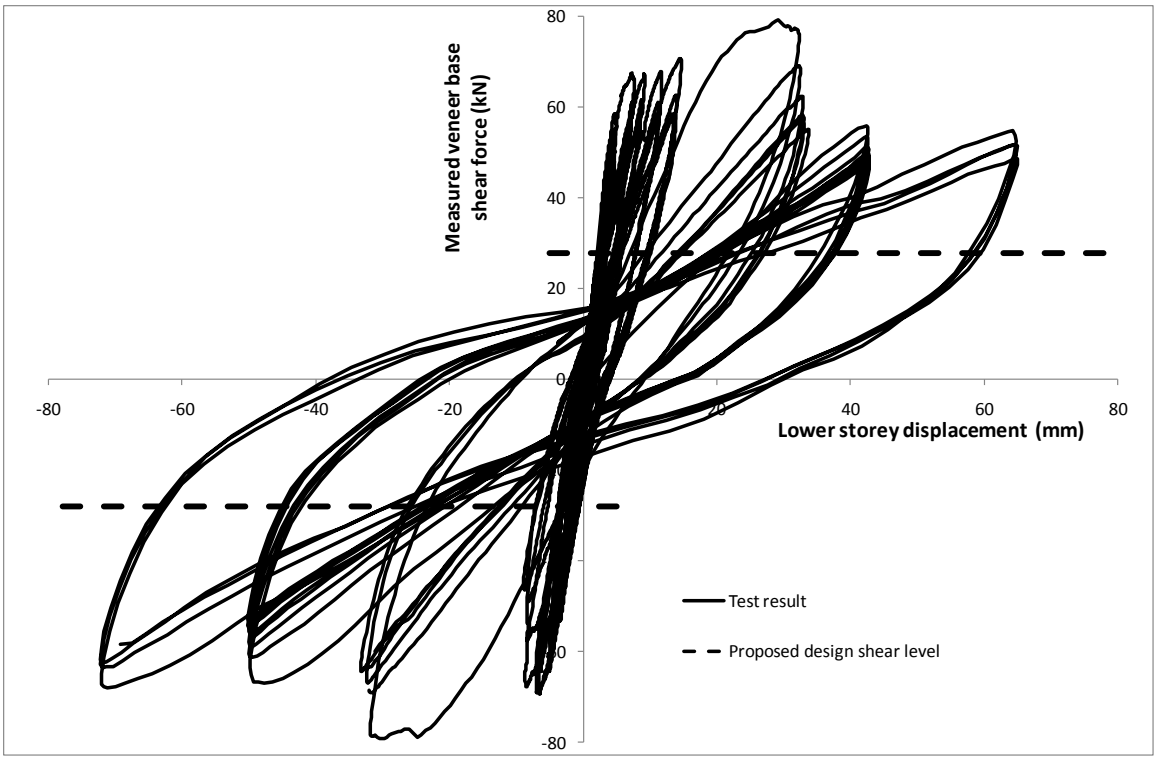

Figure 16. Comparison of design shear resistance for the lower-storey veneer of the two-storey building and the measured shear force at the bottom of the veneer

5. SUMMARY, CONCLUSIONS AND DISCUSSION

5.1 Testing undertaken

A two-storey brick veneer building with plan dimensions 6.7 x 3.9 m was cyclically racked in increasing displacements up to a roof displacement of ±143 mm and first floor displacement of ±69 mm. At the maximum displacements large cracks formed in the veneer and a few bricks near window edges fell. The veneer resisted large shear forces which peaked at first floor displacements of ±33 mm.

During subsequent demolition it was noted that no ties had cracked or ruptured and all ties were still firmly screwed to the LTF.

Initially the test was performed under load control with the applied force at the roof being twice that at the floor of the first storey. This complied with the force distribution assumed in the derivation of NZS 3604 earthquake demands. However, by the time the top-storey shear strength had been exceeded there was still little cracking in the bottom storey and the first floor displacement was low. Hence, to induce damage in the lower storey the loading was changed to deflection control with the displacement of the first floor being set to approximately half that at the roof.

Veneer cracks were carefully recorded at each test stage. Sometimes cracks which were clearly visible at peak load in one stage closed and could not be seen at peak loads in subsequent stages if other nearby cracks had formed.

Only a few veneer cracks occurred for top floor displacements up to ±30 mm and these were narrow at peak loads and closed to become invisible to the naked eye at unload, except that cracks in the top spandrel could still easily be seen.

The major deformation mechanism for top floor displacements up to ±46 mm was rocking of the upper-storey panels about cracks emanating from window corners. These were mainly horizontal cracks on Side 1 and diagonal cracks in the middle spandrel on Side 2. One vertical crack did occur in the middle spandrel. The horizontal cracks closed to be difficult to see at unload but the vertical and stepped cracks could sometimes be seen without difficulty. In the unload state the cracks in the top spandrel were most easily seen compared with other cracks. At this stage of the testing, the cracking in the lower storey was fine and difficult to detect even at peak loads.

At top floor displacements up to ±64 mm, damage was largely confined to the upper storey which is not surprising as the corresponding peak first floor deflection was only ±12 mm even though the veneer was carrying 69 kN in shear. The cracks in the lower storey veneer were still very fine.

The test regime then changed to deflection control. Subsequently, major and new cracks occurred mainly in the middle spandrel. Crushing at the bottom window corners occurred due to the high axial stress at these locations as the panels above rocked, pivoting at these corners.

Three bricks fell during the course of the testing and some bricks adjacent to the bottom of the bottom windows crushed but generally the veneer remained firmly attached to the framing. Vertical veneer cracks occurred near corners in the latter

stages of the tests but separation of side and end veneer did not occur. Cracks largely closed on unload but the residual crack width near the end of the testing would be unacceptable to a house owner. Some of the cracks at this stage cut across the bricks themselves rather than purely following the mortar beds. Consequently, the veneer would likely be condemned and subsequently demolished. All ties remained firmly attached to both brick mortar and the LTF at test completion.

Measurements of the slip of the veneer relative to the LTF, both in-plane and out-of-plane, are presented in this report. The in-plane slip was only approximately 20% of the LTF movement at the corresponding height. The out-of-plane movement of the veneer relative to the LTF was less than 3 mm along the sides. On the end walls the veneer tended to move away from the LTF (by a process of the 'L-shaped ties' straightening) but this was generally less than 6 mm.

Measured vertical movement of the veneer relative to the LTF is presented in this report. Values were generally more than the horizontal slip.

Measurements of total upward movement of the veneer were made at 128 locations for three stages of the test. These were used to plot panel rotations against height up the panel and these confirmed that much of these rotations occurred at the cracks emanating from the bottom corners of top windows. It was only in the latter stages of the test that panel rotations at the cracks emanating from the bottom corners of bottom windows were large. The rotations were integrated to give veneer horizontal deflections and this showed that most of the veneer displacement was due to rotation of the veneer rather than shear slip or other forms of deformation. Shear slip was observed along some upper-storey cracks in the latter stages of the test. Inspection showed that mortar dowels had been ground off in these locations.

It is concluded that two-storey brick veneer with construction similar to that tested could sustain design level in-plane displacements with only minor damage to the veneer. Only a few bricks are expected to fall at twice the design level displacements. The brick veneer will resist high in-plane seismic shear forces which will result in building displacements being far lower than design level displacements calculated ignoring the veneer shear stiffness contribution.

5.2 Previous work

Previous work at BRANZ (Thurston and Beattie 2008a, 2008b, 2008c) on buildings with single-storey brick veneer tied to LTF framing has shown that this type of construction has high resilience to both in-plane shaking and imposed seismic cyclic displacements. There was a good agreement between the shear load transferred to the veneer and predictions using a theory which used measured tie load versus displacement characteristics.

5.3 Comparison of test results and theory for two-storey construction

Two models for predicting the seismic in-plane resistance of the brick veneer building are discussed in Section 4.2 and 4.3 respectively. The most successful was a simplified model which gave reasonable predictions for the upper storey and was a little unconservative for the lower storey. This lack of conservatism here was attributed to diagonal cracking of the middle spandrel which was not considered in the model.

A recommended design veneer shear resistance, for use in NZS 3604, was developed in Section 4.4. The design method was shown to be very conservative relative to test results for both the two-storey building and a single-storey building tested previously but is still proposed for adoption as discussed in Section 5.4. A comparison of the proposed brick veneer DBR and the total building demand shear force for various building shapes showed that the maximum resistance provided by the veneer was 29% for single-storey buildings and 18% for two-storey buildings. The exceptions were for a small building of aspect ratio 2:1, where:

- For a single-storey building the ratio was 32% if there was a heavy roof and 49% if there was a light roof
- For a two-storey building the ratio was 26% if there was a heavy roof and 30% if there was a light roof.

5.4 Recommendations for changes to NZS 3604

Brick veneer is far more resilient to earthquake loads in buildings using modern construction materials and methods than was the case with historic construction. NZS 3604 can take advantage of this improvement of performance by allowing two-storey veneer construction within its scope and by attributing a bracing function to the veneer.

It is proposed that NZS 3604 now allow two-storey brick veneer construction without requiring specific design. However, the NZS 3604 revision may need to prohibit two-storey veneer construction where the openings in the lower storey are too large or the piers too narrow or the openings in upper and lower storeys are located inappropriately with respect to each other. Suitable clauses to capture this have yet to be developed.

A simple method to calculate the bracing resistance provided by brick veneer was derived for both single and two-storey buildings. It is proposed that this is incorporated into the next revision of NZS 3604. The main assumption was that the veneer may **only** carry the seismic in-plane inertia load attributed to it by NZS 3604. The proposed DBR is:

$$DBR = KxHxL \quad \ldots (10)$$

Where:

H is the storey height in metres for single-storey buildings or the upper of two storeys and H = the height from the concrete floor slab to the eaves for the lower storey bracing
L is the wall length in metres
K is given in Table 2.

It is intended that this method be only applicable to brick veneer of similar construction to that tested, namely:

Required veneer features

- The mortar has a compressive strength of at least 12.5 MPa
- The bricks have a height to length ratio no greater than 0.5

- The bricks have full depth holes comprising not less than 12% of the horizontal cross-section of the brick and having a minimum dimension of 20 mm.

6. REFERENCES

MonierBrick. 2006. *MonierBrick Two Storey Building System – Design Note C1.*

MonierBrick. 2008. *MonierBrick Steel-less Lintels – Design Note A7.*

Okail HO, Shing PB, Klingner RE and McGinley WM. 2008. 'Seismic Performance of Clay Masonry Veneer'. *Proceedings of the 14th World Conference on Earthquake Engineering*. Beijing, China, 12-17 October 2008.

Shelton RH. 2007. 'The Engineering Basis of NZS 3604'. BRANZ *Study Report 168*. BRANZ Ltd, Judgeford, New Zealand.

Shing. 2008. Personal communication.

Standards Australia/Standards New Zealand. 2000. AS/NZS 2699.1. *Built-in Components for Masonry Construction – Part 1: Wall Ties.* SA, Sydney, Australia and SNZ, Wellington, New Zealand.

Standards New Zealand. 1986. NZS 3112: Part 2 *Code of Practice for General Structural Design and Design Loadings for Buildings*. SNZ, Wellington, New Zealand.

Standards New Zealand. 1992. NZS 4203 *Code of Practice for General Structural Design and Design Loadings for Buildings*. SNZ, Wellington, New Zealand.

Standards New Zealand. 1999. NZS 3604 *Timber-framed Buildings*. SNZ, Wellington, New Zealand.

Standards New Zealand. 2001. NZS 4210 *Masonry Construction: Materials and Workmanship.* SNZ, Wellington, New Zealand.

Thurston SJ and Beattie GJ. 2008a. 'Seismic Performance of Brick Veneer Houses. Phase 1. Cyclic and Elemental Testing of Clay Brick Veneer Construction'. BRANZ *Study Report 189*. BRANZ Ltd, Judgeford, New Zealand.

Thurston SJ and Beattie GJ. 2008b. 'Seismic Performance of Brick Veneer Houses. Phase 2. Shake Table Tests on a Clay Brick Veneer Room'. BRANZ *Study Report 190*. BRANZ Ltd, Judgeford, New Zealand.

Thurston SJ and Beattie GJ. 2008c. *Seismic Performance of Brick Veneer Houses.* Proceedings of the 2008 NZSEE Conference, Wairakei, New Zealand.

Thurston SJ and Beattie GJ. 2008d. 'Seismic Performance of Brick Veneer Houses. Phase 3. Shake Table Tests on a Concrete Brick Veneer Room'. BRANZ *Study Report 191*. BRANZ Ltd, Judgeford, New Zealand.

APPENDIX A CYCLIC TESTING OF ROOM 1

A.1 Construction

The test building is shown in Figure 3 and Figure 4. It was a two-storey, single-room brick veneer construction with each storey having a nominal 2.4 m stud height. It had plasterboard-lined light timber-framed (LTF) walls, brick veneer on all four sides and a timber-framed plasterboard-lined ceiling. Figure 18 defines the labelling given to the corners, sides and ends. Figure 19 and Figure 20 provide cross-sectional views. Figure 21 to Figure 23 provide drawing elevations of the veneer walls which give the panel and window labelling used. For instance in Figure 21 the brickwork to the Left Hand Side (LHS) of the windows is referred to as Panel A and this consists of a lower panel (Panel AL) and an upper panel (Panel AU). The LHS vertical edge of Panel A is referred to as A1 and the Right Hand Side (RHS) as A2; similarly for Panels B and C.

On Side 2 (Figure 22) it is a little more complicated as the windows are offset. The top edges of the windows are labelled F3, G3, G4 and H3 as shown.

The brickwork above the top windows is referred to as the 'top spandrel', between the two window levels as the 'middle spandrel' and below the bottom windows as the 'bottom spandrel'.

Construction details are given below:

General:

- The outside dimensions of the veneer were: 6.73 m long x 3.93 m wide by 5.5 m high.
- The walls incorporated window and door openings as shown in Figure 21 to Figure 23. Glazed aluminium windows were used in window openings S1A (Figure 21), S2A and S2B (Figure 22). These were removed part-way through Phase G of this project as discussed later.
- The LTF wall framing was constructed from 90 x 45 mm kiln-dried radiata pine timber with a maximum stud spacing of 600 mm.
- The timber wall framing and the roof were essentially the same as described in the Phase 1 study report (Thurston and Beattie 2008a) and only brief details will be given here. The first floor was constructed from 190 x 45 timber joists spanning in the short direction and blocked at the ends and mid-span. The flooring was 20 mm particle board. The roof of the building was similar but consisted of 140 x 45 mm joists and the top cladding was 10 mm medium density fibreboard (MDF). A 13 mm standard plasterboard ceiling was fixed as per the manufacturer's instructions at both levels, with all joints being paper-taped and stopped.
- The plasterboard wall linings were only lightly fixed to the timber framing. In the upper storey the lining was fixed with 32 mm x 6 g drywall screws at the

sheet corners and then at 600 mm centres around the perimeter of each sheet. The wall/ceiling junction was paper-taped and stopped but the vertical joints, including at the room corners, were not. The same construction was used in the lower storey except that the fixings were at 300 mm centres.

Brickwork:

- The veneer consisted of 58 courses of clay bricks placed in a running bond pattern. Hot-dipped galvanised steel ties were placed on top of the 2nd, 6th, 10th, 14th … 50th, 54th and 57th level of bricks and were screwed to the timber studs. The bricks were interlocked at the corners as shown in Figure 25. The top of the brickwork stopped 240 mm below the roof.
- Details of the bricks, brick ties and mortar are summarised in Section 1.5.
- Lintel supports are detailed in Figure 21 to Figure 23. All windows having brickwork lintels above were spanned by 60 x 60 x 6 mm mild steel angles with 100 mm seating as specified in Section 11.7.6 of NZS 3604 except:
  - A 65 x 10 mm steel flat lintel bar spanned the door in End 1, called Door E1A in Figure 23.
  - Door E1B and Window E2B (Figure 23) did not have brickwork above the opening.
  - Window S1A (Figure 21) did not use a steel lintel but instead used soldier bricks above the window with two ties in every perpend. (Note: MonierBricks only specifies two ties in every second perpend (MonierBricks 2008). As no window frame was used in this opening, an LTF support was used as shown in Figure 3 to simulate the support a window would provide should the brick veneer courses above loosen.
  - Window S2D (Figure 21) did not use a steel lintel but instead used soldier bricks above the window with two ties in every second perpend (MonierBricks 2008).
  - Window S2C (Figure 21) did not use a steel lintel but instead used one tie in every perpend for two layers in the brickwork of normal running bond (MonierBricks 2008).

Foundations:

- The LTF was constructed on a timber foundation beam bolted to the laboratory strong floor, as shown in Figure 18 to Figure 20 and Figure 24.
- The brick veneer was constructed on a 250 universal column (UC) steel ring beam laid on its side. The top portion of the UC was filled with concrete to provide a bed for the brick veneer. The ring beam was supported on rollers as shown in Figure 19 and Figure 20 which enabled it, when filled with concrete, to be rolled on the laboratory strong-floor with a horizontal force of 0.3 kN. However, horizontal movement of the ring beam was precluded during the test by using horizontal ring-beam restraint elements that incorporated load cells as shown in Figure 18 and Figure 20.

A.2 Test method

The test process was to horizontally displace the roof and also the first floor to separate deflection regimes to simulate the motion expected in large earthquakes. This was achieved by using a computer-controlled actuator at each of these two levels (as shown in Figure 20). Each reacted against a strong wall. The actuators were located at building mid-width.

The roof was displaced to increasing displacements in each of nine test stages referred to as Stage A to Stage I. Details are summarised in Table 6. For test Stages A to F the ratio of load applied at the roof to load applied at the first floor was 2.0. This was based on the loading distribution adopted by NZS 3604 (Shelton 2007). However, as the bottom storey was significantly stiffer and stronger than the top storey, when the upper storey reached peak lateral strength no greater shear load could be imposed into the lower storey. The displacement of the lower storey at this stage was relatively small (approximately ±12 mm). Subsequently the actuator at the first floor level was controlled to move approximately half the displacement of the top actuator. Full details are given in Table 6.

Some of the applied load was transferred to the brick veneer by the brick ties and a small portion by the window frames between the LTF and veneer. The horizontal load resisted by the brick veneer was measured using the load cells in the ring beam restraint elements, as shown in Figure 18.

After Stage D the upper-storey horizontal plasterboard joints cracked at the junction between LTF walls and ceiling and also the joints at the junctions of the walls. After Stage F the upper-storey lining fixings had sufficiently damaged the surrounding plasterboard that the bracing resistance provided by the plasterboard had largely dissipated. After completion of Stage G the lining in both storeys had partially fallen.

A.3 Instrumentation

Panel locations referred to in the description below are defined in Figure 21 to Figure 23. The linear potentiometers were read continuously whereas the manual measurements were only taken at some peak loads.

The in-plane displacement of the timber framing relative to the veneer was measured to determine whether the ties had been extended close to their limit in the tests and for calibration of any computer modelling. This was measured using linear potentiometers at four places at the top of the side wall veneer as shown in Figure 26 and four places at the top of the bottom-storey window level by cutting holes in the plasterboard lining as shown in Figure 27. In addition, a ruler was glued to the veneer at the sill of upper-storey window openings. These gauges are summarised in Table 7 and the window and panel labels referred to are defined in Figure 21 and Figure 22.

Table 6. Measured floor displacements, applied and resisted loads

Stage	Number of cycles	Nominal displace. of the roof of the building (mm)	Bottom horizontal Restraints			Applied loads			Measured floor horizontal displacements	
			Side1 Load (kN)	Side2 Load (kN)	Total Load (kN)	Roof load cell (kN)	First floor load cell (kN)	Total = Lower Storey Shear Load (kN)	Roof (mm)	First floor (mm)
A+		+8mm	18.4	18.4	36.2	35.7	24.6	54.6	8.1	3.5
A-	3	-8mm	-18.1	-17.3	-35.4	-34.1	-16.7	-47.0	-8.0	-2.5
Ave.			18.3	17.8	35.8	34.9	20.6	50.8	8.0	3.0
B+		+14mm	29.5	29.1	58.6	52.2	31.5	81.1	14.1	4.9
B-	3	-14mm	-25.3	-28.0	-53.3	-48.3	-21.3	-69.3	-14.2	-3.5
Ave.			27.4	28.6	55.9	50.2	26.4	75.2	14.2	4.2
C+		+24mm	31.3	37.2	67.6	60.9	37.4	94.9	23.7	7.6
C-	3	-24mm	-29.7	-34.7	-64.4	-56.9	-25.8	-81.6	-23.9	-5.1
Ave.			30.5	35.9	66.0	58.9	31.6	88.2	23.8	6.4
D+		+35mm	28.2	39.2	67.4	61.4	37.9	95.6	34.3	9.2
D-	3	-35mm	-31.9	-37.4	-69.3	-61.5	-28.8	-87.8	-34.7	-6.6
Ave.			30.1	38.3	68.4	61.5	33.3	91.7	34.5	7.9
E+		+46mm	28.9	39.2	68.1	62.1	35.9	95.7	44.8	11.6
E-	3	-46mm	-33.5	-35.8	-69.0	-62.5	-32.0	-88.5	-46.8	-7.1
Ave.			31.2	37.5	68.5	62.3	33.9	92.1	45.8	9.4
F+		+64mm	31.7	39.2	70.8	63.7	37.9	100.7	65.5	14.6
F-	3	-64mm	-33.9	-33.9	-67.8	-61.0	-28.5	-88.2	-63.8	-9.0
Ave.			32.8	36.5	69.3	62.3	33.2	94.4	64.7	11.8
G+		+82mm	38.7	41.1	79.3	42.2	84.7	123.1	77.2	33.0
G-	6	-82mm	-42.2	-38.4	-79.2	-41.4	-74.4	-111.3	-84.6	-33.0
Ave.			40.5	39.8	79.2	41.8	79.6	117.2	80.9	33.0
H+		+110mm	29.2	26.8	55.9	41.9	67.3	86.9	109.5	42.7
H-	8	-110mm	-35.1	-31.9	-66.8	-37.4	-68.3	-96.2	-109.4	-50.1
Ave.			32.2	29.3	61.4	39.7	67.8	91.5	109.5	46.4
I+		+143mm	26.6	28.5	54.8	21.1	64.9	83.9	142.8	64.9
I-	4	-143mm	-36.4	-31.6	-68.0	-29.8	-59.0	-86.2	-142.6	-72.2
Ave.			31.5	30.0	61.4	25.4	61.9	85.1	142.7	68.6

Table 7. Horizontal displacement of LTF relative to the veneer

No	Panel	Location of gauge	Averaged peak displacement (mm)				
			Stage B	Stage D	Stage F	Stage G	Stage H
1	A2	Top of veneer	4.20	8.20	10.24		
2	B2	Top of veneer	4.64	6.01	7.84	10.91	16.04
3	F2	Top of veneer	5.75	11.68	15.93	16.01	26.22
4	G2	Top of veneer	3.89	4.15	5.79		
5	A1	Top of lower storey window	0.31	0.62	1.46	3.41	
6	B1	Top of lower storey window	0.57	1.45	2.83	5.85	8.37
7	F1	Top of lower storey window	0.45	1.16	2.46	6.07	10.11
8	G1	Top of lower storey window	0.63	1.76	3.09	7.04	9.42
9		Mid-length of sill of window S1D		4.50	10.00	16.00	
10		Mid-length of sill of window S1C		1.50	7.00	13.00	
11		Mid-length of sill of window S2D		5.50	7.50	14.50	
12		Mid-length of sill of window S2C		4.00	4.50	12.50	

The out-of-plane displacement of the brickwork relative to the timber framing was measured using potentiometers at four places on the end walls as shown in Figure 28 and in 26 locations using a ruler between the veneer and LTF. This movement was considered to be important because:

- The ties in the end walls help resist the side wall veneer from sliding and large movement would indicate break down of this function.
- The side veneer can move closer to the LTF allowing more in-plane differential movement between veneer and LTF but this movement is resisted by the end veneer. If the veneer panels can move closer to the LTF when they rock, the uplift resistance to the rocking motion from the ties will be less.

It was expected that much of the horizontal displacement of the veneer would occur by rocking motion which would lift the veneer vertically. To investigate this, and for calibration of computer models, the vertical deflection of the veneer relative to the LTF was directly measured with potentiometers at four locations as shown in Figure 29 and in 13 locations using a ruler (glued to the veneer) and the LTF. These gauges are summarised in Table 8. Manual measurements are shown to an accuracy of 1 mm while the potentiometer measurements are shown to an accuracy of two decimal places.

The horizontal displacement of the building roof and first floor relative to the ground was recorded at both actuator loading points.

To measure brickwork crack widths a specially made 6 m long aluminium ruler was used to measure vertical changes in length between lines drawn on the brickwork using the arrangement shown in Figure 30. This ruler pivoted on a bottom rod. It was fixed to the veneer near the base using threaded rod glued into the veneer. The operator read the height of the scratch marks while climbing a ladder and initially recorded the information on a Dictaphone before transferring it to data sheets.

The following forces were measured with load cells:

- Horizontal load in the brick veneer via the horizontal ring beam restraint elements shown in Figure 18 and Figure 20.
- The total load applied at each actuator using the load cell in the actuator shown in Figure 20.

Table 8. Vertical displacement of LTF relative to the veneer

No	Panel	Location of gauge		Peak Uplift (mm)				
				Stage B	Stage C	Stage D	Stage F	Stage G
(a) Vertical movement of veneer side walls								
1	G3	Top of veneer	Max			9	9	17
			Min			3	3	11
2	G4	Top of veneer	Max			7	15	10
			Min			1	5	4
3	C1	Top of veneer	Max			15	32	33
			Min			8	18	24
4	C2	Top of veneer	Max			5	11	32
			Min			4	6	8
5	A1	Top of veneer	Max			5	13	15
			Min			5	8	9
6	A2	Top of veneer	Max			12	26	36
			Min			8	13	21
7	B1	Top of veneer	Max	2.28	9.35	17.56	26.14	
			Min	0.21	0.30	-0.12	5.56	
8	B2	Top of veneer	Max	2.12	7.01	10.77	23.04	
			Min	0.38	0.38	-0.10	4.93	
9	F1	Top of veneer	Max	0.87	1.10	1.33	8.04	24.00
			Min	-0.54	-0.51	-1.01	-0.82	-1.12
10	H2	Top of veneer	Max	0.91	2.50	4.71	7.36	16.62
			Min	-0.02	0.09	-0.02	0.35	-0.37
11	F2	Top of veneer	Max			15	31	36
			Min			4	5	19
12		Mid-length of sill of window S2C	Max			1	2	6
			Min			-1	2	6
(b) Vertical movement of veneer on veneer end walls								
13	J3	Bottom corner of upper storey door	Max			3	2	4
			Min			0	0	3
14	K3	Bottom corner of upper storey door	Max			3	-1	5
			Min			0	0	2
15	J3	Very top of veneer	Max			8	14	20
			Min			5	6	9
16	K3	Very top of veneer	Max			4	16	17
			Min			5	8	12

A.4 Test results

A.4.1 Hysteresis loops for load in brick veneer

A plot of the upper-storey shear force versus upper-storey displacement is shown in Figure 31. Note that the upper-storey shear load is taken as the load applied at the roof. This would have been partially resisted by the lined LTF. As the upper-storey lining was only screwed at 600 mm centres and vertical joints were not stopped, the upper-storey LTF bracing is expected to be low, particularly at large displacements when the lining fixings had effectively failed.

The backbone curve in Figure 31 is approximately a trilinear shape having an initial elastic portion to a yield force of 60 kN at 10 mm deflection. After a flat yield plateau to approximately 50 mm, the resistance drops.

A plot of the lower-storey shear force (i.e. force applied at roof plus first floor) versus displacement of the first floor is shown in Figure 32.

Note that in loading Stages A to F the shear force in the lower storey was limited to 1.5 times the shear force in the top storey. This only induced an average of approximately 12 mm lower-storey displacement. Subsequent load stages were to predetermined lower-storey displacements which resulted in higher lower-

storey peak shear forces. The peak lower-storey shear load in Stage G averaged 117 kN at 33 mm displacement which was 88% higher than the peak shear load resisted by the upper storey. Subsequently the lateral load resistance of the building dropped.

The windows in the lower storey were removed prior to Stage H. Subsequent cycles showed a small drop off in lower-storey shear load which is attributed to this construction change (see Figure 32).

A plot of the total horizontal load recorded by the ring beam restraints (i.e. transferred through the brick veneer) versus first floor displacement is shown in Figure 33. From a comparison with Figure 32 it can be seen that the veneer is carrying approximately two-thirds of the applied lateral load.

A.4.2 Brick veneer crack pattern

Cracking detected at peak loads was marked onto prepared drawings similar to Figure 21 to Figure 23 except every 5th mortar line was labelled. These labels were also marked with felt pen onto the bricks at each building corner. This enabled the observed veneer cracks to be accurately marked on the drawings. These cracks have been redrawn in Figure 34 to Figure 41 for the various stages of test. Sometimes cracks which were clearly visible at peak load in one stage closed and could not be seen at peak loads in subsequent stages if other nearby cracks had formed.

Only a few veneer cracks occurred in test Stages B and C as shown in Figure 34 and Figure 37. These were narrow at peak loads and closed to become invisible to the naked eye at unload except cracks in the top spandrels could easily be seen after completion of Stage C.

Cracks in Stages D and E were sufficiently wide at peak loads to be seen in photographs and the most significant are shown in Figure 48 to Figure 52 for cracking above the top windows. General cracking is shown in Figure 55 to Figure 64 for cracking in Stage D and Figure 63 to Figure 70 for Stage E. The horizontal cracks closed and were difficult to see at unload but the vertical and stepped cracks could sometimes be seen without difficulty. Figure 71 to Figure 73 show the most significant of these. The cracks above all upper-storey lintels were most easily seen in the unload state.

The major mechanism for Stages A to E was rocking of the upper-storey panels about cracks which emanated from window corners. These were mainly horizontal cracks on Side 1 (Figure 55, Figure 56, Figure 63 and Figure 64) and diagonal cracks in the middle spandrel on Side 2 (the most significant being Figure 67 and Figure 68 for Panel F although Figure 69 and Figure 70 are other examples). A vertical crack did occur in the middle spandrel at Panel A of Side 1 under pull load in Stage E. The cracking in the lower storey (shown in Figure 35 and Figure 38) was fine and difficult to detect even at peak loads. Cracking above the top storey lintels at peak loads was wide in Stages D and E, as noted above.

At peak loads in Stage F the veneer cracks were sufficiently wide to be able to be seen in total building width photographs (e.g. Figure 74 and Figure 75 for Side 1 at peak push and pull respectively). Corresponding photographs for Side 2 are

Figure 84 and Figure 85. It can be seen that damage is largely confined to the upper storey which is not surprising as the peak lower-storey deflection was only 12 mm, even though the veneer carried 69 kN in shear which was 73% of the applied load. Although cracks did occur in the lower-storey veneer (Figure 34 to Figure 41), the cracks were very fine and cannot be seen in the photographs. Close-up photographs of the veneer cracking in Stage F are shown in Figure 76 to Figure 83 for Side 1 and Figure 84 to Figure 88 for Side 2. Figure 89 shows the cracking in End 2. Note the vertical cracks near Corner 3.

In Stage G the test regime changed to deflection control to enable greater lower-storey deflections to be imposed. Figure 90 and Figure 91 show the cracking in Side 1 at peak push and pull loads respectively. Major cracks occurred mainly in the middle spandrel, as shown in Figure 92 and Figure 93. Crushing at the bottom window corners occurred as shown in Figure 94 and Figure 95 due to the high axial stress at these locations as the panels above rocked and pivoted at these corners. Figure 96 and Figure 97 show the cracking in Side 2 at peak push and pull loads respectively. It can be seen that the most severe cracking is in the middle spandrels and the brickwork above pivot points on these spandrel cracks.

Figure 98 and Figure 99 show the cracking in Side 1 and Figure 101 and Figure 103 show the cracking in Side 2 from Stage I loading. Damage is severe in all spandrels and from cracks emanating from all window corners. However, only a few isolated bricks fell and the panels showed little cracking over the depth of the windows.

At test completion it was concluded that generally the veneer remained firmly attached to the framing. Vertical veneer cracks occurred near corners in the latter stages of the tests but separation of side and end veneer did not occur. Cracks largely closed on unload but the residual crack width near the end of the testing would be unacceptable to a house owner. Some of the cracks at this stage cut across the bricks themselves rather than purely following the mortar beds. Consequently, the veneer would likely be condemned and subsequently demolished. All ties remained firmly attached to both brick mortar and the LTF at test completion.

A.4.3 Movement of the bases of LTF walls and base beams

Uplift of both the LTF wall and base beam was measured at the edges of wall openings and room corners and horizontal slip was measured at mid-length of wall elements. The maximum movement monitored did not exceed 1 mm.

A.4.4 Horizontal movement of brick veneer relative to LTF wall

Table 7 summarises the measured horizontal movement of the brick veneer relative to the LTF. The values shown have been averaged over the peak push and pull measurements for each stage of loading. Measurements No 5-8 in Table 7 were by ruler and the rest were continually recorded by a displacement gauge.

The horizontal differential movement tends to increase with height up the veneer. The differential movement was small relative to the adjacent LTF overall movement (as summarised in Table 6) showing that brickwork must have moved horizontally thereby reducing the demand deformations on the ties.

Note, where no value is given in Table 7 then either no reading was taken or the values had become unreliable (e.g. the gauge probe had moved off the target).

Shear slip was observed along the some upper-storey cracks emanating from the window sill level in Stages F and later. Inspection showed that mortar dowels had been ground off in these locations (see Figure 1).

A.4.5 Vertical movement of brick veneer relative to LTF wall

Table 8 summarises the measured vertical movement of the brick veneer relative to the LTF at the locations shown. Maximum and minimum values are given for the stage of loading. The minimum values are usually positive showing that cracks have not fully closed. The maximum values approximately represent the accumulated crack widths over the height of the veneer to the point being measured.

Measurements by ruler are shown to the nearest millimetre whereas measurements by displacement gauge are shown to two decimal places.

A.4.6 Absolute vertical movement of brick veneer

The measured vertical movement of the brick veneer as measured by the 6 m long aluminium rule shown in Figure 30 is summarised in Table 9. Movement is summarised for eight heights up the veneer for plan locations denoted in Figure 21 and Figure 22. If each panel rocks over like a cantilever, one vertical edge will be in tension and would be expected to lengthen and the other will be in compression and may also lengthen, but to a much lesser degree if the cracks do not fully close. Whether a particular edge is in ‘tension’ or ‘compression’ will depend on its location and whether it is a push or pull load. The results in Table 9 identify whether the measurements are for a ‘tension’ or ‘compression’ edge.

The difference between adjacent readings in a row of the table indicates the magnitude of the crack width should a crack occur in the intermediate height. Thus, in Stage D at location B1 a crack width of 17 mm (=17-0) width occurred between 3.053 and 3.569 m height. This height range included the horizontal crack from the bottom of the upper-storey window. In Stage G this had increased to 24 mm (=30-6) width. In Stage G a crack of 20 mm (=21-1) had opened at the bottom of the bottom-storey window at F2 and 16 mm at C1.

As expected, uplift increases from Stage D to F to G, particularly in the lower storey, as cracking was not observed here in the early stages. The only observed uplift of the veneer from the concrete foundation on the side walls was at A1 and the measurements indicate this reached 6 mm in Stage G.

The uplifts averaged over the six tension locations (and also the six compression locations) are plotted in Figure 42 for Stage D, F and G. It can be seen that most of the uplift for Stages D and F occurs between 3.05 and 3.57 m (i.e. encapsulates the horizontal cracks from the bottom of the upper-storey windows). However, for Stage G much of the uplift also occurs below 0.99 m (i.e. encapsulates the horizontal cracks from the bottom of the bottom-storey windows).

It is hypothesised that most of the veneer movement is due to rocking at cracks. At each level, panel rotation can be calculated from the values in Table 9 taking the difference in uplift between the tension and compression end of a panel and

dividing by the horizontal distance between the measurement points. Figure 43 provides a plot of the average rotation from the push and pull over all panels. As expected, most of the rotation occurs at the cracks emanating from the bottom corners of the top windows for Stages D and F but there is also a significant rotation at the cracks from the bottom window corners in Stage G.

The rotations can be integrated up the height of the veneer to produce deflections. Averaged results are given in Figure 44. These are compared with the LTF deflection profiles in Figure 45 to Figure 47. Also shown in these figures are the measured in-plane deflections plotted from the LTF deflection line, as shown by the double-headed arrows. If the veneer movement was purely due to rotation about cracks the dots would coincide with the calculated veneer deflection lines. The difference is due to measurement error, brick shear slippage, in-plane deflection of the studs and differences between actuator deflection and the deflection of wall top plates. Some horizontal slippage was noted in the latter tests at the horizontal cracks emanating from the bottom of the upper-storey windows. However, in general most of the veneer displacement was due to rotation of the veneer above on veneer cracks.

A.4.7 Out-of-plane movement of brick veneer relative to LTF wall

Table 10 summarises the averaged measured out-of-plane movement of the brick veneer relative to the LTF at peak loads for three stages of the test. Values are positive if the veneer has moved away from the LTF – by a process of the 'L-shaped tie' straightening as shown in Figure 17. No slip of the tie in the mortar or tie connection failure was observed in the tests or could be seen after dismantling of the veneer at test completion.

Table 9. Upward movement of veneer

Peak Push Tension end	Stage	Location up scratch mark up height of veneer (m)							
		0.172	0.473	0.989	1.677	2.279	3.053	3.569	4.773
Location A1	D	1	0	0	1	1	5	9	9
	F	3	2	2	2	2	14	22	20
	G	7	6	6	7	7	14	20	20
Location B1	D	0	1	1	0	0	0	17	18
	F	0	1	5	4	4	4	36	37
	G	0	0	7	6	6	6	30	32
Location C1	D	1	0	1	1	0	1	15	18
	F	0	0	3	3	2	3	28	32
	G	0	0	16	16	15	17	25	29
Location F2	D	0	2	3	2	4	14	14	14
	F	0	4	4	4	6	25	27	27
	G	1	21	21	21	23	28	30	29
Location F3	D					2	2	20	20
	F					4	4	40	39
	G					17	20	41	42
Location G2	D	0	1	2	2	1			
	F	1	0	3	3	3			
	G	0	0	7	9	7			
Location G4	D					1	3	11	11
	F					3	5	20	21
	G					6	0	23	22
Location H2	D	0	1	1	0	1	8	8	0
	F	0	0	1	1	1	17	18	16
	G	0	4	4	4	4	22	23	23
Averages	D	0.3	0.8	1.3	1.0	1.3	4.7	13.4	12.9
	F	0.7	1.2	3.0	2.8	3.1	10.3	27.3	27.4
	G	1.3	5.2	10.2	10.5	10.6	15.3	27.4	28.1

Peak Pull Comp. end	Stage	Location up scratch mark up height of veneer (m)							
		0.172	0.473	0.989	1.677	2.279	3.053	3.569	4.773
Location A1	D	1	0	0	1	0	0	1	0
	F	1	0	-1	1	0	2	4	3
	G	1	0	0	1	1	3	6	
Location B1	D	0	0	0	-1	0	0	0	5
	F	0	0	0	0	0	0	-1	8
	G	-1	-1	-2	-1	0	0	0	
Location C1	D	0	0	1	0	0	1	0	8
	F	0	0	0	0	1	2	4	9
	G	0	0	0	1	0	4	6	
Location F2	D	1	0	1	0	2	3	3	3
	F	0	-1	0	0	2	9	10	10
	G	0	-1	0	0	4	21	22	
Location F3	D					1	1	2	2
	F					2	5	6	5
	G					8	17	17	
Location G2	D	0	0	0	0	0			
	F	0	-1	-1	0	0			
	G	0	0	-1	-1	0			
Location G4	D					0	0	1	1
	F					0	-1	5	5
	G					0	0	2	
Location H2	D	-1	0	-1	0	0	0	1	1
	F	-1	0	-1	0	1	1	2	2
	G	0	0	1	1	1	5	5	
Averages	D	0.2	0.0	0.2	0.0	0.4	0.7	1.1	2.9
	F	0.0	-0.3	-0.5	0.2	0.8	2.6	4.3	6.0
	G	0.2	-0.3	-0.2	0.0	2.0	7.0	7.9	

Table **9 … Continued**

Peak Pull Tension end	Stage	Location up scratch mark up height of veneer (m)							
		0.172	0.473	0.989	1.677	2.279	3.053	3.569	4.773
Location A2	D	1	1	2	1	0	1	6	17
	F	1	3	4	4	3	4	26	26
	G	0	18	19	19	18	19	36	
Location B2	D	0	0	1	2	0	0	16	18
	F	0	0	1	2	0	0	30	38
	G	-1	0	9	10	10	10	24	
Location C2	D	0	1	1	1	0	0	8	5
	F	0	0	1	1	1	2	13	16
	G	2	4	4	4	4	7	13	
Location F1	D	2	2	0	1	0	3	3	5
	F	1	1	1	1	1	4	3	19
	G	6	6	5	6	5	9	10	
Location G1	D	0	1	1	1	1	1	0	0
	F	-2	-1	2	4	3	2	0	0
	G	-2	-1	13	14	14	14	0	
Location G3	D				1	2	1	9	8
	F				2	2	2	12	10
	G				5	7	14	22	
Location H1	D	0	2	2	3	3	0	0	0
	F	0	3	4	4	4	0	0	0
	G	-1	-1	14	16	15	0	0	
Location H3	D					3	12	12	13
	F					3	24	24	26
	G					12	32	32	
Averages	D	0.6	1.0	1.0	1.2	0.2	0.8	6.8	8.3
	F	0.4	1.0	2.2	2.7	2.0	2.0	12.0	16.5
	G	1.2	4.3	10.7	11.5	11.0	9.8	13.8	

Peak Push Comp. end	Stage	Location up scratch mark up height of veneer (m)							
		0.172	0.473	0.989	1.677	2.279	3.053	3.569	4.773
Location A2	D	1	1	1	0	1	1	2	3
	F	0	0	0	0	2	3	3	5
	G	0	0	0	0	3	3	2	8
Location B2	D	0	0	1	1	-1	1	1	1
	F	0	0	0	1	-2	3	4	12
	G	0	0	0	1	3	4	5	20
Location C2	D	0	0	1	0	0	0	0	-1
	F	0	0	1	0	0	0	1	0
	G	1	1	1	1	1	2	3	5
Location F1	D	0	0	-1	0	-1	-1	0	0
	F	0	-1	-1	0	0	1	-1	1
	G	1	0	0	0	0	1	1	2
Location G1	D	-1	1	1	0	2	2		
	F	0	1	1	0	4	4		
	G	-2	-1	0	1	4	4		
Location G3	D				2	1	2	1	3
	F				3	5	4	2	8
	G				7	7	14	1	12
Location H1	D	-1	-1	-1	1	2			
	F	0	0	0	1	2			
	G	-1	-1	0	1	2			
Location H3	D					2	1	1	2
	F					2	2	2	3
	G					3	5	5	7
Averages	D	0.2	0.3	0.7	0.2	0.2	0.5	0.6	0.4
	F	0.0	0.0	0.2	0.3	1.0	2.2	1.8	4.5
	G	0.2	-0.2	0.2	0.7	2.2	2.8	2.8	8.8

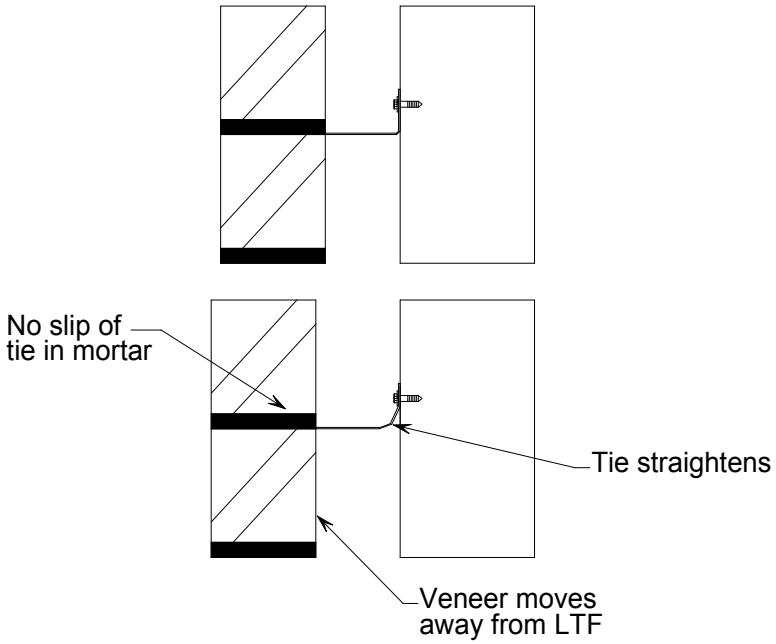

Figure 17. Tie straightening allows brick veneer to move away from LTF

(a) Out-of-plane movement measured at end walls.

When the LTF floor diaphragm was moved away from a veneer end wall this tended to put the tie in the end wall into tension. Peak displacements measured for this situation were categorised as 'tension' movements. The converse was categorised as 'compression' movements. More movement of the veneer relative to the LTF was measured near the corners of end walls than at the middle and the data has been separated in Table 10 to show this.

Table 10 shows that generally the movement of the veneer was away from the LTF. More movement occurred at the top of the veneer than at the sill of upper-storey windows. At peak loads under the category 'compression' the gap between veneer and LTF had sometimes remained open.

(b) Out-of-plane movement measured at side walls

Out-of-plane movement was small along the sides of the building.

Table 10. Gauges measuring out-of-plane displacement of LTF relative to the veneer

	End walls						Side walls	
	At very top				Sill of upper storey windows			
	Tension		Compression		Tension	Compression	At very top	Sill of upper-storey windows
Stage	Near corners	Near middle	Near corners	Near middle	Near middle	Near middle		
D	10.3	4.0	3.8	2.3	0.2	-1.3	0.9	1.6
F	15.8	5.3	7.3	4.0	0.1	-1.1	0.6	1.7
G	18.5	5.3	12.5	5.0	3.1	0.7	2.3	2.9

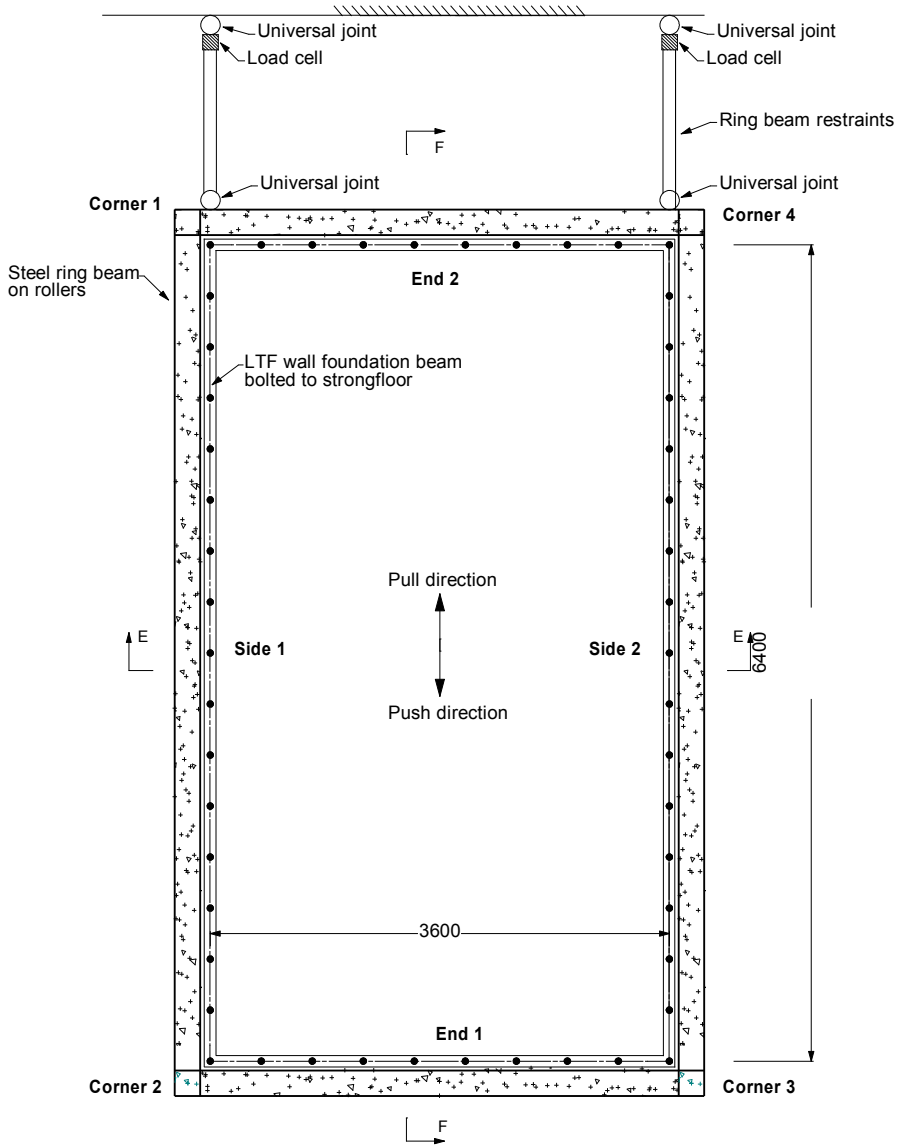

Figure 18. Plan view of building foundation ring beams supporting the veneer and the LTF foundation beams

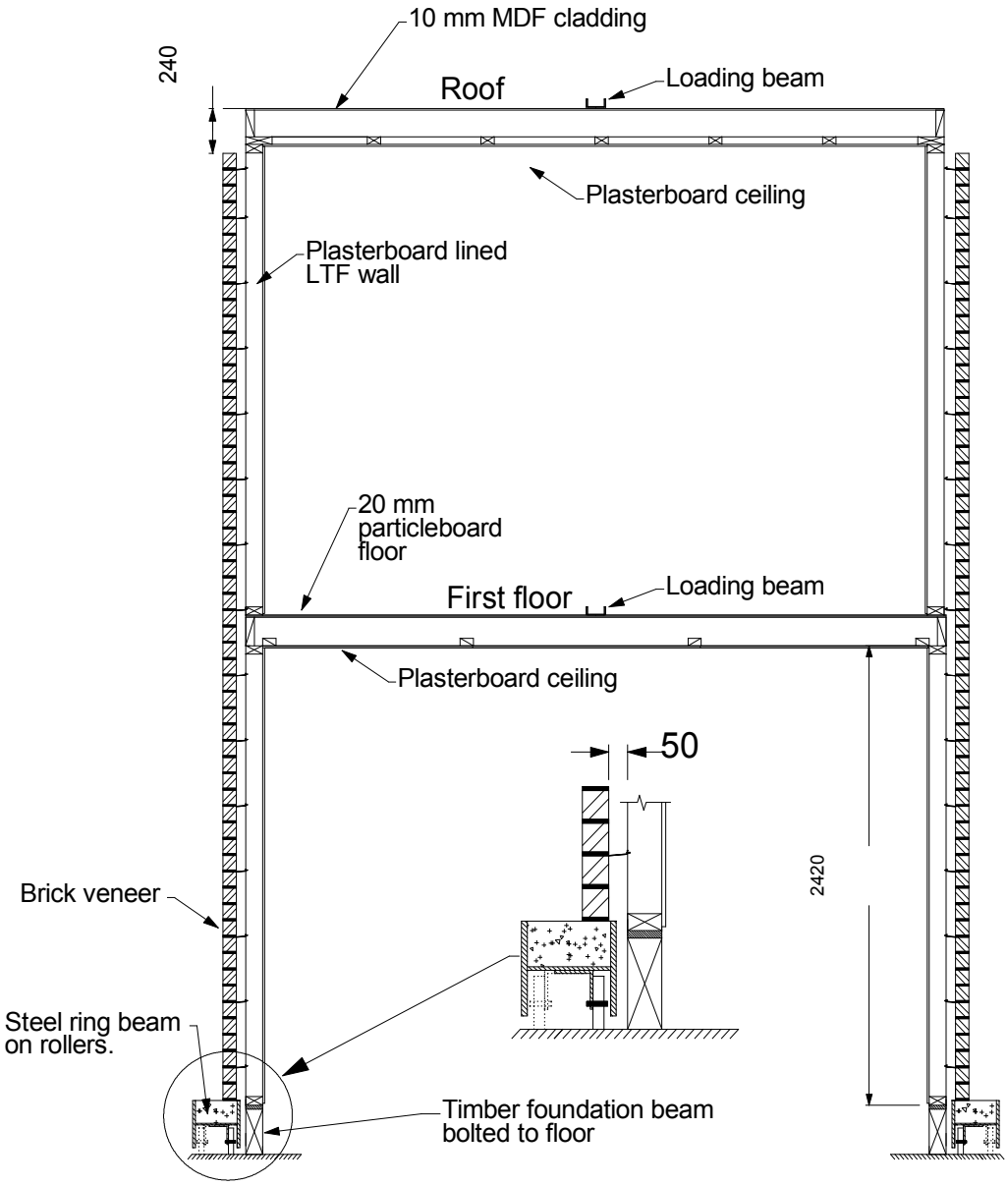

Figure 19. Section E-E through Room 1 (see Figure 18 for location)

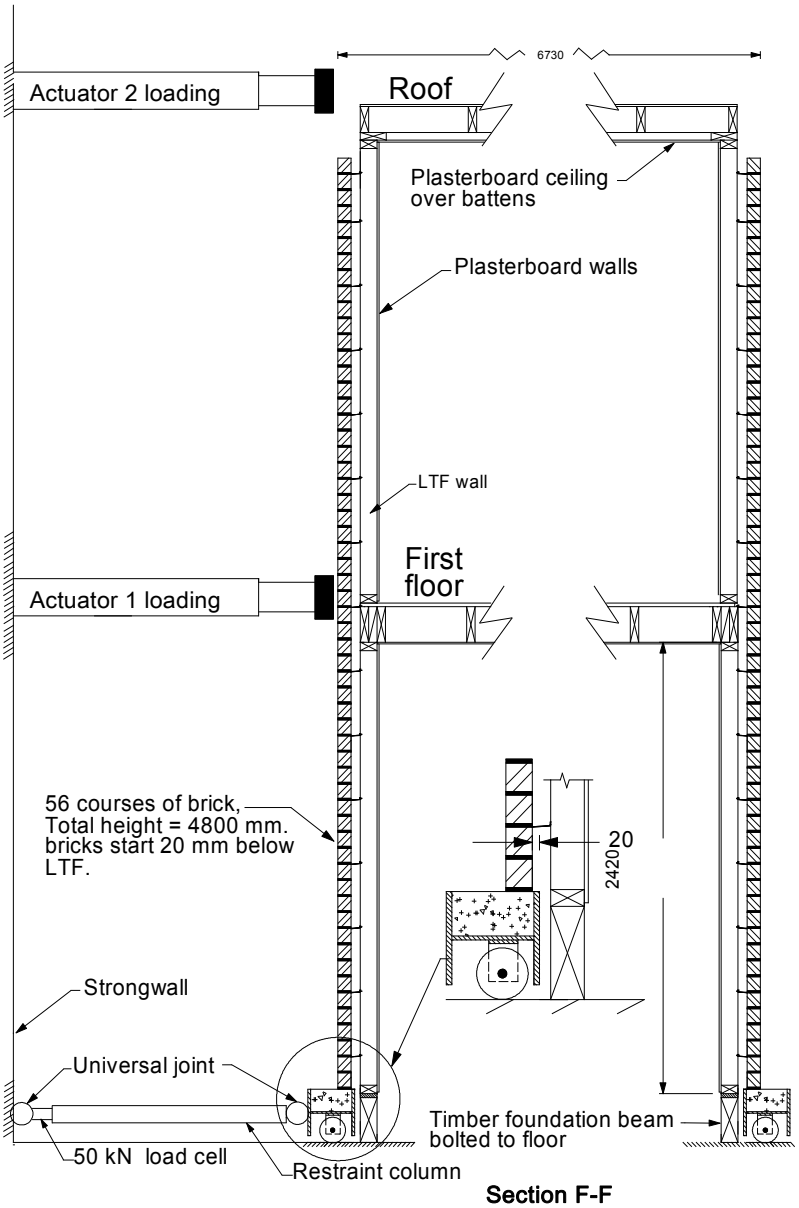

Figure 20. Section F-F through Room 1 (see Figure 18 for location)

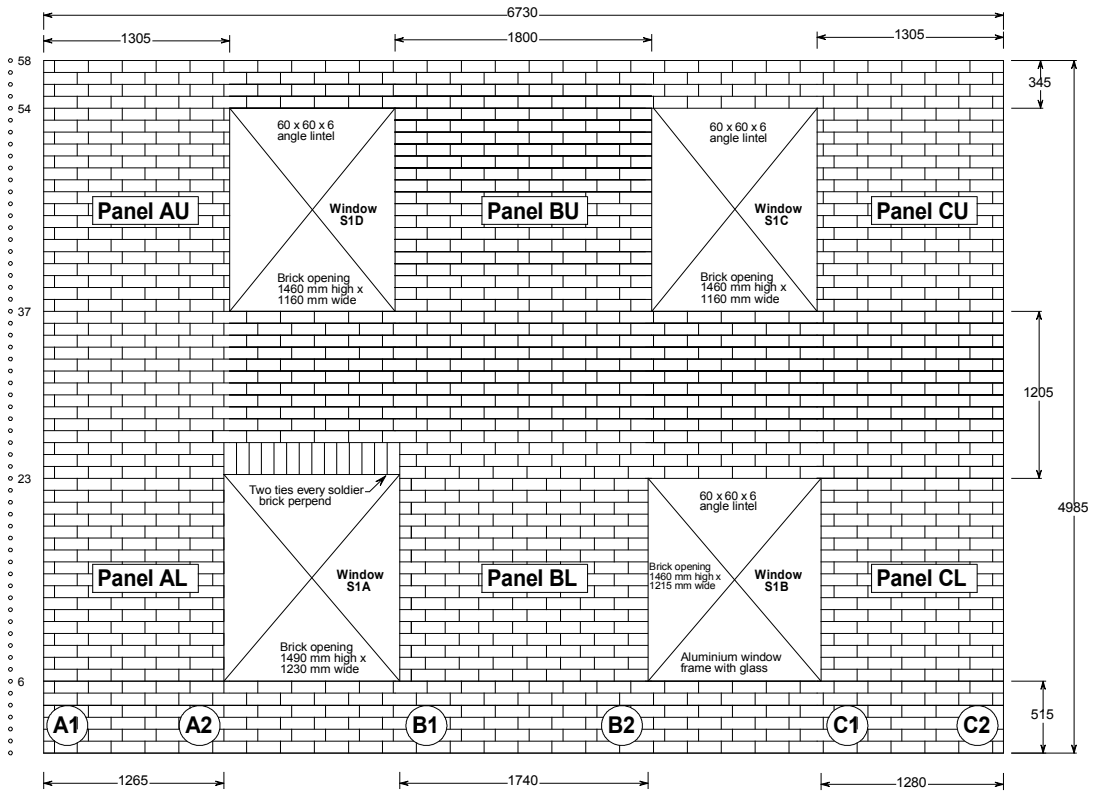

Figure 21. Side 1 elevation

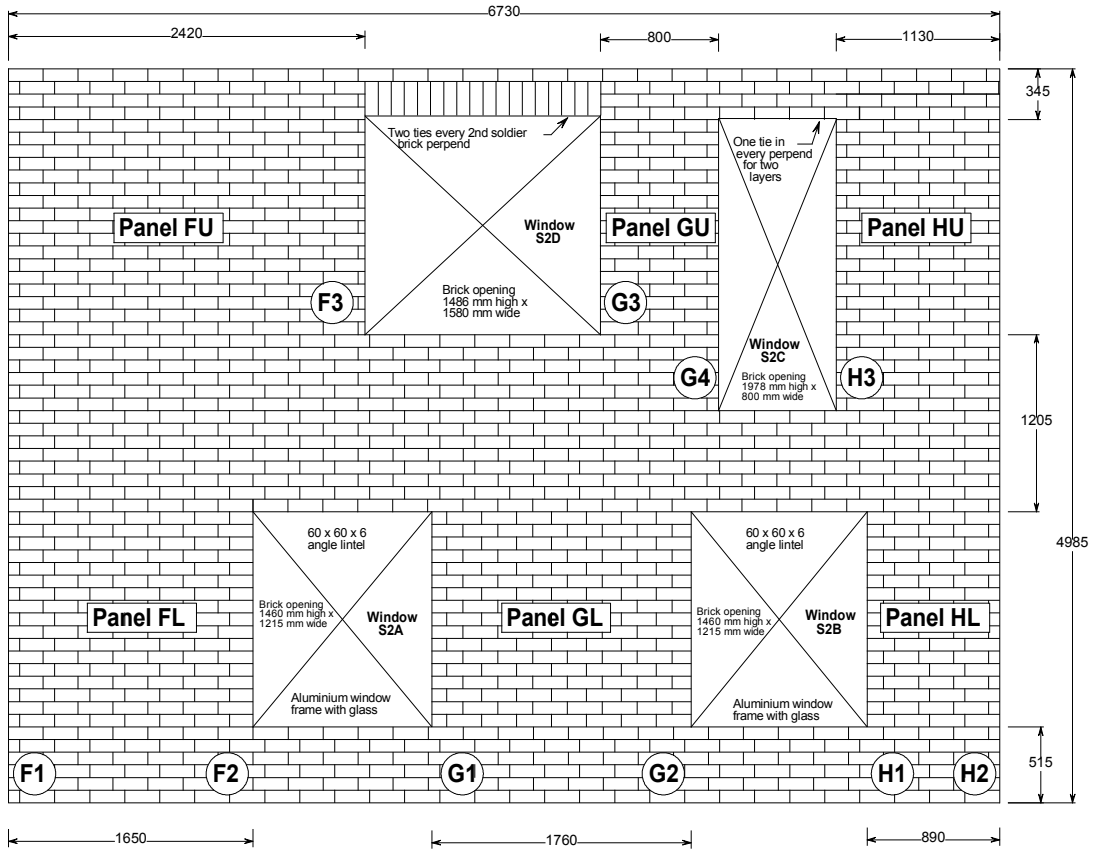

Figure 22. Side 2 elevation

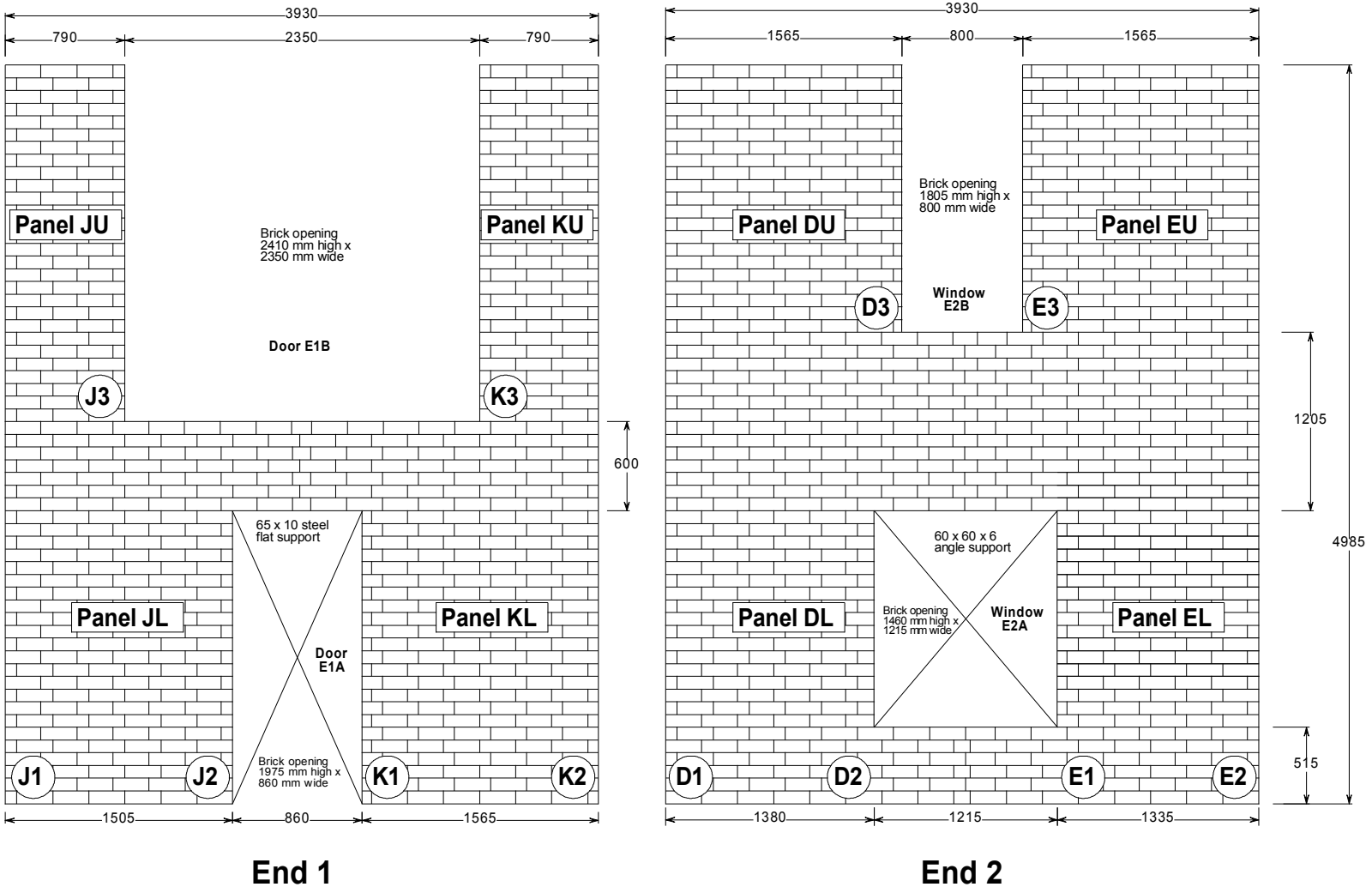

Figure 23. Building end elevations

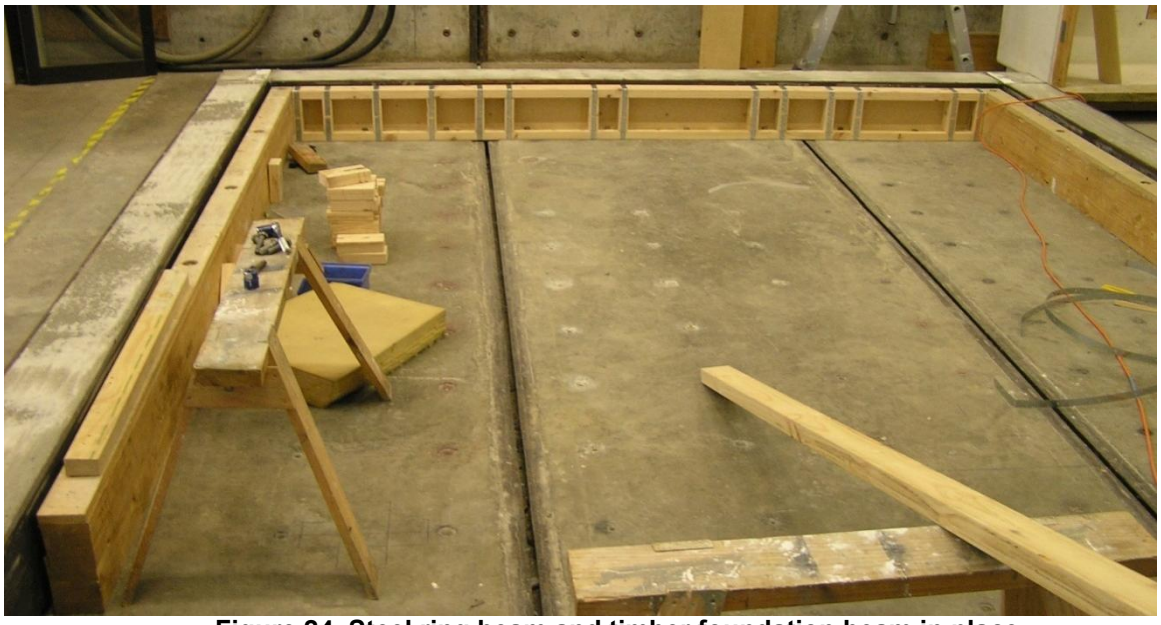

Figure 24. Steel ring beam and timber foundation beam in place

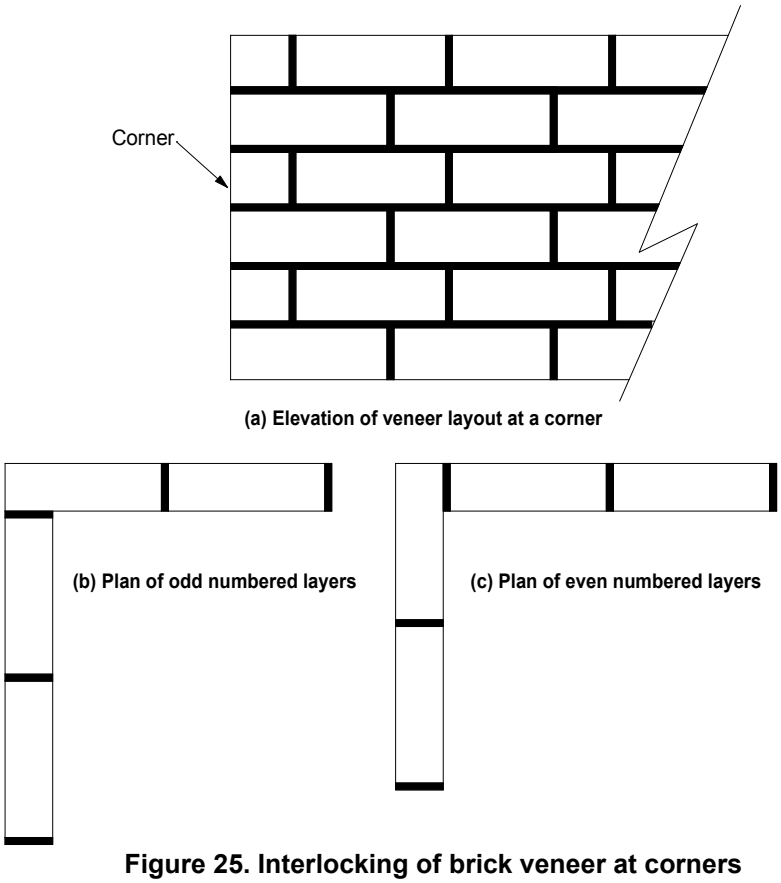

Figure 25. Interlocking of brick veneer at corners

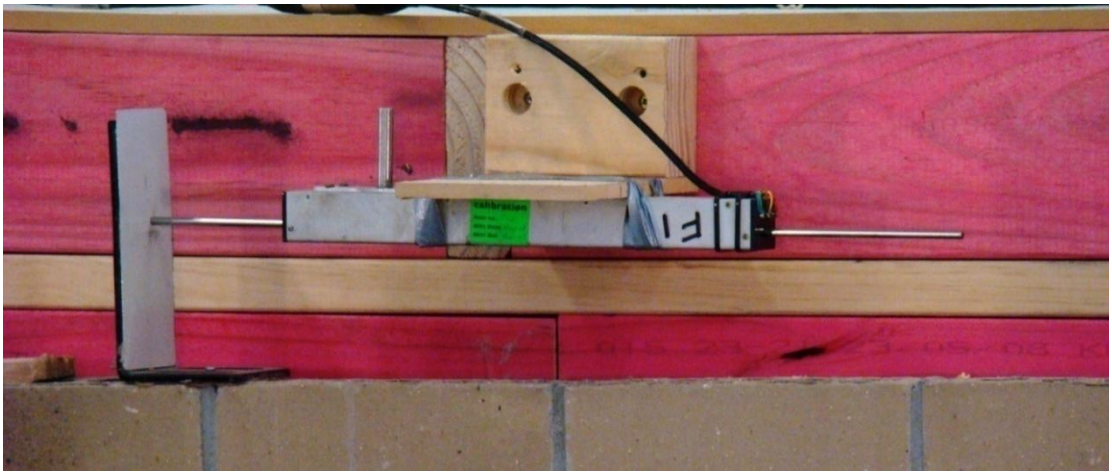

Figure 26. Measurement of horizontal in-plane displacement of LTF relative to veneer at the top of the veneer

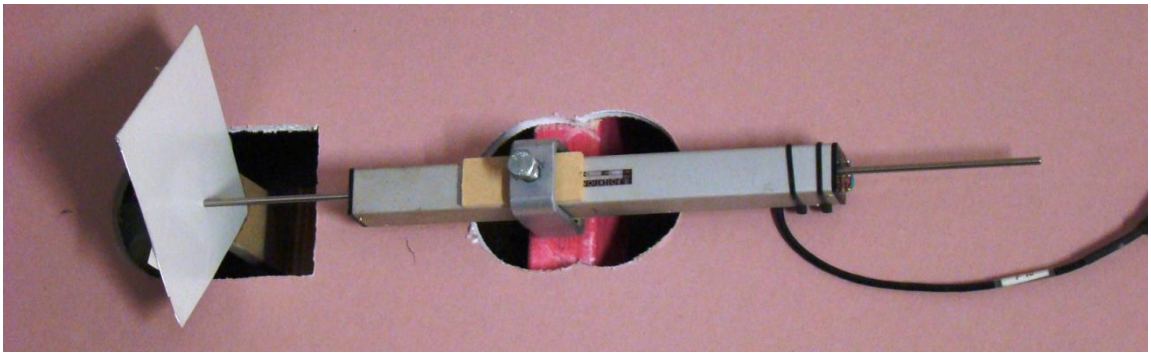

Figure 27. Measurement of horizontal in-plane displacement of LTF relative to veneer at top of lower-storey windows

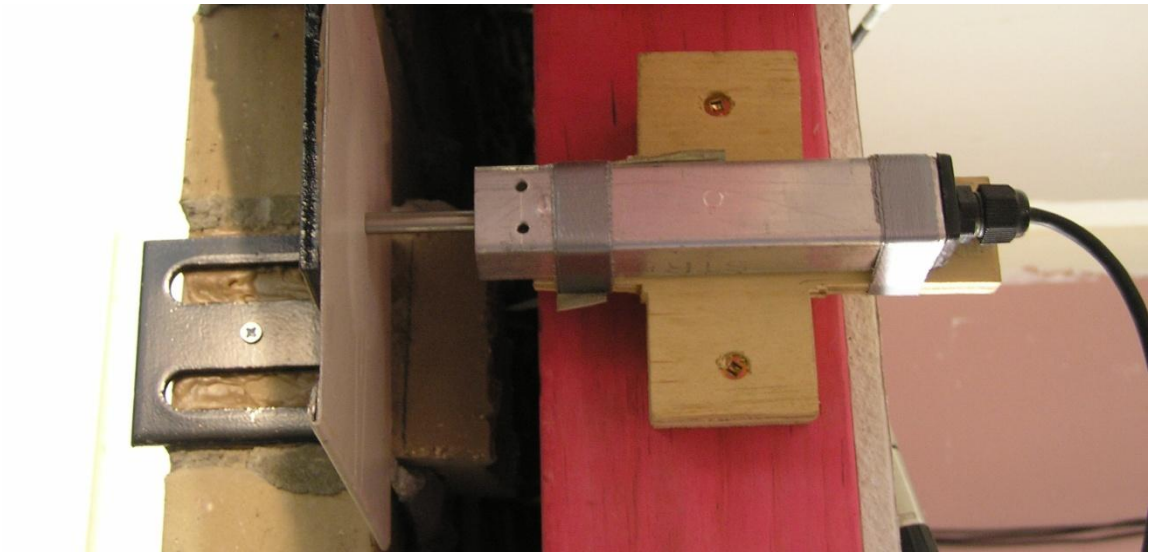

Figure 28. Measurement of out-of-plane displacement of LTF relative to the veneer

Figure 29. Measurement of vertical displacement of LTF relative to the veneer

Figure 30. Measurement of veneer crack width by measuring height to scratch marks at eight locations up the height of the veneer

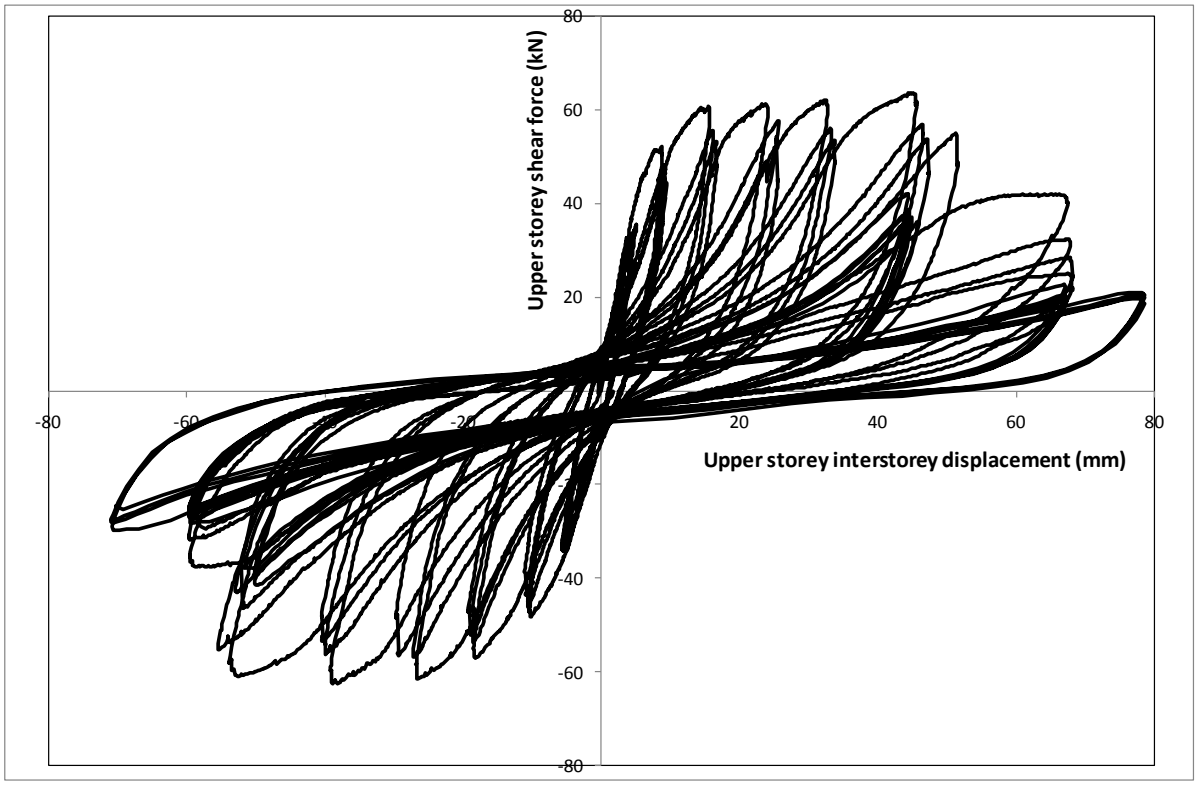

Figure 31. Upper-storey shear force versus upper-storey displacement

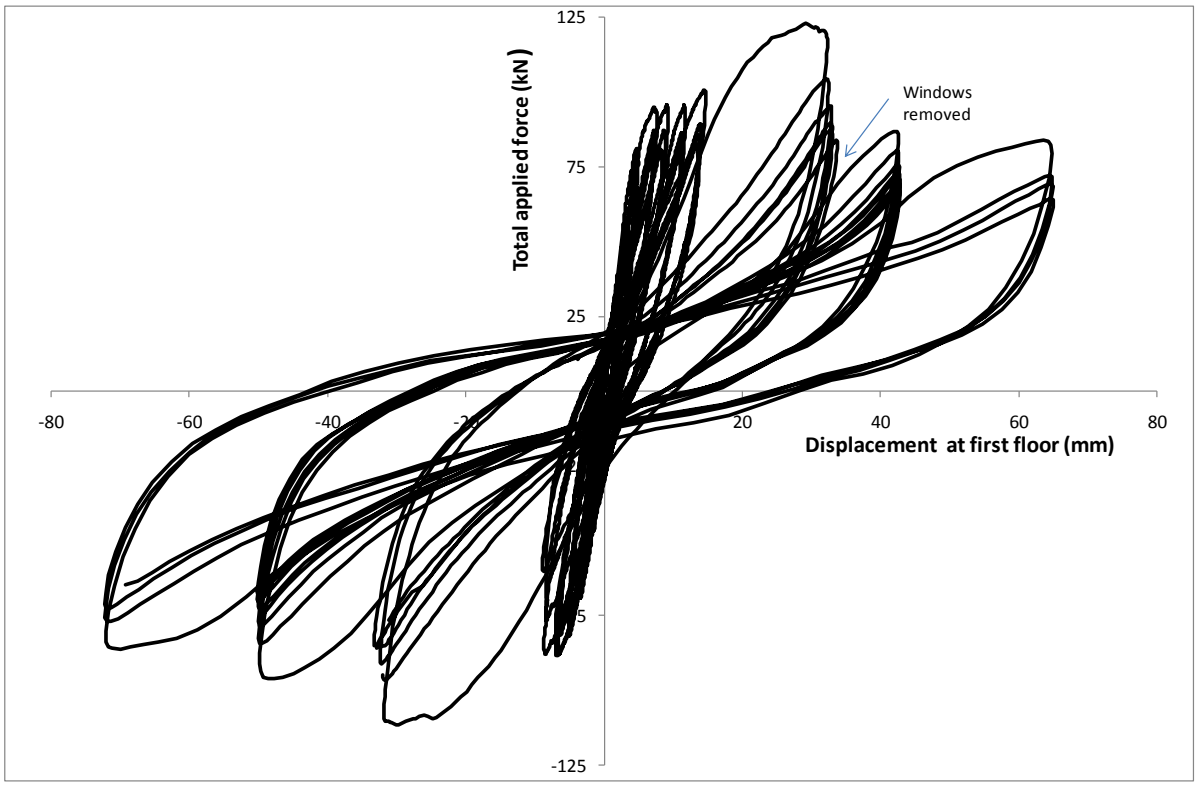

Figure 32. Total applied force at roof plus first floor versus displacement of first floor

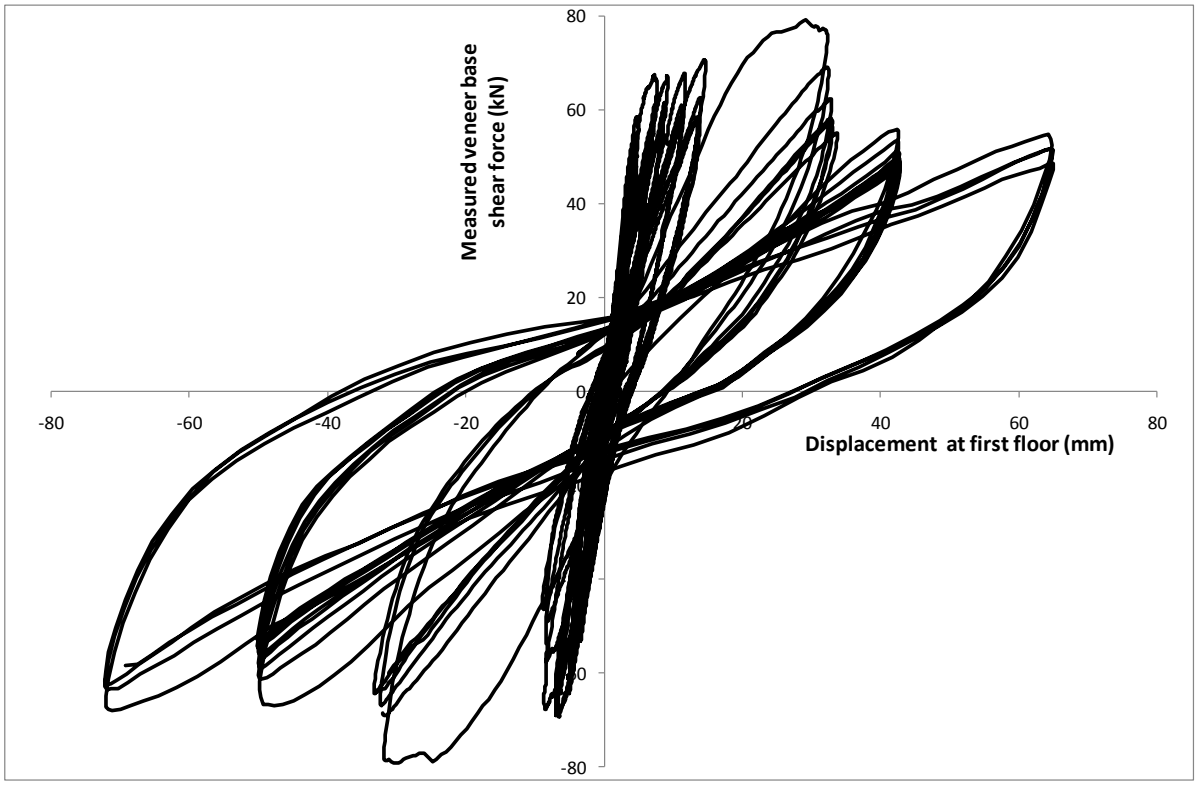

Figure 33. Measured shear force at base of veneer versus displacement of first floor

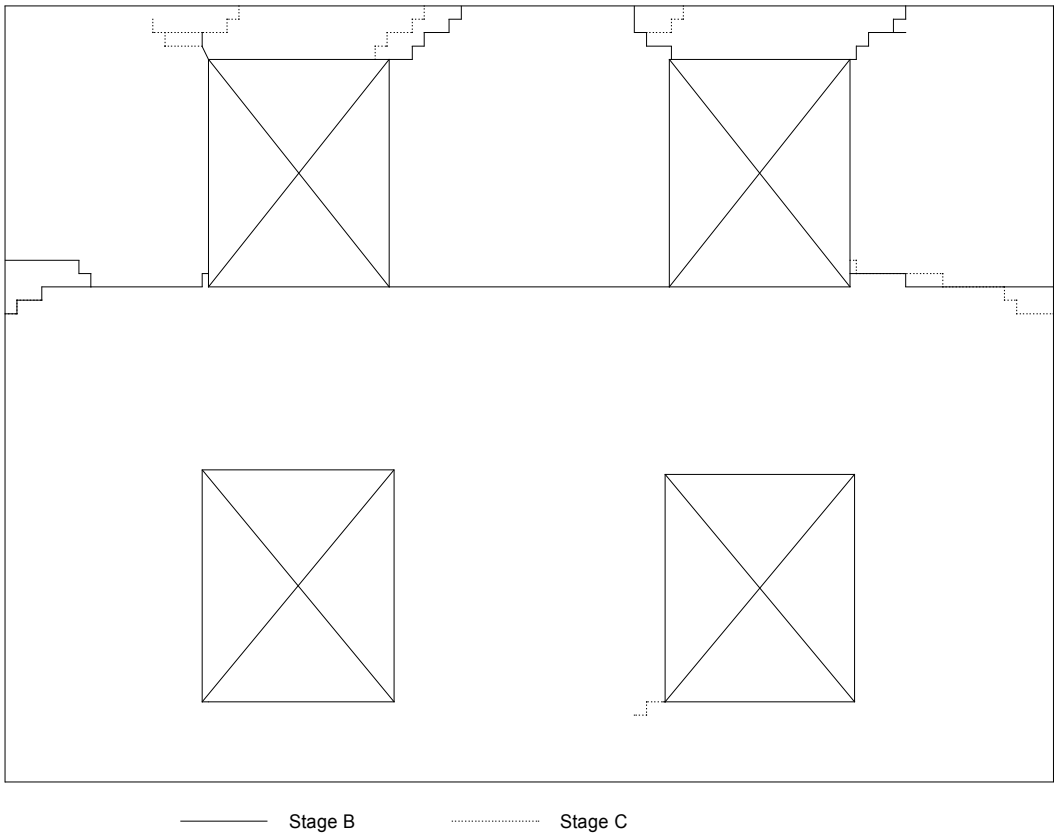

Figure 34. Cracks in Side 1 noted during Stages B and C

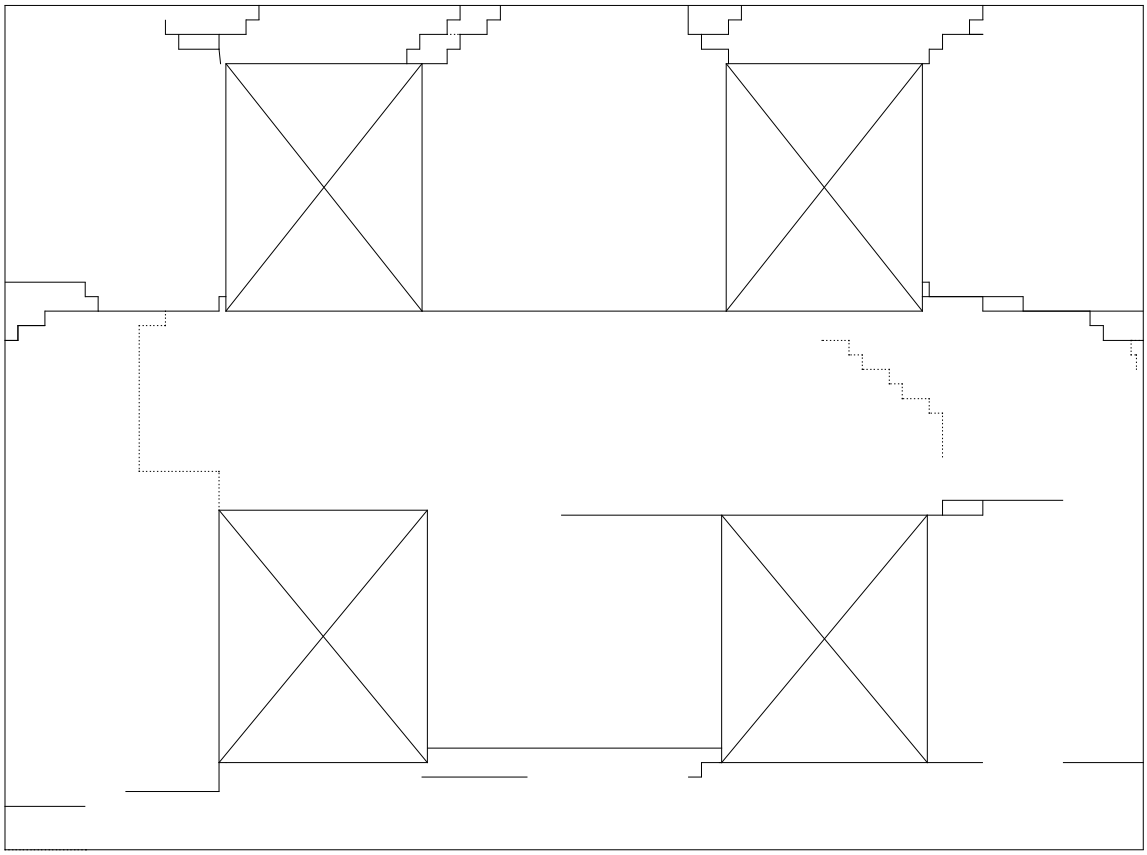

Figure 35. Cracks in Side 1 noted up to the end of Stage E

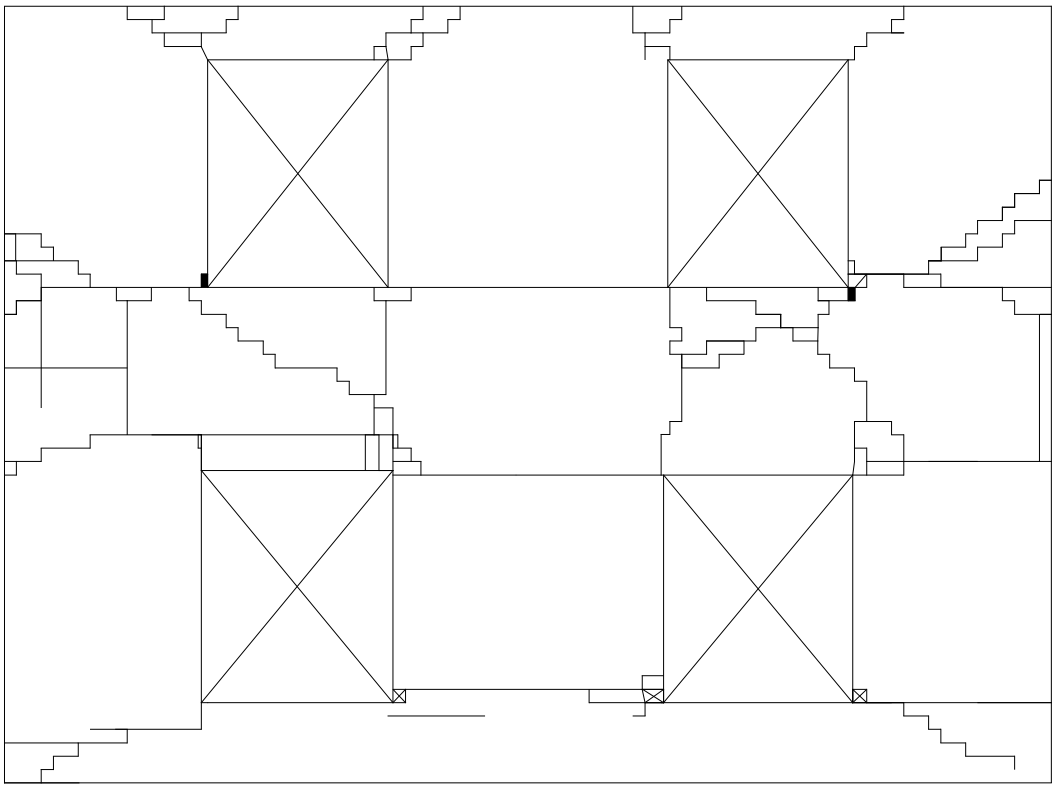

Figure 36. Cracks in Side 1 noted up to the end of Stage G

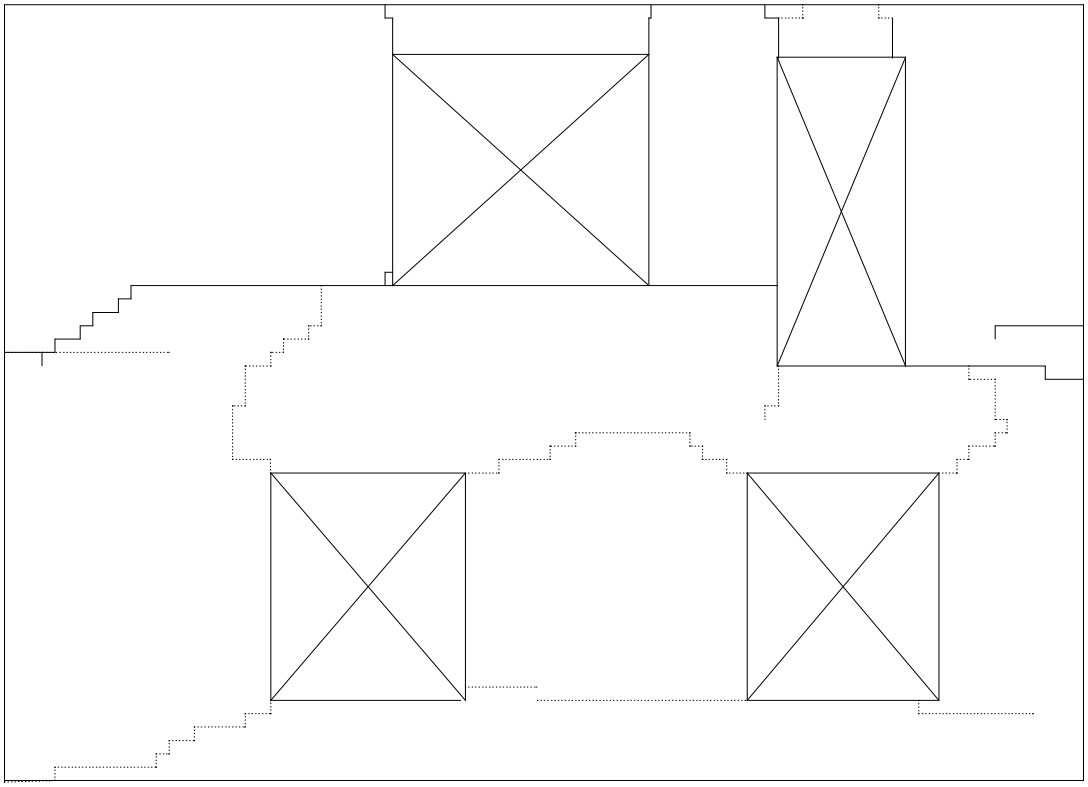

Figure 37. Cracks in Side 2 noted during Stages B and C

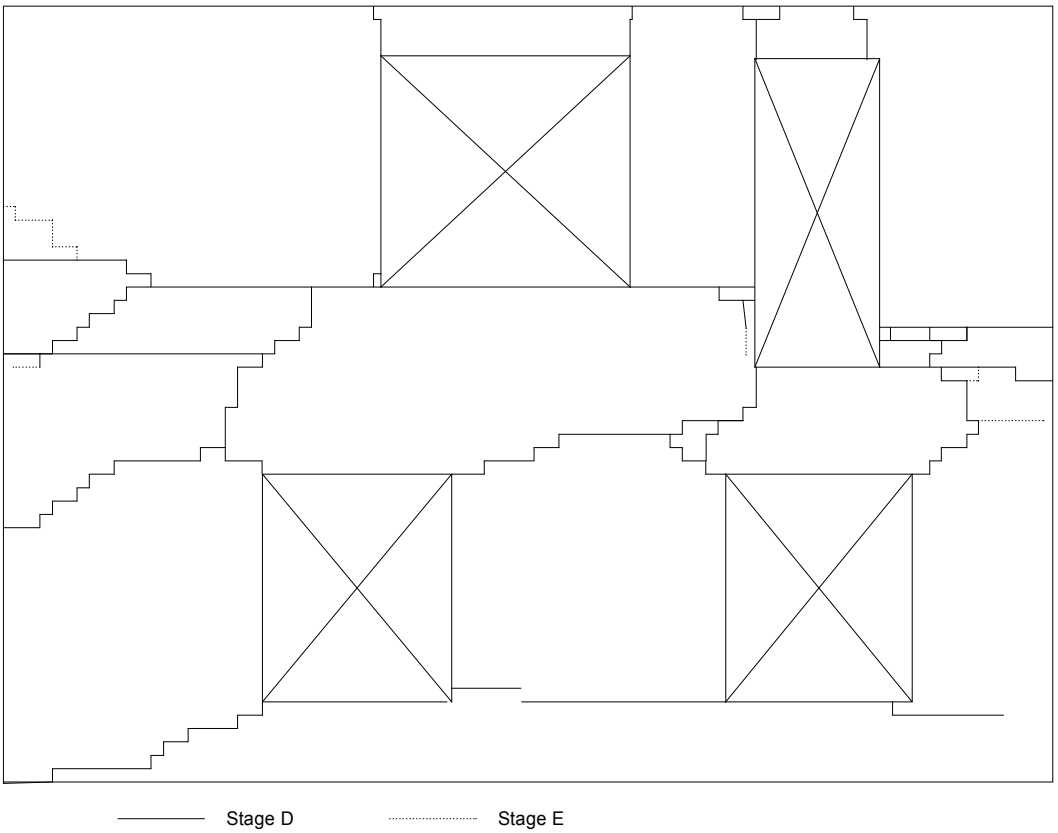

Figure 38. Cracks in Side 2 noted up to the end of Stage E

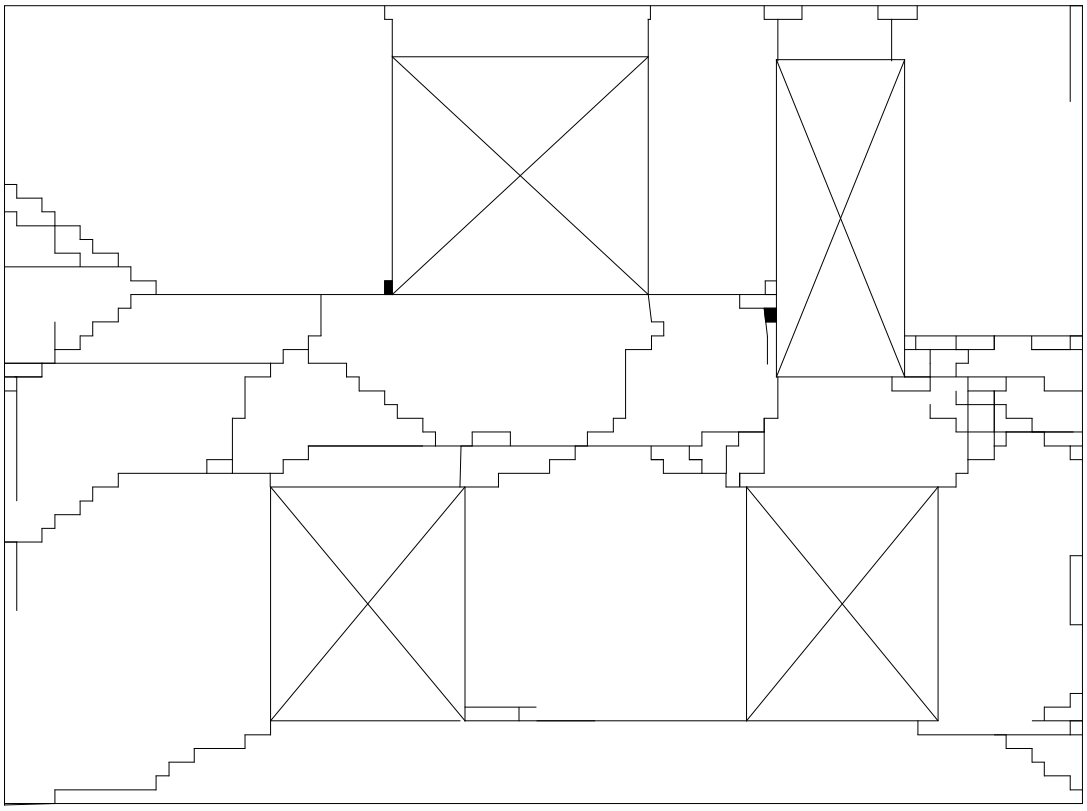

Figure 39. Cracks in Side 2 noted up to the end of Stage G

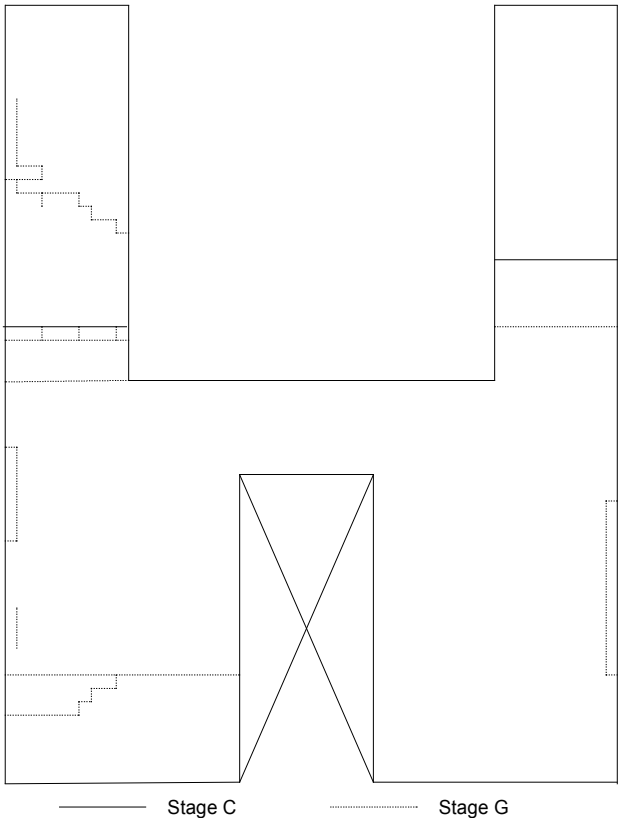

Figure 40. Cracks in End 1 noted up to the end of Stage G

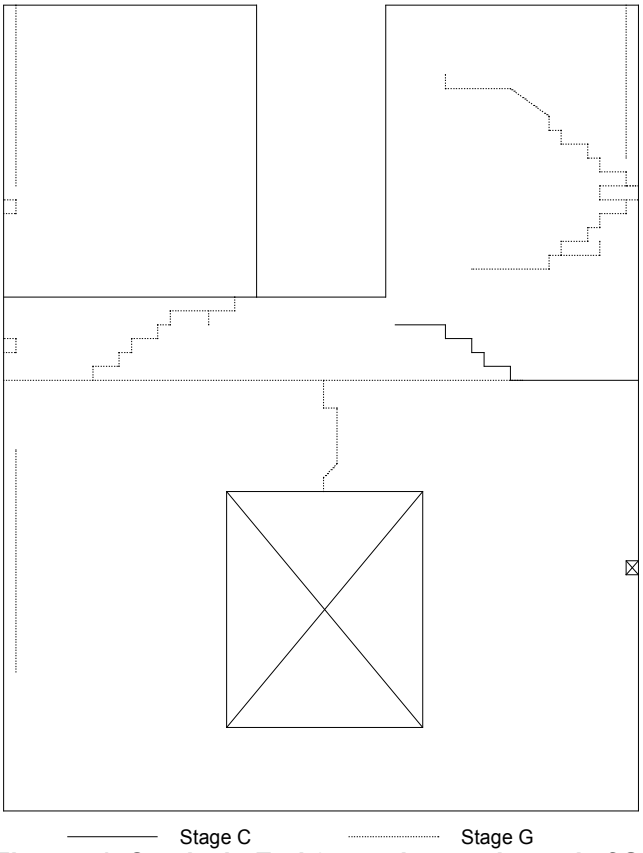

Figure 41. Cracks in End 2 noted up to the end of Stage G

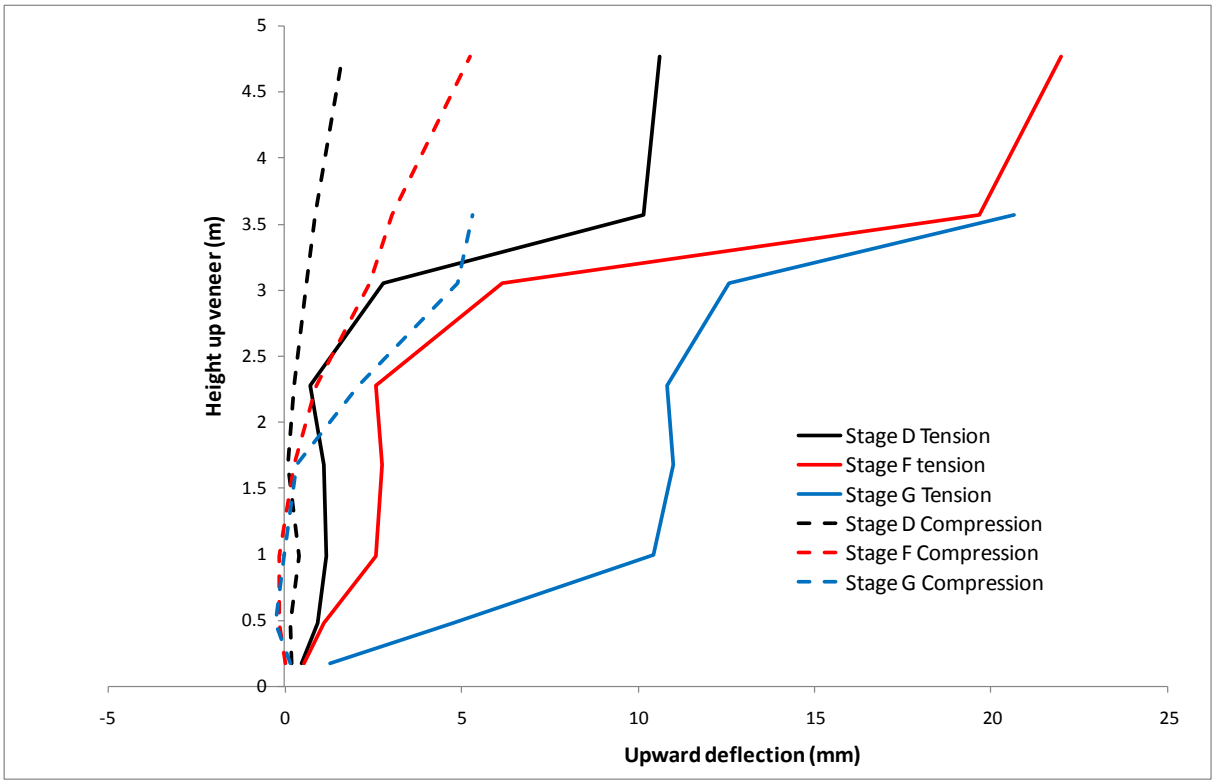

Figure 42. Measured veneer upward deflection

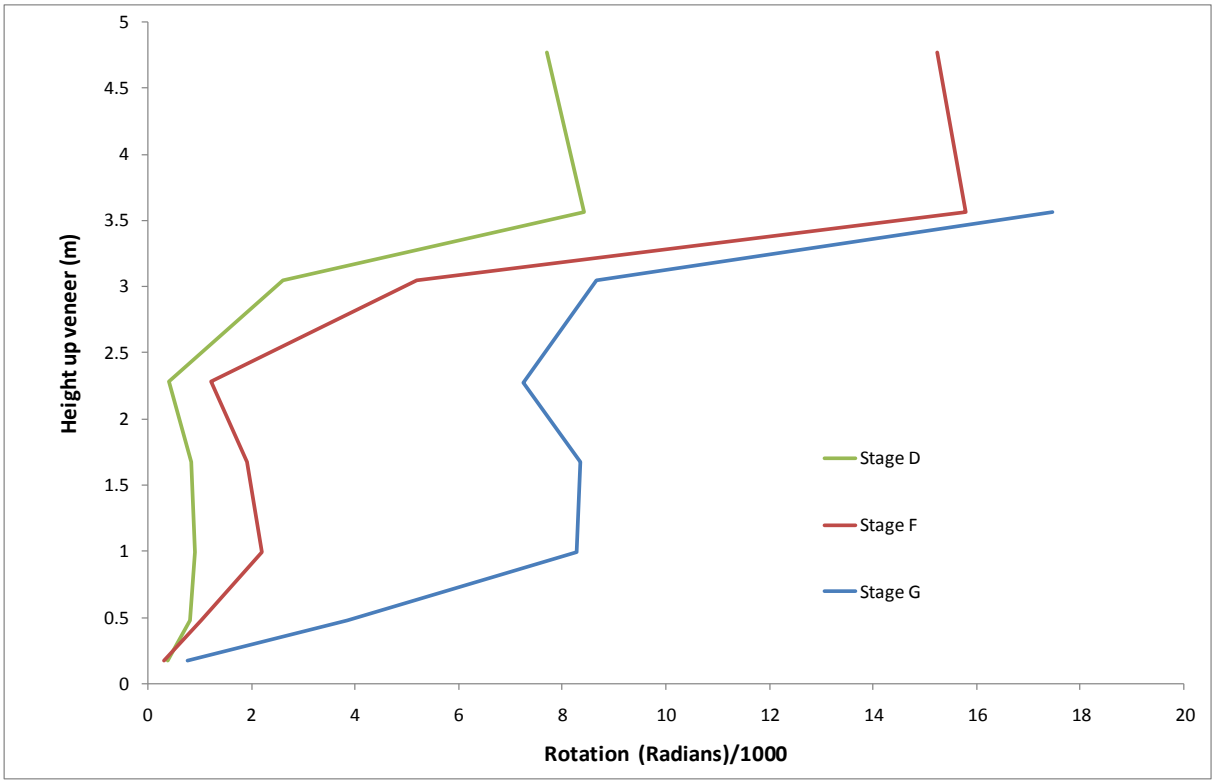

Figure 43. Relationship between veneer rotation and height up veneer

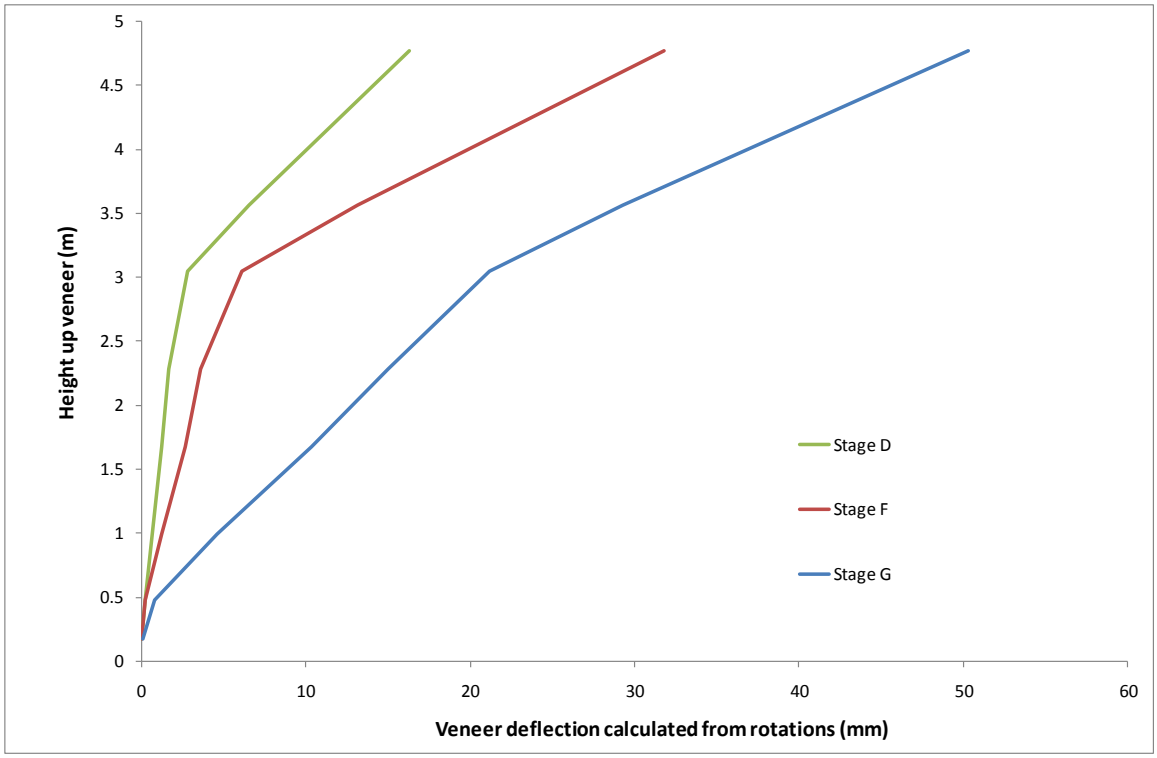

Figure 44. Veneer deflection profile calculated from the veneer rotations

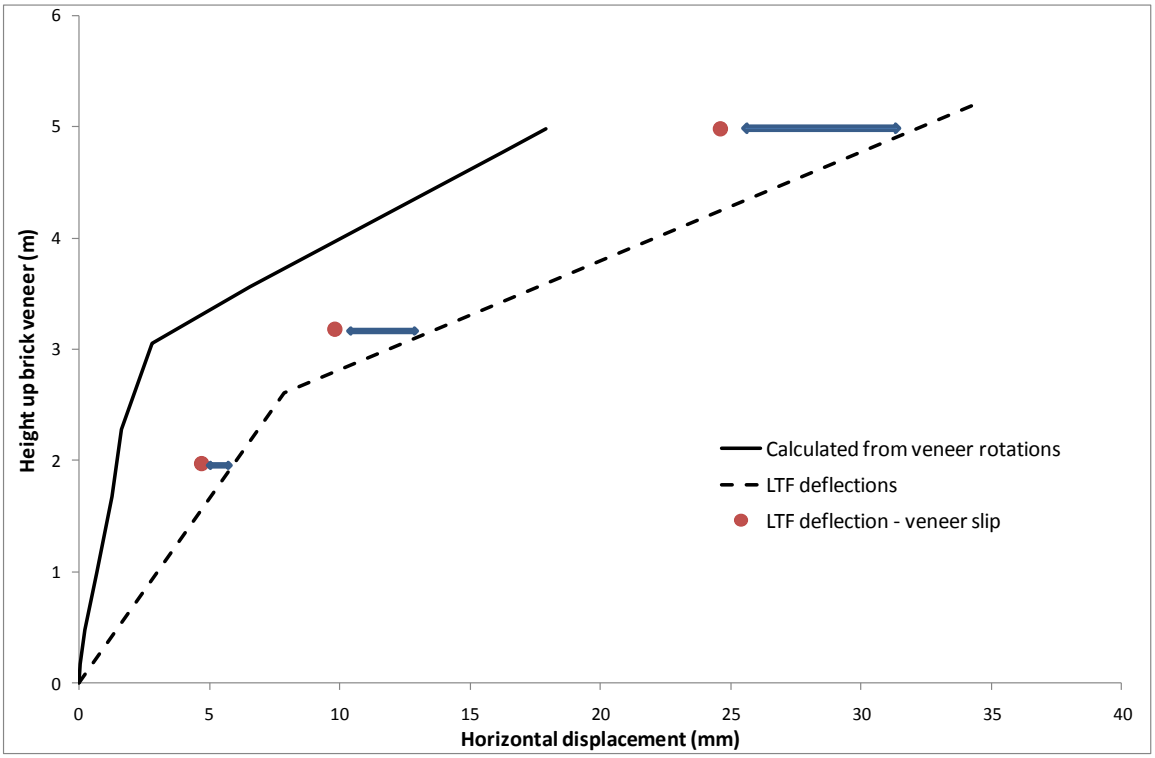

Figure 45. Veneer deflection profile compared to LTF and tie deflections at Stage D

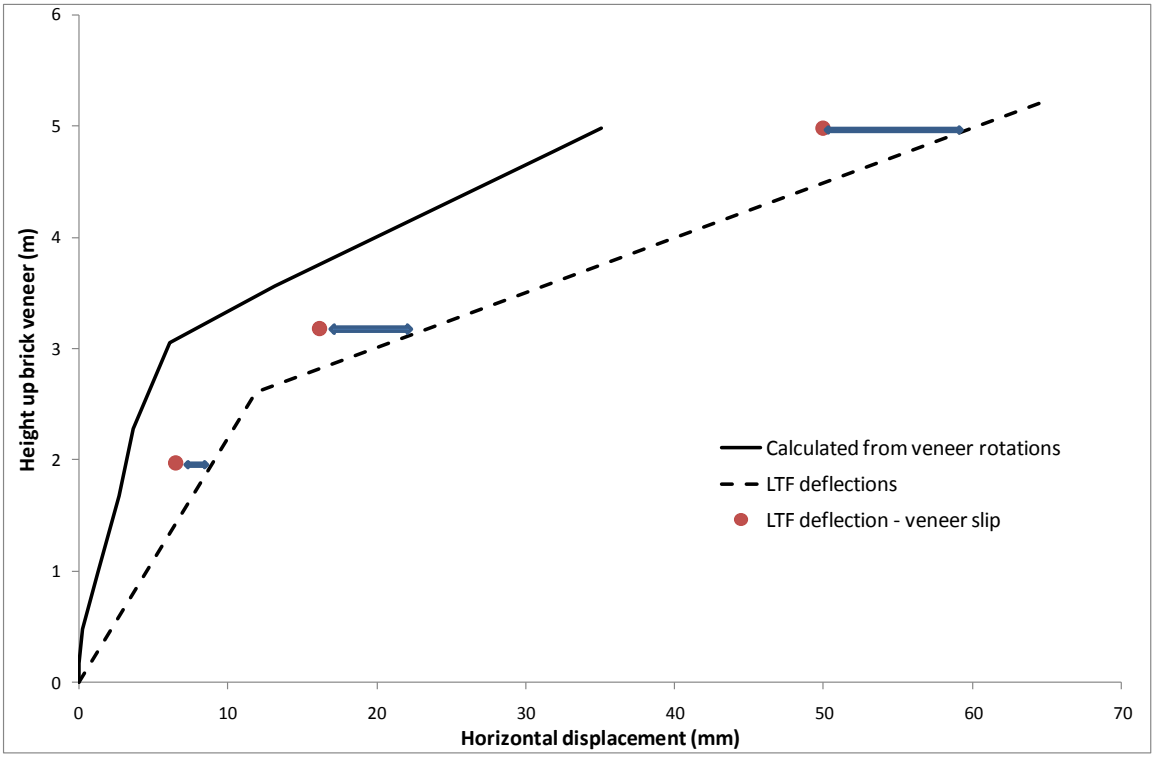

Figure 46. Veneer deflection profile compared to LTF and tie deflections at Stage F

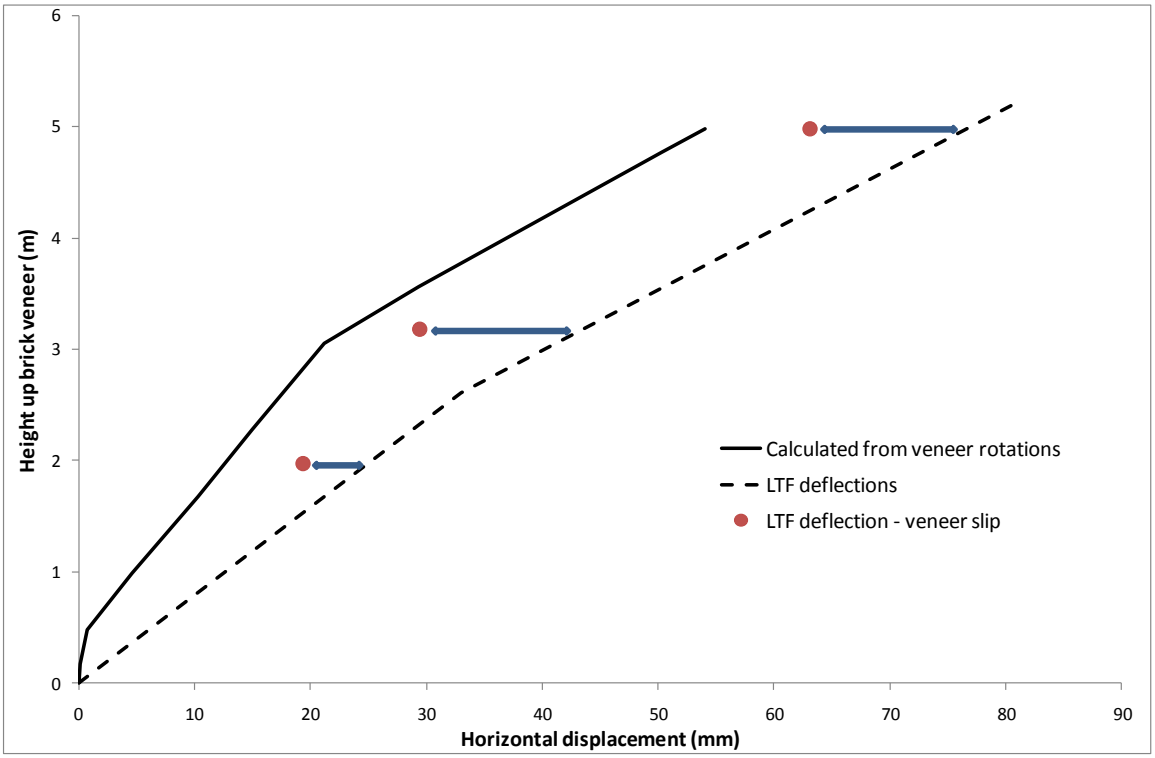

Figure 47. Veneer deflection profile compared to LTF and tie deflections at Stage G

Figure 48. Lintel cracking above Side 1 Window S1D at peak push in Stage D

Figure 49. Lintel cracking above Side 1 Window S1C at peak push in Stage D

Figure 50. Lintel cracking above Side 2 Window S2C at peak push in Stage D

Figure 51. Lintel cracking above Side 2 Window C peak pull in Stage D

Figure 52. Lintel cracking above Side 2 Window S2C at peak pull in Stage E

Figure 53. Lintel cracking above Side 1 Window S2C at peak pull in Stage F

Figure 54. Lintel cracking above Side 1 Window S1C at peak pull in Stage G

Figure 55. Cracking in Side 1 veneer at Panel B at peak pull in Stage D

Figure 56. Cracking in Side 1 upper-storey veneer at Panel B at peak push in Stage D

Figure 57. Cracking in Side 1 upper-storey veneer at Panel A at peak push in Stage D

Figure 58. Cracking in Side 1 veneer at Panel A at peak pull in Stage D

Figure 59. Cracking in Side 1 upper-storey veneer at Corner 2 at peak push in Stage D

Figure 60. Cracking in Side 1 upper-storey veneer at Corner 2 at peak pull in Stage D

Figure 61. Cracking in Side 2 upper-storey veneer at Panel H at peak pull in Stage D

Figure 62. Cracking in Side 2 upper-storey veneer at Panel G at peak pull in Stage D

Figure 63. Cracking in Side 1 upper-storey veneer at Panel B at peak push in Stage E

Figure 64. Cracking in Side 1 upper-storey veneer at Panel B at peak pull in Stage E

Figure 65. Cracking in Side 1 upper-storey veneer at Panel A at peak push in Stage E

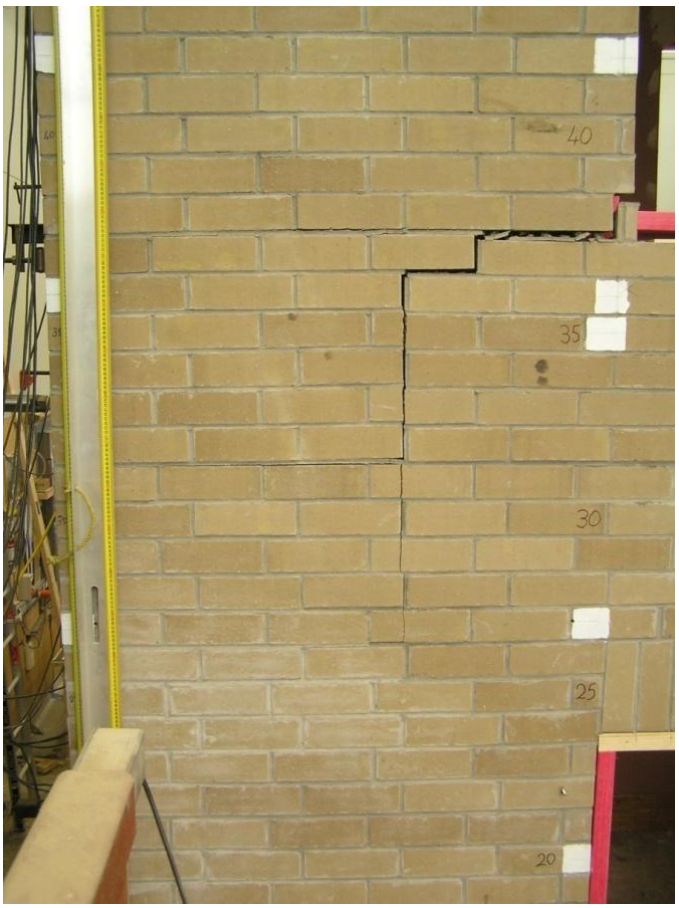

Figure 66. Cracking in Side 1 veneer at Panel A at peak pull in Stage E

Figure 67. Cracking in Side 2 upper-storey veneer at Panel F at peak pull in Stage E

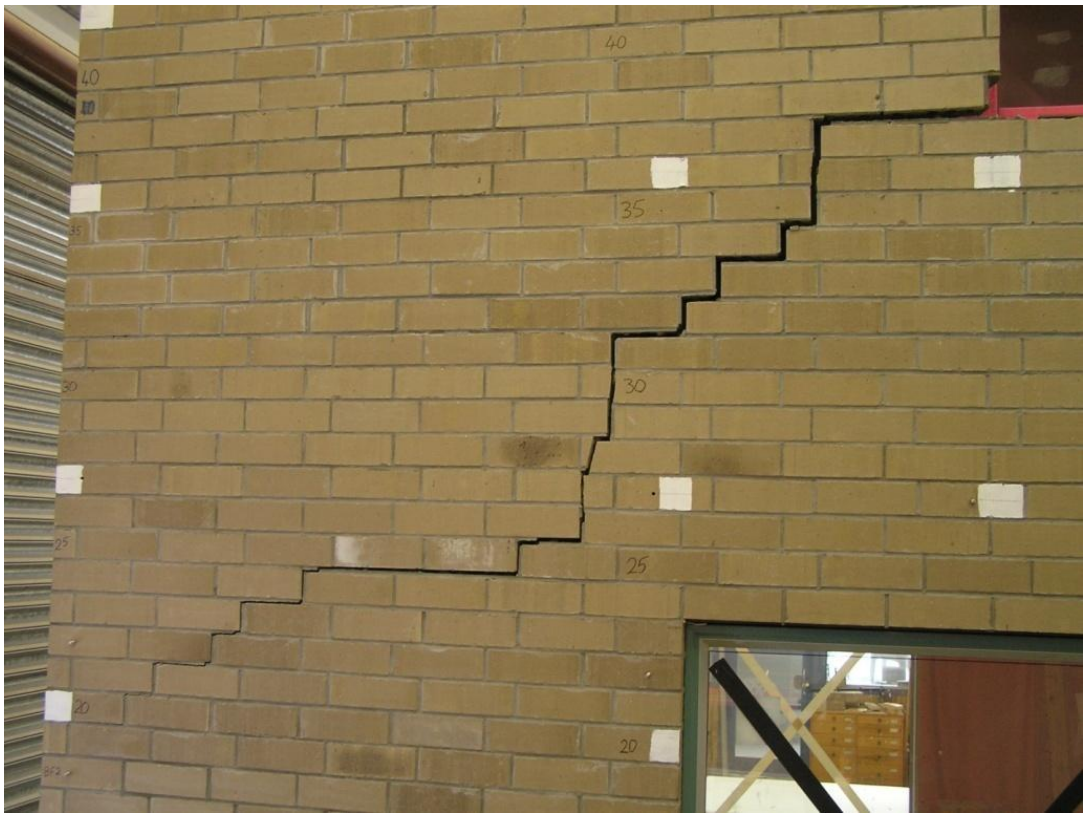

Figure 68. Cracking in Side 2 veneer at Panel F at peak push in Stage E

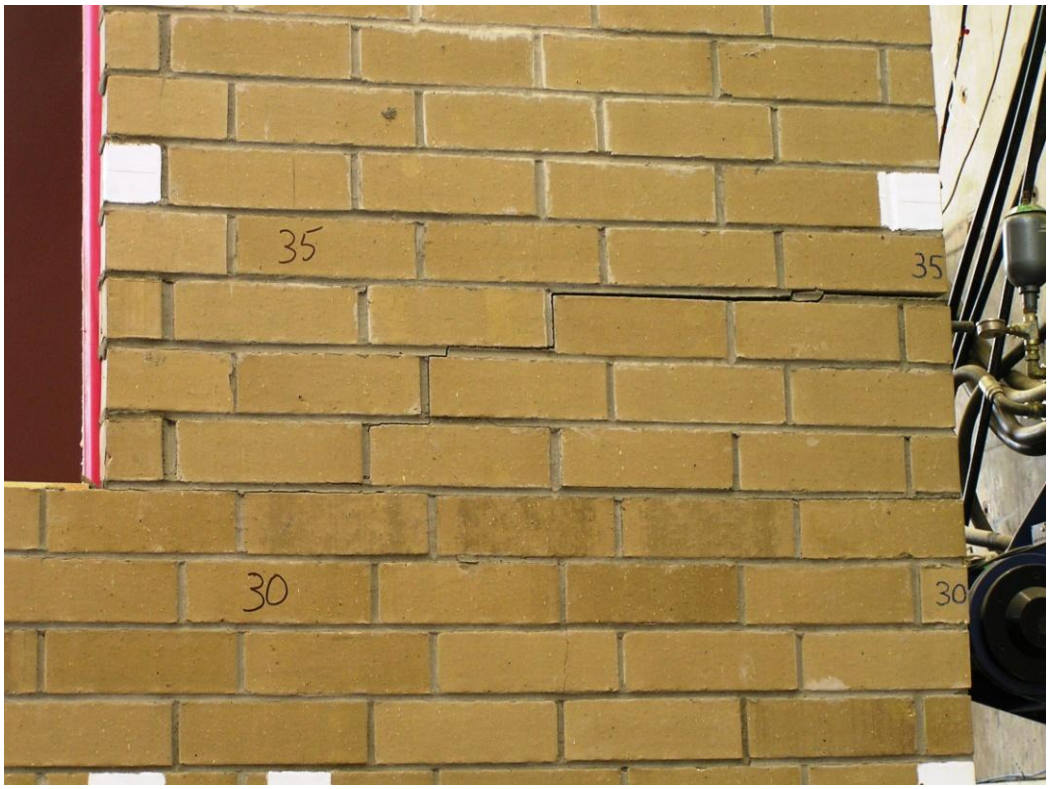

Figure 69. Cracking in Side 2 upper-storey veneer at Panel H at peak push in Stage E

Figure 70. Cracking in Side 2 upper-storey veneer at Panel G at peak pull in Stage E

Figure 71. Residual cracking Side 1 Panel F veneer at zero load after Stage E cycling

Figure 72. Residual cracking in Panel A Side 1 veneer at zero load after Stage E cycling

Figure 73. Residual cracking in Side 1 veneer above a top window at zero load after Stage E cycling

Figure 74. Cracking in Side 1 veneer at peak push in Stage F

Figure 75. Cracking in Side 1 veneer at peak pull in Stage F

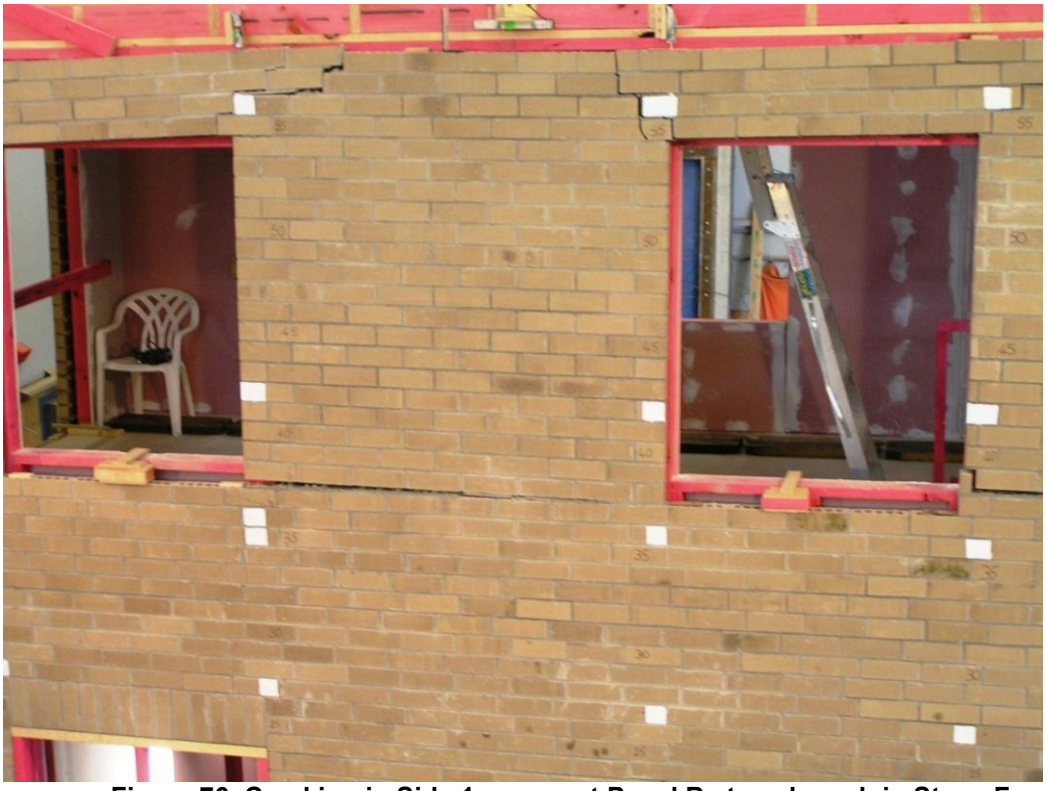

Figure 76. Cracking in Side 1 veneer at Panel B at peak push in Stage F

Figure 77. Cracking in Side 1 veneer at Panel B at Peak pull in Stage F

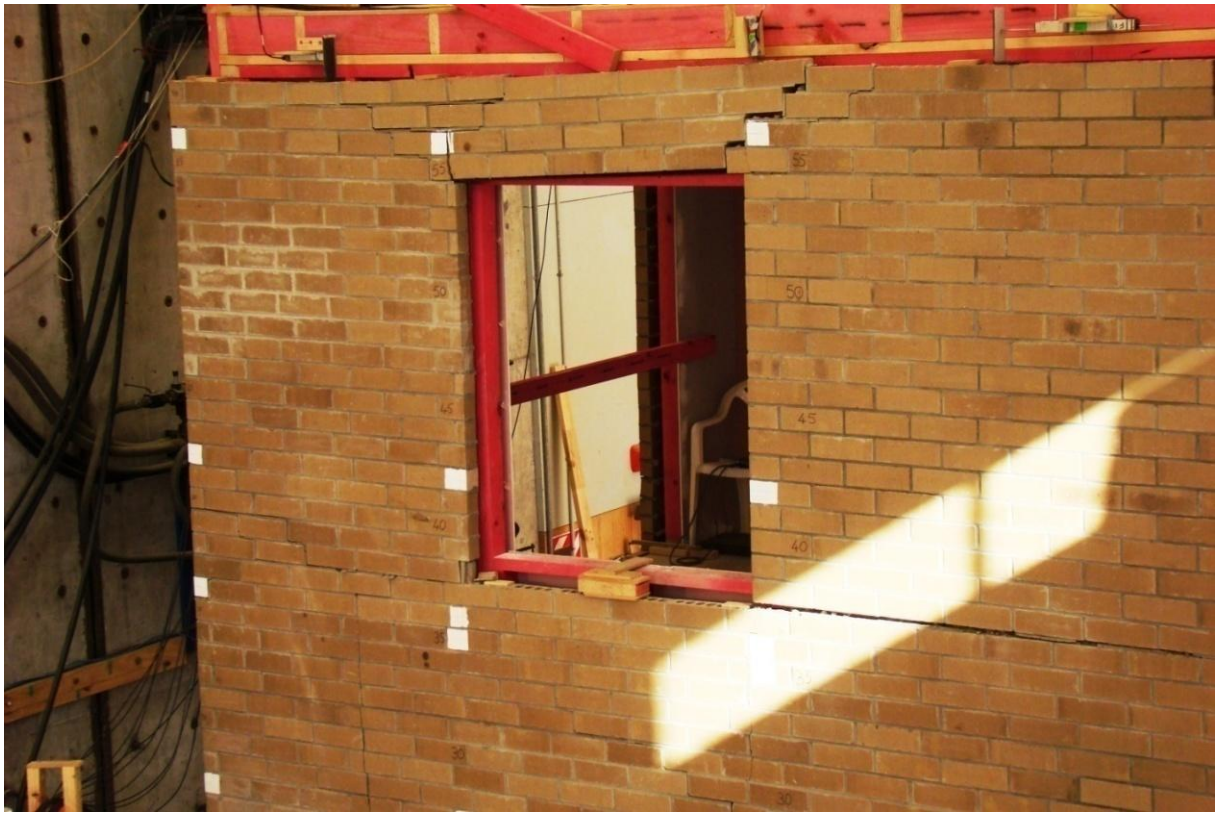

Figure 78. Cracking in Side 1 veneer at Corner 1 at peak push in Stage G

Figure 79. Cracking in Side 1 veneer at Corner 2 top window at peak push in Stage F

Figure 80. Cracking in Side 1 veneer at Panel B at peak pull in Stage F

Figure 81. Cracking in Side 1 veneer at Corner 1 at peak pull in Stage F

Figure 82. Cracking in Side 1 veneer at Panel C top window at peak push in Stage F

Figure 83. Cracking in Side 1 veneer at Panel C at peak push in Stage F

Figure 84. Cracking in Side 2 veneer at peak push in Stage F

Figure 85. Cracking in Side 2 veneer at peak pull in Stage F

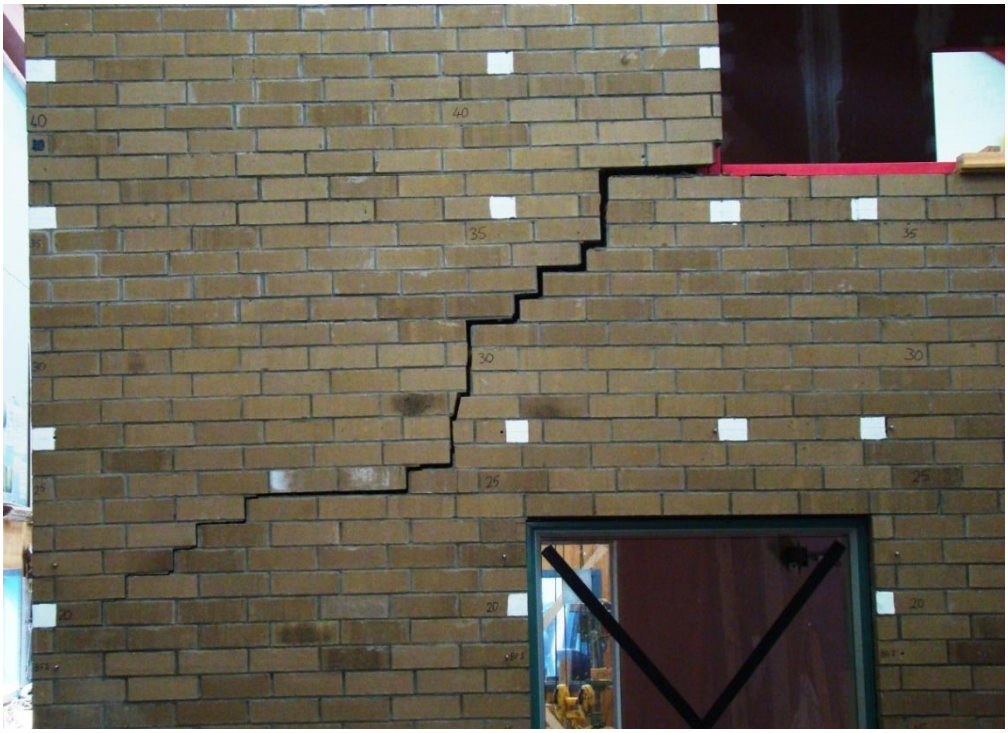

Figure 86. Cracking in Side 2 veneer at Panel F peak push at Stage F

Figure 87. Cracking in Side 2 upper-storey veneer at Panel H at peak push in Stage F

Figure 88. Cracking in Side 2 upper-storey veneer at Panel G at peak push in Stage F

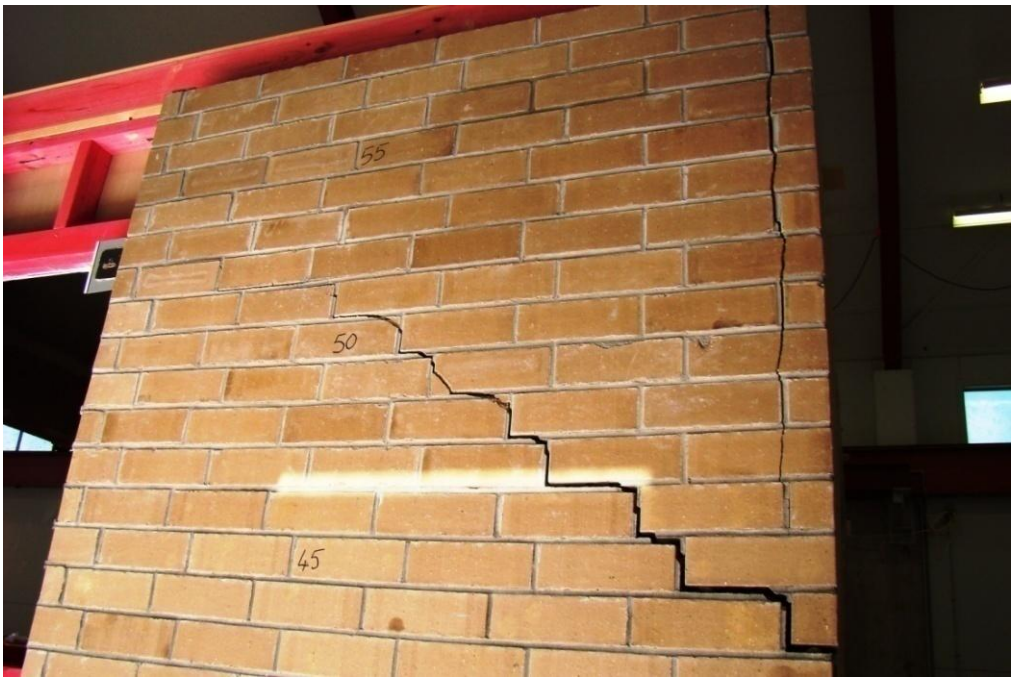

Figure 89. Cracking in End 2 veneer at Corner 3 at peak pull in Stage F

Figure 90. Cracking in Side 1 veneer at peak push in Stage G

Figure 91. Cracking in Side 1 veneer at peak pull in Stage G

Figure 92. Cracking in Side 1 veneer at Corner 2 middle spandrel at peak push in Stage G

Figure 93. Cracking in Side 1 veneer at Corner 2 middle spandrel at peak pull in Stage G

Figure 94. Brick crushing in Side 1 lower-storey veneer at Window S1B in Stage G

Figure 95. Brick damage in Side 1 lower-storey veneer at Window S1A in Stage G

Figure 96. Cracking in Side 2 veneer at peak push in Stage G

Figure 97. Cracking in Side 2 veneer at peak pull in Stage G

Figure 98. Cracking in Side 1 veneer at peak push in Stage I

Figure 99. Cracking in Side 1 veneer at peak pull in Stage I

Figure 100. Cracking in Side 2 veneer at peak push in Stage I

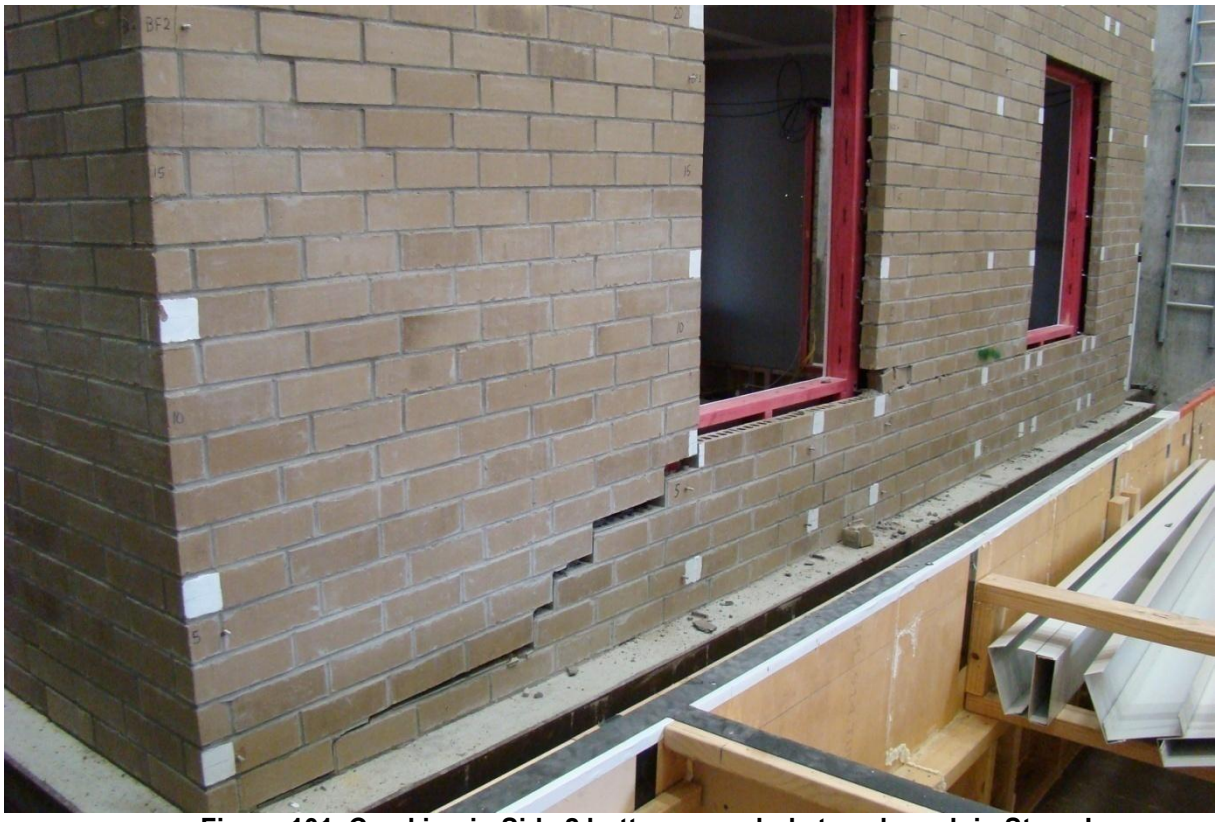

Figure 101. Cracking in Side 2 bottom spandrel at peak push in Stage I

Figure 102. Cracking in Side 2 veneer at peak pull in Stage I

Figure 103. Cracking in Side 2 bottom spandrel at peak pull in Stage I

APPENDIX B SMALL-SCALE BRICK TESTS

B.1 Introduction

A tradesman laid the bricks which were subsequently tested as described in this Appendix. The tests included:

- Horizontal shear tests on the concrete brick walls laid along a concrete foundation edges as described in Section B.2.
- Tension tests measuring the bond strength of both clay and concrete bricks which were mortared to a concrete foundation as described in Section B.3. These tests are referred to as 'plucking' tests.
- Bond wrench tests measuring the bond between concrete bricks as described in Section B.4.

B.2 Shear tests on low concrete brick walls

B.2.1 Specimen construction

Three concrete foundations were constructed. Details are given in Figure 104. The top surface of one of these was painted with two coats of Mulseal (a bitumen impregnated liquid which dried to give a surface texture and appearance much like tar). The foundation top edge was rebated 45 mm deep by 90 mm by using lengths of timber having the same cross-section dimensions on the two upper long edges of the mould. Such construction methods are typical on building sites. The concrete needed to flow under the timber which resulted in the surface of the rebate having some voids and lack of smoothness due to entrapped air.

The Mulseal was three days old at the time bricks were mortared into position. All brick veneer specimens were left outside to weather for approximately eight months before testing.

Each foundation had two brick walls, each being only two bricks high. Two shear tests were performed on each wall as shown in Figure 105. An axial load applied to the wall helped resist overturning and provided some shear friction resistance. The axial load was applied using a fulcrum system and the applied load was measured directly using the load cell shown in Figure 105 and Figure 106 .

B.2.2 Shear Test 1. Brick-to-foundation shear strength and slip coefficient

In this test on each wall a horizontal load was applied to the bottom layer of bricks and a reaction applied at the bottom of the foundation beam at the opposite end of the specimen, thus measuring the brick-to-foundation shear strength. Results are summarised in Table 11 for concrete brick mortared to a bare concrete foundation and Table 12 for brick mortared to Mulseal-coated concrete foundation. The axial load used in the calculation included the applied load as measured by the load cell, the weight of equipment which loaded the joint which was not measured by the load cell and also the weight of brick above the joint. In all cases failure was between the mortar and brick for part of the foundation length and mortar and substrate for the remainder of the length, as shown in Figure 107.

Figure 104. Concrete beam used as a foundation to fix bricks and application of shear load

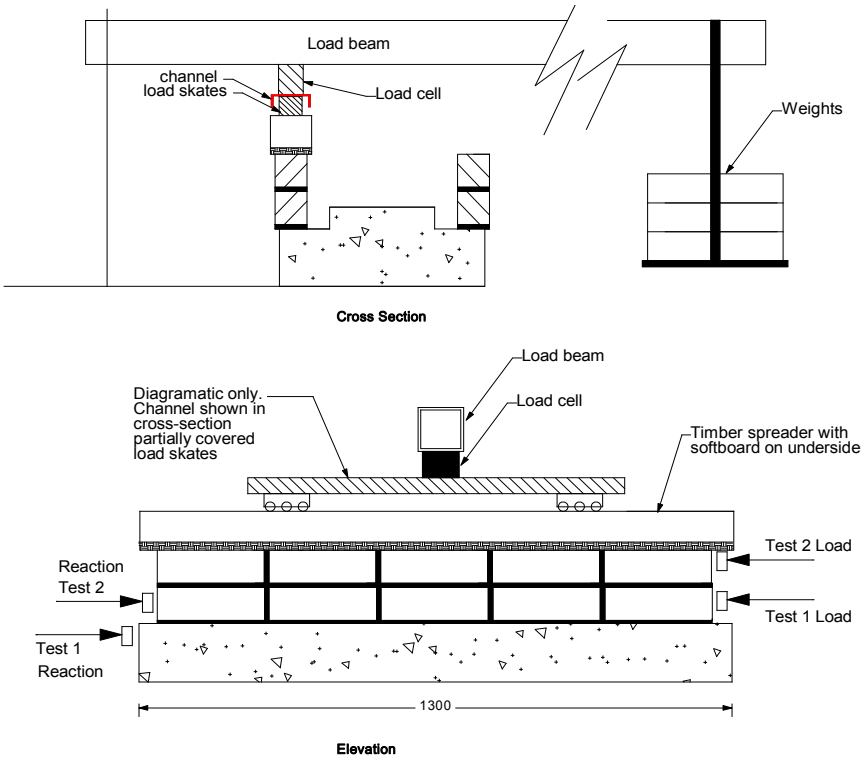

Figure 105. Shear test set-up for both brick-to-brick and brick-to-foundation tests

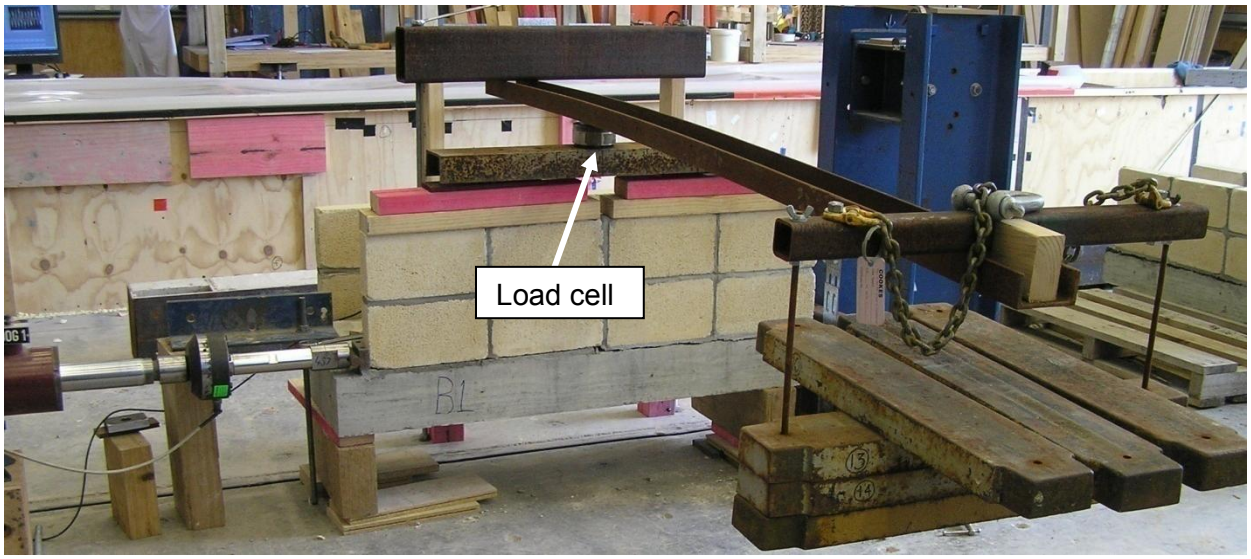

Figure 106. Shear test set-up for brick-to-concrete foundation joint

(a) Brick-to-bare concrete foundation

The load was applied in four stages as shown in Figure 108. A medium level axial load of 54 kPa was first imposed and then shear load applied until shear failure occurred. The brick-to-concrete foundation cracked for the full length and the resisted load fell quickly with increased actuator displacement and began to flatten out. The peak shear load labelled in Figure 108 was used to compute the peak shear stress given in Table 11.

The axial load was then almost doubled to approximately 94 kPa. Table 11 gives the corresponding axial stress (called Axial Stress 2). (To relate this to typical axial pressures for concrete brick veneer in actual construction, note that a 2.2 m high concrete brick veneer of the construction tested has a self-weight axial load of approximately 38 kPa on the concrete foundation.) The resisted shear load stayed almost constant with increased actuator displacement and the average shear load was used to calculate the slip shear stress. The ratio of the slip shear stress to Axial Stress 2 was called the shear friction coefficient μ2 and this is given in Table 11.

The axial load was then reduced to the original level. Table 11 gives the corresponding axial stress (called Axial Stress 3). Again the resisted load stayed almost constant with increased actuator displacement and the average shear load was used to calculate the slip shear stress. The ratio of the slip shear stress to Axial Stress 3 was called the shear friction coefficient μ3 and this is also given in Table 11.

(b) Brick-to-Mulsealed concrete foundation

The peak shear strength of the brick-to-Mulsealed concrete connection averaged 629 kPa (Table 12) which is 53% more than that for the brick-to-concrete foundation. Post-cracking, the shear friction coefficient was only 76% that measured for direct mortaring bricks to a concrete foundation. Thus, if a Mulsealed joint at a bottom of a panel is pre-cracked by rocking, it will slip at a lower shear load than a corresponding panel directly mortared to a concrete foundation. However, based on the test results, from a structural perspective, Mulseal is still considered to be a suitable damp-proof course.

Table 11. Brick-to-concrete foundation test results

Specimen Number	Axial Stress 2 (kPa)	Axial Stress 3 (kPa)	Peak shear stress (kPa)	Shear Friction μ2	Shear Friction μ3
1	94	54	379	0.91	0.96
2	92	54	468	0.90	1.03
3		54	445		
4	95	55	351	0.84	0.86
Mean			**411**	**0.88**	**0.95**
COV			**0.13**	**0.04**	**0.09**

Table 12. Brick-to-Mulsealed concrete test results

Specimen Number	Axial Stress 2 (kPa)	Axial Stress 3 (kPa)	Peak shear stress (kPa)	Shear Friction μ2	Shear Friction μ3
5	95	57	629	0.71	0.72

B.2.3 Shear Test 2. Brick-to-brick shear strength and slip coefficient

In this test a horizontal load was applied to the top layer of bricks and a reaction applied at the bottom layer of bricks at the opposite end, as shown in Figure 109, thus measuring the brick-to-brick shear strength. Test results are summarised in Table 13.

Table 13. Brick-to-brick test results

Specimen Number	Axial Stress 2 (kPa)	Axial Stress 3 (kPa)	Peak shear stress (kPa)	Shear Friction μ2	Shear Friction μ3
1	88	52	581	1.06	1.01
2	91	51	792	1.05	1.12
5	95	54	819	1.01	1.03
Mean			**687**	**1.05**	**1.06**
COV			**0.22**	**0.01**	**0.08**

Figure 107. Typical shear failure

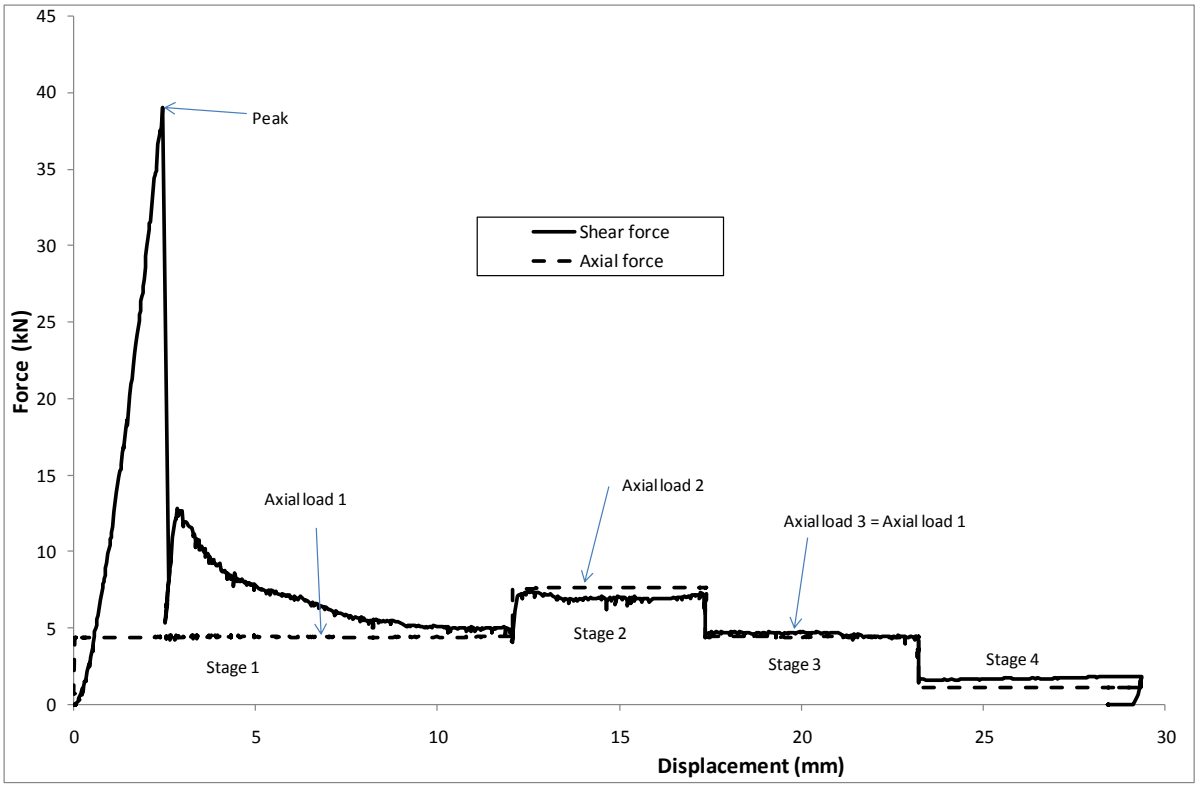

Figure 108. Typical plot of shear force and axial load versus actuator movement

B.2.4 Comments on the brick shear test results

Clearly the shear friction measured is a function of slip displacement and to a lesser extent the axial load. Values given are significantly greater than the shear friction values of 0.63 measured for Room 2. Several causes of this incompatibility are possible:

- The brick ties may have been applying a net uplift force on the veneer panels in the room tests
- The concrete surface in Room 2 was trowelled smoother than used for the small sample tests
- The measurement of shear force in the veneer may have been underestimated due to friction in the UC support rollers.

The peak shear strength of the brick-to-brick interface averaged at 687 kPa (Table 13) which is 67% more than the corresponding value for the brick-to-concrete foundation of 411 kPa (Table 11). This may be partially due to the weaker bond for mortar cast against bare concrete which may have 'sucked' moisture from the mortar.

Figure 109. Set-up for brick-to-brick joint shear test 2

B.3 Plucking tests

Plucking tests were performed as shown in Figure 110 with the results summarised in Table 14. Plates were bolted together each side of the bricks, thus effectively clamping the brick to the plates. These were mechanically lifted off and the peak load measured by a load cell and strain indicator.

Figure 110. Plucking test set-up

Table 14. Plucking tests results

Sample	Brick/concrete		Brick/Mulseal	
1	2.21	kN	8.68	kN
2	2.575	kN	9.99	kN
3	3.115	kN	9.65	kN
4	1.825	kN	11.66	kN
5	2.735	kN	11.49	
6	2.030	kN		
7	2.235	kN		
Mean	2.389	kN	10.294	kN
SDEv	0.444	kN	1.267	kN
Cov	0.186		0.123	
Mean bond stress	118	kPa	668	kPa

Eighty to ninety percent of the brick-to-concrete failure occurred at the interface of the mortar and the concrete rather than between the mortar and the brick. A similar percentage occurred at the Mulseal/mortar interface in the brick-to-Mulseal specimens. The mortar-to-Mulseal bond was far higher than the mortar-to-concrete bond strength.

Although an effort was made to make the loading concentric, accidental eccentricities are likely to have influenced the above results.

B.4 Concrete brick bond wrench tests

Tests were performed in accordance with NZS 4210 (NZS 2001). A view of the test set-up is shown in Figure 111. Results are given in Table 15. There is a significant scatter of results, but the mean value of 859 kPa is far higher than the 118 kPa obtained from the plucking tests from a concrete foundation (Table 14).

Table 15. Bond wrench tests results

	Failure stress (kPa)
1	1093
2	1081
3	730
4	726
5	706
6	817
Mean	859
Standard Dev.	181
Cov	0.21

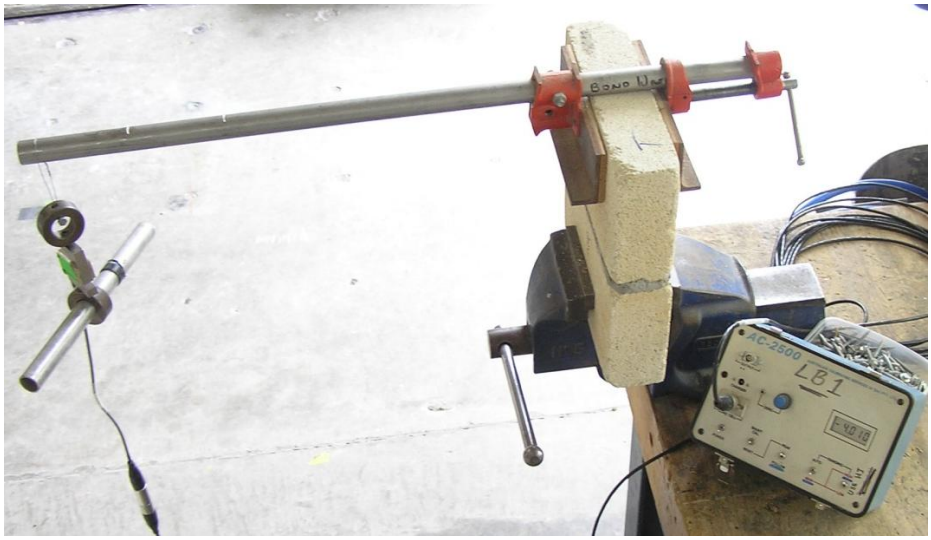

Figure 111. Bond wrench test arrangement

B.5 Mortar crushing strength

The measured crushing strength of test cylinders, made from the mortar taken from the tradesman's barrow, is summarised in Table 16. The tests were done to NZS 3112: Part 2 (SNZ 1986). The average strength of the standard 28-day cured mortar was 20.2 MPa which is 62% more than the 12.5 MPa minimum strength specified by NZS 4210 (SNZ 2001).

Table 16. Measured mortar crushing strength

	Age (days)	Density kg/m^3	Strength (MPa)	Group Average (MPa)	Curing
1	15	1890	17.5	17.3	Standard curing
2		1900	17.5		
3		1890	17.0		
4	15	1870	15.0	16.2	Double bagged sealed and stored by test room
5		1870	16.5		
6		1880	17.0		
7	15	1760	12.5	12.8	Stored in air by test room
8		1750	12.5		
9		1750	13.5		
10	28	1920	20.5	20.2	Standard curing
11		1900	20.0		
12		1900	20.0		

APPENDIX C ANALYSIS OF TWO-STOREY HOUSE

C.1 Computer model

A Ruaumoko computer model predicting the backbone curve of the inter-storey shear force versus displacement relationship for the two-storey brick veneer test house was developed. The model depicted in Figure 112 represents Side 1 of the test house. It consists of three columns connected by brick ties at each height where they were used in the test house.

All column elements in Figure 112(b) were specified as sufficiently stiff so that any flexural or shear deformations of the columns was negligible in the model. The centre column represents the LTF. This is assumed to be pinned at ground level and first floor level so that within each storey it has a linear relationship between height and displacement as shown in Figure 112(a). This is representative of LTF shear wall displacements.

At the first floor level the X and Y movements of node 55 were set constant with respect (slaved) to node 9 to ensure no separation.

The left hand side (LHS) column represented the end brick veneer panels. It was connected to the middle column with appropriate springs to represent the axial load properties of Type EM end wall ties, as specified in Table 2 of AS/NZS 2699.1 (SA/SNZ 2000). A horizontal crack was assumed to exist at the top and bottom of window openings and thus nodes 19, 23, 27 and 31 are separated from the structure above as shown, but with the adjacent upper nodes slaved to ensure they deformed with the same X and Y movement as the corresponding lower nodes.

The right hand side (RHS) column represented the side brick veneer walls including the corner portions. It was connected to the middle column with appropriate springs to represent the horizontal ties using the properties presented in Section D.1 of Thurston and Beattie (2008a). A horizontal crack was assumed at the top and bottom of window openings and thus nodes 35, 41, 46 and 52 are separated from the structure above as shown, but with the adjacent upper nodes slaved to ensure they deformed with the same X and Y movement as the corresponding lower nodes.

The nodes at 37 and 48 were partially restrained from rotating using rotational springs with yield properties based on the theory in Section 4.3.2. This assumes that the rocking motion of the brickwork piers is resisted by the self-weight of the piers, the apportioned weight of the brickwork above and the resistance from the apportioned brick ties to their uplift in the Y direction. The spring properties of the brick ties in the Y direction were determined from the test results in Appendix B.

The spandrels were assumed to force the horizontal displacement of the corresponding levels of LHS and RHS brickwork to be the same. Nodes were slaved accordingly.

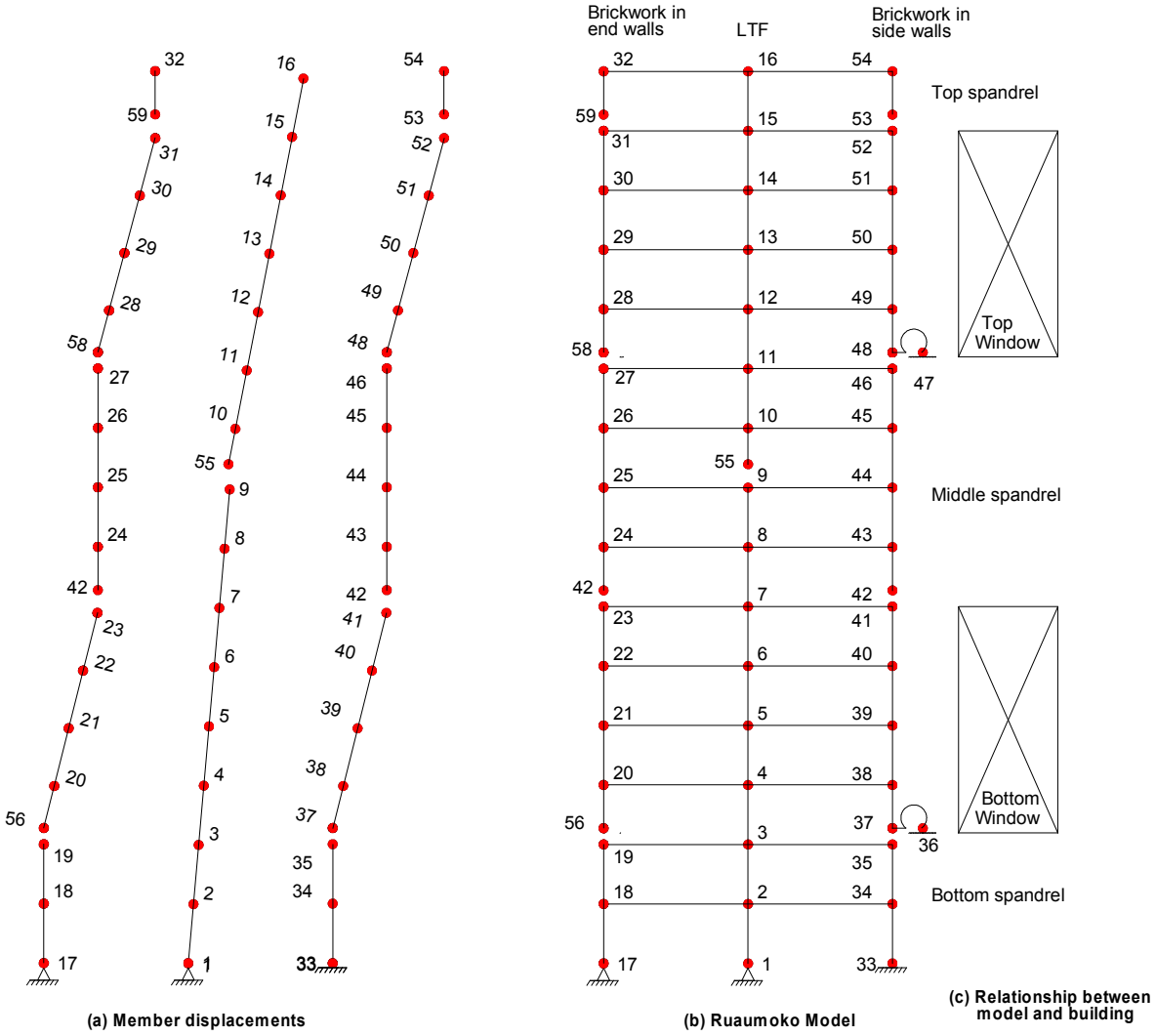

Figure 112. Computer model of two-storey building